UNIVERSITY OF INSUBRIA

Doctoral School of Experimental and Translational Medicine

Ph.D. Program in Neuroscience – XXXI Cycle

Proteomics and network analysis identify common and specific pathways of neurodegeneration

Tutor: Dr. Tiziana Alberio

Coordinator: Prof. Daniela Negrini

PhD thesis of:
CHIARA MONTI

Ad Anna,

A Luigi

Index

Abstract

Neurodegenerative diseases are characterized by the progressive loss of specific neurons in selected regions of the nervous system. The main clinical manifestation (movement disorders, cognitive impairment, and/or psychiatric disturbances) depends on the neuron population being primarily affected. Parkinson's disease (PD) is a common movement disorder, whose aetiology remains mostly unknown. Progressive loss of dopaminergic neurons in the *Substantia Nigra* causes an impairment of the motor control. Some of the pathogenetic mechanisms causing the progressive deterioration of these neurons are not specific for PD but are shared by other neurodegenerative diseases, like Alzheimer's disease (AD) and amyotrophic lateral sclerosis (ALS).

In this context, the main aim of the present thesis is to dissect specific and common pathways of neurodegeneration, in order to focus on PD specific mechanisms and to delineate a PD macromolecular landscape, eliminating common signs of neuronal loss. The different projects developed during my Ph.D. programme aimed to achieve this final goal.

First of all, to distinguish between general and PD-specific patterns of neurodegeneration, a meta-analysis of the literature of all quantitative proteomics investigations of neuronal alterations in different models of PD, AD, and ALS was performed (Meta-Neuro project). Afterwards, all proteomics data were merged with genetics information retrieved from the DisGeNET database. By using open-source bioinformatics tools, it was possible to identify biological processes specifically affected in PD, *i.e.*, proteolysis, mitochondrion organization and mitophagy. Moreover, four cellular component complexes were found to be mostly involved in the pathogenesis: the proteasome complex, the protein phosphatase 2A, the chaperonins CCT complex and the complex III of the respiratory chain. Eventually, this analysis highlighted a close relationship between PD and ALS.

In order to dissect the particular relationship between PD and ALS, the ProLyPALS project aimed at the analysis of ALS patients showing parkinsonian signs and symptoms (ALS-PD), who may evidence those proteins and biochemical pathways altered by both diseases. Indeed, the frequency of extrapyramidal symptoms in ALS patients is significantly higher than in the general population. To study these complex and multifactorial pathologies, a holistic approach may give a global view on the pathogenetic processes at the basis of neurodegeneration. The nature of samples available for this kind of studies is an issue in

neuroscience research. In this project, peripheral blood mononuclear cells (PBMCs) were considered a good cellular model for a better understanding of ALS and PD, because of the easiness of sampling, their ability to patrol what is happening at the central level and the involvement of the immune system in the pathogeneses. The ultimate goal of this approach was the characterization of ALS-PD patients, based on a model constructed from the differences evidenced in the PBMCs proteome of ALS and PD subjects. Therefore, ALS and PD proteomes were used to construct the predictive model and ALS-PD subjects were predicted as ALS or PD, depending on the discriminant function previously generated. Total proteins from PBMCs lysates of each patient were separated through two-dimensional electrophoresis (2-DE). Around 400 spots in each 2-DE map were matched. Consequently, the 54 spots able to better discriminate between ALS and PD patients were selected by Wilcoxon test. Among them, 33 spots were selected to build a Linear Discriminant model, as the one with the best sensibility and specificity. The proteins at the basis of the model were identified by LC-MS/MS. The role of each feature contributing to the discriminating function was investigated, to evidence the biochemical pathways specifically altered by one of the two pathologies. Some of them have already been associated with either disease, for example a feature selected by the model was the Cu,Zn-superoxide dismutase-1 (SOD1), linked to familial ALS, whereas another one, fibrinogen, was already found to be reduced in T-lymphocytes of PD patients. Eventually, the model was used to predict the classification of the ALS-PD patients. Four ALS-PD subjects were classified as ALS patients, while five subjects resulted to be more similar to PD patients. Their classification as PD subjects instead of ALS can be due to several factors: early appearance of parkinsonism, severity of parkinsonian signs, familiarity with PD, mutations in genes commonly involved in PD.

Mitochondria seem to have a pivotal role in PD pathogenesis. Several pieces of evidence are present in the literature and emerged by the results of the two first projects of the present thesis (Meta-Neuro and ProLyPALS projects). Many neurodegenerative diseases are only associated with alterations at the mitochondrial level, whereas the impairment of the mitochondrial quality control could be a primary event in PD pathogenesis. Indeed, several molecular pathways implicated in PD aetiology converge on mitochondria. To focus on the main mitochondrial processes involved in PD, PD-specific proteins obtained by the meta-analysis (Meta-Neuro project) were mapped on the functional mitochondrial human proteome network (MitoNet project). This network was built retrieving information from neXtProt, the reference database for the Human Proteome Project (HPP) metrics, about both nodes (mitochondrial proteins) and edges (gold binary interactions). This analysis highlighted that 31% of PD-specific proteins were mitochondrial proteins or associated with mitochondria. Moreover, the over-representation analysis highlighted the central role of mitophagy, mitochondrial protein import and mitochondrial transport as PD specific pathways.

At the end of my Ph.D. programme, I tried to make a step forward in the use of bioinformatics tools to investigate PD specific mechanisms. In particular, I aimed at the generation of a dynamic model of the "PD mitochondrion", to describe mathematically what happens in mitochondria of PD patients. The proposed model focused on a particular type of cellular model of PD (human neuroblastoma cells treated with mitochondrial toxins). The model adopted a fuzzy logic-based formalism that allows the temporal simulation of the system and the representation of heterogeneous cellular components and processes. To this purpose, preliminary data were collected about several proteins involved in mitochondrial dynamics, such as mitophagy, fusion and fission. Next steps will be the generation of many other wet results and their integration, to generate membership functions of the fuzzy-model, with the final aim to use the virtual "PD mitochondrion" as a simulation platform.

PART I

Introduction and

Scope of the thesis

1.1

Introduction

From reductionism to systems biology

Methodological reduction is based on the idea that complex biological systems could be explained by investigating their individual components. A common example of this type of strategy is the dissection of biological systems into their constituent parts (Strange, 2004), for instance, the investigation of cellular populations or organs is used to comprehend the organism status and the study of cellular biochemical components is exploited to understand cell phenotype. This method drove the research in the last half of the 20th century and it has been effective in explaining the chemical basis of numerous living processes.

However, biological systems are clearly much more than the sum of their parts and the behaviour of complex physiological processes cannot be explained, or even predicted, by studying how the parts work in isolation. For instance, PARK7 gene encodes for DJ-1 protein (Protein/nucleic acid deglycase DJ-1) that plays an important role in cell protection against oxidative stress and cell death, acting as oxidative stress sensor and redox-sensitive chaperone and protease. Deletions and loss-of-function mutations in the human PARK7 gene have been associated with several diseases such as a familiar form of Parkinson's disease (PD) (Tang et al., 2006), amyotrophic lateral sclerosis (ALS) (Annesi et al., 2005) and dementia (Rizzu et al., 2004). Furthermore, an increase of DJ-1 level promotes cell survival (Kim et al., 2005) and it is involved in advanced stage ovarian carcinomas (Davidson et al., 2008), in renal carcinoma (Sitaram et al., 2009) and in prostate cancers (Tillman et al., 2007). In all these pathologies, DJ-1 function and/or level are altered, but this alteration leads to different clinical features. Therefore, other factors, such as the specific cellular type, the micro- and macro-environment and epigenetic factors influence the epiphenomenon. Thus, interactions between the individual parts of given system, as well as influences from environmental factors and the genetic background, give

rise to a systems behaviour, which are absent in the individual components (Alm and Arkin, 2003; Van Regenmortel, 2004). Emergent properties have their own causal powers, which are not be predicted from lower-level (as it happens for resultant properties). For instance, the experience of pain can alter human behaviour, but the biochemical pathways activated in the neurons (lower-level) in the perception of pain are not the cause of the altered behaviour, as the pain itself has causal efficacy (Morowitz, 2002). Reductionists advocate the idea of "upward causation" by which molecular states bring about higher-level phenomena. The hierarchical structure present in biological systems implies that what happens at a certain scale (*e.g.* at the cellular level) is strongly linked to the other scales (*e.g.* at the tissue level). These levels interact in many ways: negative feedback and feed-forward control. Therefore, it is impossible to predict the whole phenomenon by linear mathematical models that disregard cooperativity and non-additive effects, but it is necessary the adoption of multi-scale mathematical methods, where the output of each model being the input of another model that operates on a different scale.

Moreover, biological systems present other essential properties:

- Robustness: the capability of systems to adapt and be impervious to change in the environment, thanks, for example, to the presence of redundant components that can act as a backup when individual components fail (Kitano, 2002).
- Modularity: biological systems are composed of subsystems communicating with each other even if they are physically and functionally insulated. Thus, the failure of one module does not necessarily spread to other modules (Alm and Arkin, 2003).
- Biological systems are open: they are able to exchange matter and energy with their environment, so they are not in thermodynamic equilibrium.

For all the above-mentioned reasons, systems biology has emerged as the successor of reductionism (Kitano, 2002; Kitano, 2002; Pennisi, 2003, Bizzarri et al., 2013).

The aim of systems biology is to integrate experimental data to build predictive models, whose numerical simulations can elucidate the emergent properties of the system in both physiological and pathological conditions (Medina, 2013; Noble, 2011; Longo et al., 2012). Mathematical modelling helps in revealing possible counterintuitive mechanisms and in generating new hypotheses that can be tested in laboratory. Simulation of the temporal evolution can show the system dynamics in a wide variety of perturbed conditions, considerably reducing the cost and time of experiments. The iterative process (Figure 1.1) of prediction, computational simulation and experimental validation allows to refine the model, in order to obtain the most accurate depiction of the real system, along with clarity, simplicity and a reduced number of free parameters (Fasano et al., 2016; Bartoccio and Liò, 2016).

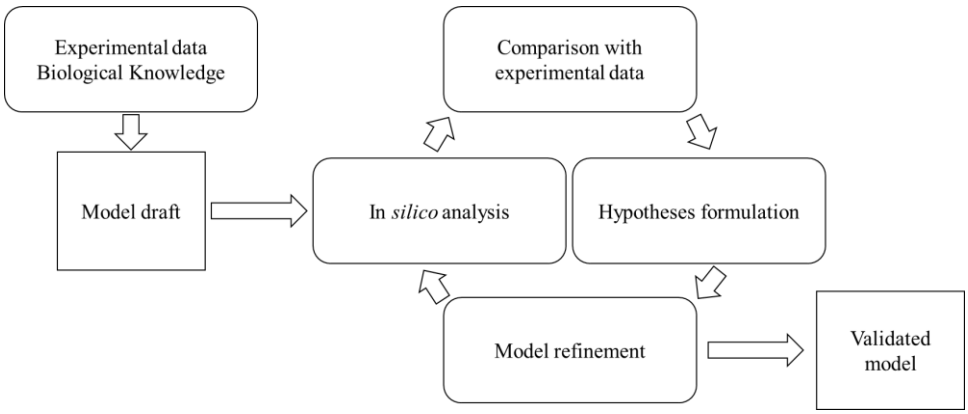

Figure 1.1: Schematic representation of the iterative process of construction and validation of a mathematical model. Data from *in silico* analysis are compared to the experimental ones, in order to formulate new hypotheses and refine the first model draft. A validated model is the starting point for a deeper and predictive computational analysis.

To formulate a mathematical model that describes the system, it is essential to know elements and dynamics activated in response to specific environmental or genetic perturbations and supplement this information to identify the rules of system control and regulation. To these purposes, several tools can be used, such as pathway and network analysis (Fasano et al., 2016).

Pathway analysis

Biological knowledge has been organized in several databases, which encode biological knowledge of molecular mechanisms, proteins sequences, proteolytic peptides and proteins interactions data (Table 1.1).

Table 1.1: Main protein databases.

Database name	URL	Reference
Uniprot	http://www.uniprot.org/	Chen et al., 2017
neXtProt	http://www.nextprot.org/	Gaudet et al., 2017
UniGene	https://www.ncbi.nlm.nih.gov/unigene/	NCBI Resource Coordinators, 2018
RefSeq	https://www.ncbi.nlm.nih.gov/refseq/	O'Leary et al., 2016
GenBank	https://www.ncbi.nlm.nih.gov/genbank/	Benson et al., 2005
MissingProteinPedia	http://missingproteins.org/	Baker et al., 2017
Human Protein Atlas	https://www.proteinatlas.org/	Thul and Lindskog, 2018
MEROPS	https://www.ebi.ac.uk/merops/	Rawlings et al., 2018
Pride	https://www.ebi.ac.uk/pride/archive/	Vizcaíno et al., 2016
ProteomeXchange	http://www.proteomexchange.org/	Deutsch et al., 2017
Peptide Atlas	http://www.peptideatlas.org/	Deutsch et al., 2015
STRING	https://string-db.org/	Szklarczyk et al., 2017
BioGRID	https://thebiogrid.org/	Chatr-Aryamontri et al., 2017
IMEX	https://www.imexconsortium.org/	Orchad et al., 2012
IntAct	https://www.ebi.ac.uk/intact/	Orchard et al., 2015
Gene Ontology consortium	http://geneontology.org/	The Gene Ontology Consortium, 2017
WIKIPATHWAY	https://www.wikipathways.org/index.php/WikiPathways	Slenter et al., 2018
Pathway Commons	http://www.pathwaycommons.org/pc/	Cerami et al., 2010
Reactome	https://reactome.org/	Fabregat et al., 2018
KEGG	https://www.genome.jp/kegg/	Kanehisa et al., 2017

Many databases have become accessible in the last decade (Khatri et al., 2012; Ramanan et al., 2012) and some of them provide platforms to directly analyse proteomics data, such as pathway databases (*e.g.* Reactome (Fabregat et al., 2018) and KEGG (Kanehisa et al., 2017) databases) (Goh et al., 2012). Relevant functional relations may be obtained also from the Gene Ontology (GO) database, in which gene functions are described in terms of three different main aspects: the molecular function (MF), the cellular component (CC) and the biological process (BP) (The GO Consortium, 2017). Other possible platforms for the interpretation of proteomics data are secondary databases (which collect

information from other public pathway databases), such as Pathway Commons (Cerami et al., 2010) and WIKIPATHWAYS (Slenter et al., 2018).

Using data stored in pathway databases, it is possible to analyse lists of proteins resulting from proteomics studies. The analysis of pathways can be used to generate a hypothesis, through an inductive method, and to attribute an expectation value to it (Khatri et al., 2012). To this purpose an over-representation analysis (ORA) can be performed to functionally explain changes at protein level. In the ORA, the hypergeometric test (Fisher's test) is normally used to compute a p value for each over/under-represented pathway. Fisher's test is a conditional test, where the p value for an over-represented pathway is calculated from the number of differentially expressed proteins in the experimental list and in a reference database, assigned or not to a given pathway (Fasano et al., 2016).

Network analysis

Based on the rationale that interacting proteins share common functions or take part to common processes, it is possible to build biological networks. The biological network is a graph defined by two sets: a set of nodes, representing biological components (such as proteins, genes) and a set of edges, that connect nodes, representing physical or functional interactions.

Networks can be analysed using several topological measures that can help elucidate potential therapeutic targets and/or biomarkers (degree of connectivity, betweenness centrality and clustering coefficient) (Santiago and Potashkin, 2014). Eventually, protein networks may be further analysed in terms of pathways to show how protein clusters are functionally linked to specific processes (Wu et al., 2014; Laukens et al., 2015).

Several software is available to generate and visualize biological networks. Cytoscape is the most used, since it provides an open-source environment for network generation, visualization and analysis (Shannon et al., 2003). Moreover, several modules are available to customize the Cytoscape environment, in particular tools to perform the ORA on networks or to analyse topological elements (clusters or subnetworks). In addition to Cytoscape, other open-source platforms are available to visualize and analyse networks, such as Gephi – The Open Graph Viz Platform –for network manipulation (Bastian et al., 2009) and Pajek, for large networks (Mrvar and Batagelj, 2016).

To build a biological network, information present in public databases that store molecular interaction data can be used (*e.g.,* BioGRID (Chatr-Aryamontri et al., 2017), IntAct (Orchard et al., 2015), and STRING (Szklarczyk et al., 2017)). Each of them has advantaged and disadvatages (Table 1.2). Several

efforts have been made to put under a single consortium (the IMEx consortium) the whole information available on protein–protein interactions (PPI) (Orchad et al., 2012) (Table 1.2).

Table 1.2: Advantages and disadvantages of main open source PPI databases.

Database name	Advantages	Disadvantages
IMEx	• Contains physical interactions data • Contains data of several organisms • Is a secondary database • Contains data of several public interaction database (*e.g.*, IntAct, BioGRID and Uniprot) • A plugin in Cytoscape is available	• Redundant information • The user is overwhelmed with too much information • No quality control of data available • A graphical software is necessary to visualize the network
IntAct	• Contains physical interactions data • All interactions are derived from literature curation or direct user submissions • A plugin in Cytoscape is available	• The user is overwhelmed with too much information • No quality control of data available • A graphical software is necessary to visualize the network
STRING	• Contains physical and functional interactions data • Contains data of several organisms • Is a secondary database • Contains data of several public interaction databases (*e.g.*, IntAct, BioGRID) • Computes the PPI enrichment p value. It indicates that the network has significantly more interactions than expected • Performs an ORA using GO, KEGG and proteins domains databases (PFAM)	• The user is overwhelmed with too much information • No quality control of data available
neXtProt	• Contains physical interactions data • Is a secondary database • Contains data of several public interaction database (*e.g.*, IntAct, Uniprot) • Provides only highest and good quality data • Data deemed of a lower quality do not integrate	• Provides only data about human proteins • No plugin in Cytoscape is available to directly generate the network • Information is manually curated (operator-dependent and delayed update with respect to automatically annotated database)

Logic modelling

A graph can be a good representation of a biological systems, but it can provide only a static view of the underlying system. To overcome this drawback, two main modelling approaches are currently being utilized: mechanism-based models and logic-based models (Le Novère, 2015).

Mechanism-based models allow to predict the behaviour of a specific system and to track its dynamics by fixed system parameters. All the parameters (*e.g.,* diffusion, binding and reaction kinetics, concentrations of system's components) (Würstle et al., 2014) must be experimentally measured or inferred to specify the model. For example, a mechanism-based model was used to describe the glucose-insulin system and all major physiological processes involved in plasma glucose homeostasis (Figure 1.2) (Cobelli et al., 2014).

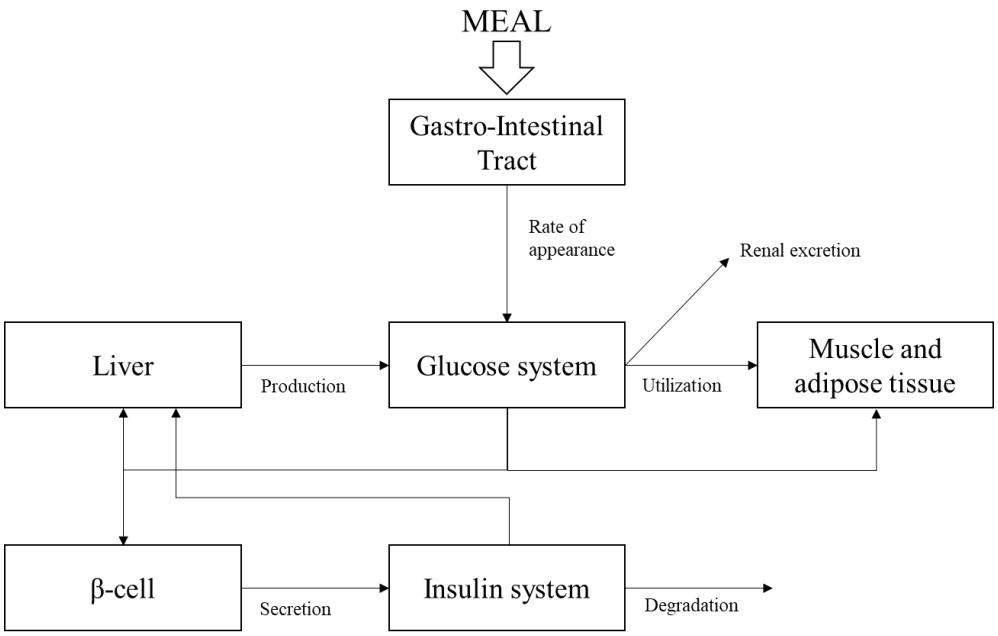

Figure 1.2: Pictorial layout of the physiological components in the glucose-insulin system model (taken from Cobelli et al., 2014).

All parameters of this model (*e.g.,* insulin secretion in the pancreas, glucose uptake in peripheral tissues, glucose production) have been obtained through the evaluation of insulin and glucose dynamics in serum and plasma (Cobelli et al., 2014). Mechanism-based model requires a huge amount of biochemical quantitative information. To overcome this limitation, logic-based models are currently emerging as an alternative to study biological events (Wynn et al., 2012).

Logic-based models are graphs based on (1) edges, (2) nodes and (3) logical rules (Morris et al., 2010). The interactions between the components of the system can be physical or functional and edges can be added also using qualitative data (Morris et al., 2010). Moreover, nodes can represent different types of information, from the presence of a protein to the activation of a biochemical pathway or the occurrence of a phenotype. Logical rules can contain one or more logic operator (*e.g.* NOT, AND, OR). Each rule should correctly describe an interaction existing in the real biological system, to make the whole model predictive. Evaluation of logical rules provides the output value of each node based on the values of input nodes (Wynn et al., 2012). Various types of logic-based model exist, differing in (1) how they handle time during simulation and (2) how they describe nodes (discrete states or continuous states).

(1) In logic-based models, simulation is usually performed in discrete time steps using a synchronous or asynchronous update (Wynn et al., 2012). In models that adopt a synchronous update method, all nodes are updated at the same time according to the values of their input nodes at the previous time step, thus the state of the network is always entirely determined by its state at the previous step. Conversely, in the asynchronous method, a randomly selected node is updated thanks to the state of the network and therefore its next state is non-deterministic. The asynchronous update method is thought to be closer to the real biological systems, but it requires to run many simulations to obtain probability distributions of output states according to given input states (Wynn et al., 2012).

(2) In the logic-based model the description of variables can be represented as discrete states (using Boolean logic) or continuous states (using fuzzy logic). Among logic-based models, Boolean models are the simplest and widely used. In Boolean logic the variables can assume only two discrete state, often represented as 0 and 1 (active/inactive, present/not present) (Wynn et al., 2012; Würstle et al., 2014). Describing all species as either \on" or \off" is clearly an unrealistic way to represent many biomolecular phenomena, which often exist in multiple states and do not show discrete transitions between one state and the other (Figure 1.3 A). This limitation can be overcome by a fuzzy logic approach. Fuzzy logic represents multi-state variables in a continuous way. In this way, intermediate states can be described (Figure 1.3 B). For these reasons, fuzzy logic is a suitable formalism to model qualitative knowledge on cellular processes, such as high or low expression of a gene, high or low activity of an enzyme, high or low concentration of a molecule, as well as their intermediate values.

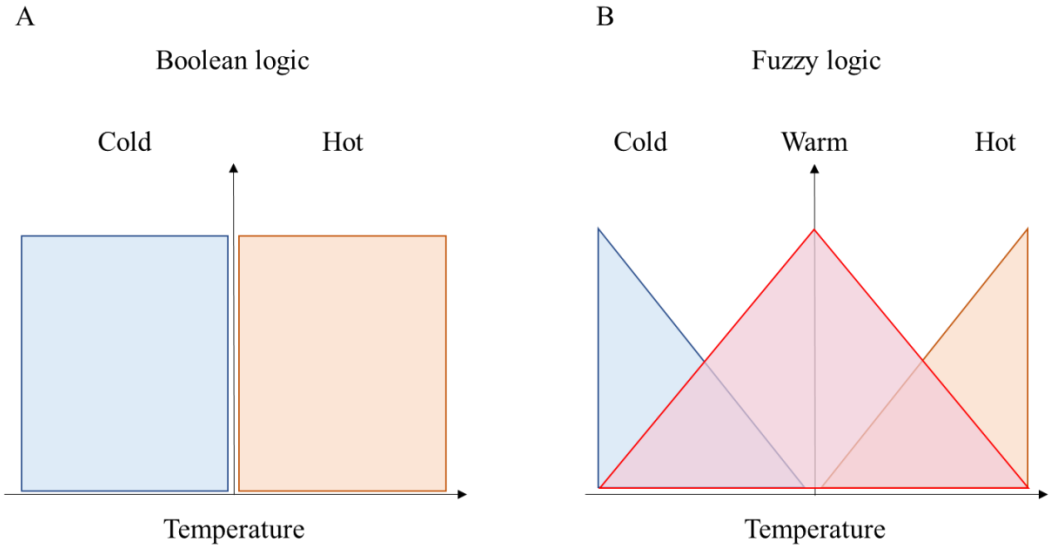

Figure 1.3: Comparison between discrete sets (A) and fuzzy sets (B), described by membership functions. Discrete sets have sharp boundaries and an input can either belong or not to a set, while fuzzy sets have smooth boundaries and an input can belong to a set up to a certain degree.

The membership degree of a fuzzy set is defined by a membership function. Membership functions describe the smooth transition from a region of inputs that is outside the set to a region that is inside the set. A linguistic variable is also defined for each of the smooth transitions. For example, in Figure 1.3, the linguistic variables are defined as "Cold", "Warm" and "Hot". Linguistic variables are meaningful terms (for example, "High" or "Low" for a fuzzy set representing the activation state of a gene), taken directly from natural language. Linguistic variables relate a common qualitative description typical of human language, to a quantitative one, represented by membership functions. Moreover, linguistic variables allow to express knowledge on the state of the node in a human-readable and easily comprehensible way, through the formulation of fuzzy "IF-THEN" rules. Fuzzy IF-THEN rules are the basic tool to capture the basic knowledge of the system and represent the interactions existing between the nodes of the modelled system. They appear in the form "\IF <antecedent> THEN <consequent>", where antecedent describes a condition and consequent describes the conclusion that can be drawn when the condition holds. For instance, considering the following rules:

- IF Glucose is Low THEN Glycolysis is Low
- IF Glucose is High THEN Glycolysis is High

where "High" and "Low" are linguistic variables associated with suitable membership functions. Together, these two rules describe a positive regulation of glucose on glycolysis output. The use of linguistic variables in fuzzy logic rules allows to represent situations in which the condition is satisfied

only to a certain degree, in contrast to classic logic rules, where a condition is either fully satisfied or not.

Proteomics approaches

Systems biology aims at studying a biological system as a whole. Therefore, disciplines that consider biological systems in a global way are the natural source of data for systems biology. "Omic" technologies are high-throughput and provide a holistic view of the molecules that constitute cells, tissues or organisms. They aim at the universal detection of genes (genomics), mRNA (transcriptomics), proteins (proteomics) and metabolites (metabolomics) in a specific biological sample, in an untargeted and unbiased manner. These techniques have many advantages: they can simultaneously consider several molecules, they are highly standardisable and easily automatized, in order to process many biological samples (Shalhoub et al., 2014; Hosp and Mann, 2017).

The term proteomics describes the study and the characterization of the proteome (complete set of proteins present in a cell, organ or organism at a given time), which conveys a snapshot of what is happening in the system under determined conditions. Indeed, environmental and cellular changes cause alterations in proteins expression, in their abundance, in their cellular or tissue localization, in their post-translational modifications (Villoslada et al., 2009). Proteomics approaches can be used for proteome profiling, for comparative expression analysis of two or more protein samples, for the localization and the identification of post-translational modifications and for the study of PPI. A wide range of proteomic approaches is available, such as gel-based applications and gel-free high throughput screening technologies.

Even if proteomics has to be considered a global approach, it is far from properly detecting all the alterations occurring in a certain condition, mainly for technical reasons. For instance, in the shotgun approach, based on data-dependent acquisition (DDA), only peptides with an intense signal are fragmented and thus identified by mass spectrometry (MS). Moreover, other limitations in current proteomics studies are the statistical analysis (*e.g.,* univariate vs. multivariate analysis, parametric vs. nonparametric analysis, multiple testing correction), the sample size (lack of an appropriate power analysis), the conservation of samples and confounding factors not appropriately taken into account (*e.g.,* age, gender, administered drugs, clinical anamnesis of subjects recruited for translational studies) (Fasano et al., 2016).

In quantitative proteomics, two approaches are possible: gel-based and gel-free (Jorrin-Novo et al., 2018; Winter et al., 2018). Independently for the strategy chosen, the quantitation of proteomes is

difficult and presents some issues. Gel-based approaches are top-down. Therefore, they directly analyse proteins. On the contrary, gel-free technologies analyse peptides and are bottom-up approaches. In the first case, the extrapolation of protein abundance is complicated by the presence of multiple proteoforms (Jorrin-Novo et al., 2018). Therefore, changes wrongly attributed to protein amounts may be due to post-translational modifications. Even in the second approach, extrapolating protein abundance from peptides is not trivial, since the information on both the identity and the amount of each protein is obtained by the peptide-to-protein mapping.

Gel-based techniques: two-dimensional gel electrophoresis (2-DE)

The two-dimensional gel electrophoresis (2-DE) entails the separation of proteins based on their isoelectric point (pI) (first dimension, by isoelectric focusing (IEF)) and their molecular weight (MW) (second dimension). During the IEF, proteins migrate through a thin gel-strip embedded with immobilized pH gradients. Migration ends when proteins reach their pI. Proteins are then separated in the second dimension (orthogonal direction) by Sodium Dodecyl Sulfate Poly-Acrylamide Gel Electrophoresis (SDS-PAGE), where SDS imparts a net negative charge, allowing proteins to separate according to MW. Proteins can be visualized using visible stains such as Coomassie blue and silver staining, or fluorescent stains such as Sypro ruby or Ru(II) tris (bathophenanthroline disulfonate) (RuBPs) staining. Although RuBPs and silver staining have a comparable sensitivity, RuBPs has good linearity, high contrast and is compatible with MS analysis. This colorant is excited by UV light of wave length around 473/488 nm. After detection of the proteins in the gels, the resulting images are quantitatively analysed to determine proteoforms (spots) changing in the experimental conditions. Those spots are excised and submitted to in-gel digestion (generally with trypsin). The resulting peptides are then eluted and analysed by MS (Rabilloud and Lelong, 2011).

2-DE analysis provides several types of information about the hundreds of proteins investigated simultaneously, including MW, pI and abundance, as well as possible post-translational modifications. 2-DE is extensively used but mostly for qualitative experiments. Indeed, this method falls short of reproducibility, it unlikely detects low abundant and hydrophobic proteins, proteins with pI < 3 or pI > 10 and with MW < 10 kDa or MW> 150 kDa. However, 2-DE is the only technique that can be routinely applied for parallel quantitative expression profiling of complex protein mixtures, such as whole cell and tissue lysates, and the most widely used method for efficiently separating proteins, their variants and modifications (Chandramouli and Qian, 2009).

Gel-free techniques: MS-based proteomics

Gel-free, or MS-based, proteomics techniques are emerging as the method of choice for quantitatively compare proteomes (Anjo et al., 2017). Label-free quantitative MS methods are based either on spectral counting or on peptide precursor ion intensities that are obtained using the first analyser of a tandem mass spectrometer. Peptides are identified across different liquid chromatography (LC) runs based on their specific retention time coordinates and precise mass to charge (m/z) values, which in principle allows the quantification of all the peptides detected from a biological sample that are within the sensitivity range of a MS analyser, independently for MS/MS acquisition. Starting from the peptide sequences obtained, proteins are identified using protein sequence databases. The stochastic precursor selection of DDA leads to under sampling of low abundant peptides. This results in missing peptide identification and reduces the number of quantifiable proteins. To overcome this limit, data-independent acquisition (DIA) was introduced as an alternative. In DIA, the entire set of peptide precursors (without a pre-selection of the precursor ions in each cycle time) is fragmented. This approach complicates the analysis in a classical database search strategy. Therefore, spectral libraries obtained by an extensive analysis of the same/similar samples by DDA are normally generated to be used in the search analysis (Koopmans et al., 2018). On the other hand, label-based proteomics relies on various isotopic labelling strategies, such as isotope-coded affinity tag (ICAT), stable Isotope Labelling by/with Amino acids in Cell culture (SILAC) and isobaric Tags for Relative and Absolute Quantitation (iTRAQ) (Ross et al., 2004).

Neurodegenerative diseases

"Neurodegenerative disease" is a collective term for a range of conditions that primarily affect neurons, in the brain (*e.g.,* Alzheimer's disease (AD) and PD), or at the periphery (*e.g.,* motor neurons in ALS).

Alzheimer's disease

AD is the most common chronic neurodegenerative disease that affects approximately 35 million people worldwide (Honig et al., 2018). The prevalence of AD is generally estimated around 6% in people over 65 years of age (Burns and Iliffe, 2009).

Early stages of AD are characterized by impairment of memory (*e.g.*, misplacing objects, forgetting conversations, problems remembering names and missing appointments) and of

visuoconstructional/visuospatial drawing (*e.g.*, clock drawing and copying of geometric figures). Language deficits are the second most prominent cognitive manifestation of AD (*e.g.,* dysnomia, verbal paraphasias, and word-finding difficulty) and in some cases they can be the initial clinical symptoms (López et al., 2008).

AD is characterized by extracellular plaques containing amyloid beta (Aβ) and intracellular neurofibrillary tangles containing hyperphosphorylated tau protein, along with synaptic and neuronal loss (Querfurth and La Ferla, 2010). Two different forms of AD have been described: sporadic and familial. In familial AD several mutations were reported such as those in the genes of Aβ A4 protein (APP), Presenilin-1 (PSEN1) and Presenilin-2 (PSEN2) (Minati et al., 2009). The investigation of the cellular function and toxicity of genes linked to monogenic forms of AD provided advances in the understanding of the molecular pathogenesis of sporadic forms. APP is a cell surface receptor and its functions are relevant to neurite growth, neuronal adhesion and axonogenesis (Chen and Bodles, 2007). Sequential cleavage by β-secretase (BACE) and γ-secretase produces the Aβ peptide fragment that aggregates into clumps called "plaques" in the brains of AD patients (PSEN1 and PSEN2 are catalytic subunits of the γ-secretase complex). Moreover, alteration of abundance of proteins involved in the degradation of Aβ and in APP intracellular trafficking (Insulin-degrading enzyme (IDE) and Ubiquilin-1 (UBQLN1)) were reported (Minati et al., 2009). Furthermore, epigenetic mechanisms are involved in AD pathogenesis (Day and Sweatt, 2011), in particular an over methylation of DNA and histone modification have been described (Day and Sweatt, 2011; Ghavami et al., 2014).

AD has been used as a reference disease for the purposes of the present thesis, since it is the most common neurodegenerative disease and it is the most studied one. Moreover, it is considered a non-motor neurodegenerative disorder. However, motor signs can be observed in AD. They may result from different underlying mechanisms, although specific factors that influence their occurrence or rate of progression are not clear (Scarmeas et al., 2011). Data about their frequencies have a large variability (frequency of motor signs in AD ranged from 6% to >50%) (Scarmeas et al., 2011). Some of this inconsistency derives from methodologic differences, including variable definitions of motor signs.

Proteomics of Alzheimer's disease

Proteomics studies in the literature are mainly focused on AD cellular and animal models and on post-mortem human brain samples. The analysis of the proteome of transgenic mice expressing N-terminal truncated Aβ highlighted alterations in several proteins involved in the mTOR/p70S6K signalling pathway and in the Rhokinase (ROCK, a downstream effector of the small GTPase Rho). These

molecular alterations preceded the onset of behavioural symptoms (Yang et al., 2013). Using a label-based approach (SILAC), it was also possible to study proteome changes in BV2 rat microglia, with Aβ fibrils. The expression of thirteen proteins were significantly regulated by Aβ (six proteins were up-regulated and 7 were down-regulated). Several of these proteins were cell membrane proteins involved in the PPAR signalling pathway and lysosomes functionality (KEGG pathway analysis) (Ma et al., 2013). Proteomics approaches allowed researchers to identified post-translational modification involved in AD pathogenesis. In particular, Zahid and co-workers, using a phosphoprotein-sensitive staining after 2-DE protein separation, observed alterations in the phosphorylation pattern in the *Substantia Nigra* (SN) and the cortex from AD cases and control subjects. They identified changes in the phosphorylation level of several proteins involved in energy metabolism pathways (*e.g.,* glycolysis) (Zahid et al., 2012). The same investigators reported a focused analysis of S-nitrosylated proteins in hippocampus, SN and cortex from AD cases and control subjects, where 45 proteins involved in metabolism, signalling, apoptosis and redox regulation were endogenously S-nitrosylated (KEGG and Reactome pathway analysis) (Zahid et al., 2013).

Parkinson's disease

PD is the most common neurodegenerative disorder after AD (Gibrat et al., 2009). The prevalence of PD is generally estimated around 1% in people over 65 years of age (de Lau and Breteler, 2006). The prevalence increases with age, with a slightly higher incidence in men with respect to women.

PD is characterized by the presence of a motor symptomatology (bradykinesia, rest tremor, rigidity and postural disturbances). In addition to the motor symptomatology of PD, some non-motor symptoms such as hyposmia, REM sleep behaviour disorder (Janković et al., 2015), personality changes, pain, paraesthesia and depression may be present and may even manifest years before the motor symptoms (Nutt and Wooten, 2005). Urinary disturbances, orthostatic hypotension and neuropsychiatric disturbances (dementia, hallucinations and delirium) usually become evident several years after the onset of the disease (Chaudhuri et al., 2005). Late-onset motor symptoms include postural instability and falls, freezing of gait, speech and swallowing difficulties.

The pathophysiology of PD involves the loss of dopaminergic neurons of the SN leading to denervation of the nigrostriatal tract and the significant reduction of dopamine (DA) at the striatal level. The degeneration of these dopaminergic neurons, which normally contain a considerable amount of neuromelanin (Dickson, 2012), produces the depigmentation of the SN. This process is usually associated with the presence of ubiquitin- and α-synuclein-positive cytoplasmic inclusions,

known as Lewy bodies (LB), within surviving dopaminergic neurons (Goedert, et al., 2013). The most abundant protein in LBs is α-synuclein (α-syn) (Stefanis, 2012):

As there are no definitive biological or imaging markers, diagnosis is based on stringent clinical criteria such as Movement Disorder Society (MDS) of the Unified Parkinson's Disease Rating Scale (MDS-UPDRS). It is a rating tool to follow the longitudinal course of PD. It is made up of the I) mentation, behaviour, and mood, II) activities of daily living and III) motor sections. All the parameters are evaluated by interview and a score is assigned to each category (from 0, normal situation, to 4, complete loss of function) (Goetz et al., 2007). Although, the diagnosis is made exclusively on a clinical basis, there are diagnostic tools that can be used to confirm the presence of dopaminergic denervation at the striatal level, thus lending support to the clinical diagnosis. These include fluorodopa positron emission tomography (FDOPA-PET) and DAT imaging with radionuclide tracers by means of single photon emission tomography (DAT-SPECT). In PD, substantial reductions in tracer uptake is observed.

Since diagnosis is mainly clinical and supporting tools are invasive, radioactive and expensive, a lot of ongoing research is devoted to the discovery of peripheral biomarkers to develop new diagnostic devices. Several evidences support the rationale to search for peripheral biomarkers of PD as early reporters of central neurodegeneration. For example, up-regulation and/or genetic/post-translational modifications of PD-related proteins should be highlight even at the peripheral level. T lymphocytes are the population of immune cells that could better reflect some of the alterations that impair the function of SN dopaminergic neurons that are primarily involved in PD pathogenesis. T lymphocytes express some dopaminergic features (receptors, transporters, vesicles) and DA plays an active role in their functions, as the activation and the differentiation of various T subtypes (Pacheco et al., 2009). Indeed, neurochemical and neuroimaging studies have shown a decreased immunoreactivity for the DA receptor in neuronal as well as in PBMCs of PD patients. In addition, the same alterations in the level of enzymes involved in the oxidative phosphorylation reported in the spinal cord of PD patients have been detected in their PBMCs (Ladd et al., 2014). Thus, peripheral blood lymphocytes may represent sensitive reporters of PD pathogenesis (Fasano et al., 2008).

Since most symptoms of PD are caused by the lack of DA in the brain, many PD drugs are aimed at either temporarily replenishing or mimicking the action of DA. Over the past half century, several progresses have been made in the treatment of PD, but levodopa, a DA precursor (L-dihydroxyphenylalanine, L-DOPA), remains the most potent drug for controlling PD symptoms. However, chronic oral treatment with L-DOPA is associated with the development of motor complications: fluctuations in motor performance, reflecting rises and falls of L-DOPA plasma levels

("on"/ "off" states), involuntary movements and painful dystonia. Another important category of antiparkinsonian drugs is represented by DA agonists, which can be used as monotherapy or in combination with L-DOPA. They exert their action by directly activating DA receptors, bypassing the presynaptic synthesis of DA. The activation of D2-like receptors (especially D3) is important for antiparkinsonian effects of DA agonists, although concurrent D1-like and D2-like stimulation is required to produce optimal physiological and behavioural effects (Jankovic and Aguilar, 2008). Some commonly used DA agonists in the clinical practice are Ropinirole, Pramipexole and Rotigotine. Other strategies to prolong DA response make use of inhibitors of enzymes that metabolize DA, such as catechol-O-methyltransferase (COMT) and monoamine oxidase (MAO). When used in a combined therapy, they extend the duration of action of L-DOPA. However, COMT inhibitors are used with caution because of hepatic side effects (Benabou and Waters, 2003).

The view of aetiological factors in PD has changed remarkably. From a purely sporadic disease, PD is now considered a multifactorial disorder, since both environmental and genetic factors contribute to the onset (Schapira and Jenner, 2011). Genetic predisposition or susceptibility is one of the major contributors to the underlying cause (Gasser, 2009). Epidemiological studies suggest that sporadic PD accounts for 85% of cases (Sun et al., 2006), whereas the remaining 15% are familial forms of PD (Schulte and Gasser, 2011). In the past decade, there has been an explosion of knowledge about the genetics of PD and 18 PD-related gene loci have been identified (Crosiers et al., 2011, Lunati et al., 2018). The most relevant are reported in Table 1.3.

Table 1.3: Some PD-related genes.

Gene	Protein function
SNCA	may be involved in the regulation of DA release and transport. Induces fibrillization of microtubule-associated protein tau.
LRRK2	positively regulates autophagy through a calcium-dependent activation of the CaMKK/AMPK signalling pathway.
PARK2	RING domain-containing E3 ubiquitin ligase involved in proteasome- dependent degradation of proteins and in mitophagy.
PINK1	protects against mitochondrial dysfunction during cellular stress by phosphorylating mitochondrial proteins. Involved in the clearance of damaged mitochondria via selective autophagy (mitophagy) by mediating activation and translocation of Parkin.
GBA	lysosomal enzyme involved in glycolipid metabolism. Homozygous mutations cause an accumulation of glucocerebroside that results in a wide spectrum of symptoms, known as Gaucher disease. However, GBA mutations in one allele have been found to increase the risk of developing PD.
PARK7	plays an important role in cell protection against oxidative stress and cell death, acting as oxidative stress sensor and redox-sensitive chaperone and protease.
VPS35	Vacuolar protein sorting-associated protein 35, component of the retromer cargo-recognition complex, is critical for the endosome-trafficking and the trans Golgi recycling of membrane-associated proteins.
EIF4G1	Eukaryotic translation initiation factor 4Gamma1, which is ubiquitous and abundantly expressed in different tissues. It operates as a scaffold protein that interacts with many initiation factors, including PABP, eIF3, two eIF4F components (eIF4E and RNA helicase eIF4A) and with the 40S ribosome.

The investigation of the cellular function and toxicity of genes linked to monogenic forms of PD provided advances in the understanding of the molecular pathogenesis of sporadic PD. Indeed, the progressive deterioration of vulnerable SN neurons in both sporadic and genetic PD forms may arise from cellular disturbances caused by alteration of DA metabolism, misfolding and aggregation of the synaptic protein α-syn (Luk et al., 2012), disruption of the autophagy-lysosome system (Moors et al., 2016), mitochondrial dysfunction (Bondi et al., 2016), endoplasmic reticulum stress (Mercado et al., 2016), dysregulation of calcium homeostasis (Rivero-Ríos et al., 2014), neuroinflammation and oxidative stress (Blesa et al., 2015).

The environmental factor that most strongly relates to the onset of PD is the aging process. Aging can lead to irreversible cellular damage, weakening cellular repair machinery and predisposing people to neurodegenerative diseases (Hindle, 2010). Mitochondrial toxins are other environmental factors that shed light on the influence of environment on PD pathogenesis. There has been increasing interest in 1-methyl-4-phenyl-1,2,3,6-tetrahydropyridine/1-methyl-4-phenylpyridinium MPTP/MPP^+

and rotenone. MPTP is a toxic molecule that is able to cross the blood-brain-barrier. Once MPTP enters in the glial cells, it is metabolized to MPP^+ by the monoamine oxidase enzyme. Then, MPP^+ accumulates in the mitochondria of the dopaminergic neurons thanks to the DAT (Ramsay et al., 1986). *In vitro* and *in vivo* studies demonstrated that, at the mitochondrial level, this toxin inhibits the activity of the complex I of the electron transport chain, thus leading to lower ATP production, increased reactive oxygen species (ROS) generation, mitophagy impairment and neuronal cell death (Gao et al., 2015; Navarro-Yepes et al., 2016). Rotenone is a lipophilic molecule that crosses the blood-brain barrier and biological membranes without using a specific receptor or transporter. Once in neuronal cells, rotenone inhibits the complex I of the mitochondrial electron-transport-chain, thus causing high ROS generation, lower ATP production and apoptotic cell death (Johnson and Bobrovskaya, 2015). After these discoveries, MPTP and rotenone toxins became of common use in research in several *in vitro* and *in vivo* models, in order to recapitulate the sporadic PD pathology.

Despite mitochondrial toxins are widely used in research, the parkinsonism induced by these compounds results from an acute toxic insult and differs from the slow and progressive disease process that characterize sporadic PD. The initial causes of the degeneration of dopaminergic neurons in PD is still unknown but altered DA homeostasis might be a key factor in the early steps of the pathogenesis (Alberio et al., 2012; Herrera et al., 2017). DA is synthesized starting from tyrosine and it is immediately stored in monoaminergic synaptic vesicles thanks to the vesicular monoaminergic transporter-2 (VMAT- 2). Since DA can auto-oxidize at neutral pH, when it accumulates in the cytosol, its auto-oxidation produces quinone species and hydrogen peroxide (Segura-Aguilar et al., 2014). The most abundant quinone species are DA quinones and amino chrome (Herrera et al, 2017). DA quinone forms adducts with several proteins (*e.g.,* Parkin), while amino chrome induces and stabilizes the formation of neurotoxic protofibrils of α-syn (Conway et al., 2001), causes dysfunction of the proteasome system (Zhou and Lim, 2009) and prevents the fusion of autophagy vacuoles with lysosomes (Paris et al., 2010). It has been demonstrated that α-syn plays an important role in DA homeostasis and that protofibrils of α-syn can modify the permeability of vesicles by forming pores, thus causing the leakage of DA from synaptic vesicles to the cytoplasm (Hastings, 2009) (Figure 1.4).

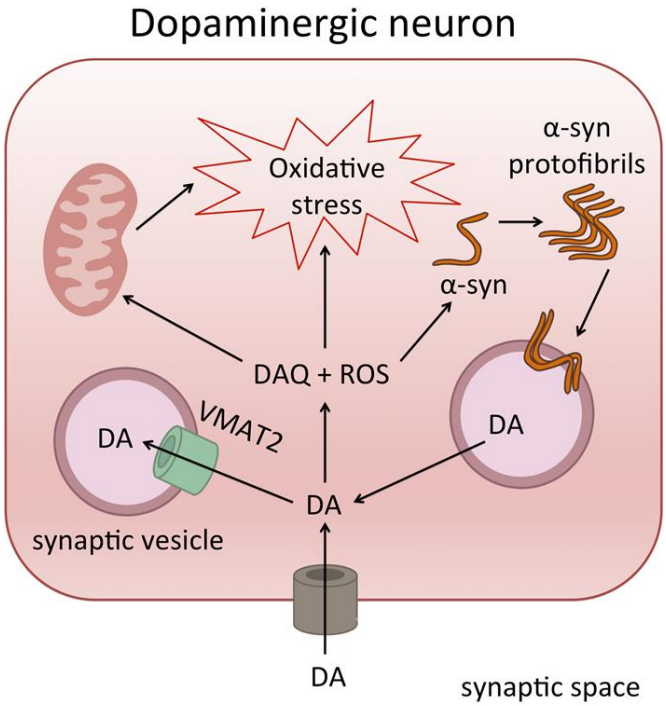

Figure 1.4: When DA is not properly stored in synaptic vesicles, it accumulates in the cytosol, thus forming quinones and increasing the ROS production. DA quinone forms adducts with several mitochondrial proteins and stabilizes the formation of α-syn neurotoxic protofibrils. In this way, altered DA homeostasis causes cellular oxidative stress and apoptotic cell death.

On this basis, several efforts have been made to develop cellular models for DA toxicity. Altered DA homeostasis in mice with reduced VMAT2 expression is enough to cause DA-mediated toxicity and progressive loss of DA neurons (Caudle et al., 2007). A cellular model often used in neurodegeneration research is the catecholaminergic SH-SY5Y human neuroblastoma cell line. This cell model expresses the DAT and DA receptors and is able to form storage vesicles, although the low activity of the VMAT2 impairs DA storage into vesicles (Mena et al., 1989). For this reason, SH-SY5Y cytoplasmic DA concentration may be increased by administering DA in the culture medium (Alberio et al., 2010).

Proteomics of Parkinson's disease

Pathogenesis of PD is still under investigation, due to its complexity in terms of current knowledge of genetic risk factors and the occurrence of several clinical phenotypes. Thus, cellular models, animal models, and post-mortem specimens from human subjects provide complementary resources. Among cellular models, the human neuroblastoma cell line SH-SY5Y has been widely used to recapitulate early stages of PD pathogenesis and to investigate mitochondrial dynamics in PD. Isolated mitochondria from SH-SY5Y exposed to a DA concentration able to induce oxidative stress were analysed by two different quantitative proteomics approaches (2-DE and shotgun proteomics).

Network analysis (IntAct) of results suggested a possible alteration of the NF-κB signalling pathway, and the hypothesis was further confirmed by the luciferase gene reporter assay (Alberio et al., 2010). Pathway analysis of mitochondrial proteins affected by DA revealed the over-representation of the Parkinson Disease and the Parkin– ubiquitin proteasomal system pathways and of gene ontologies associated with the generation of precursor metabolites and energy, unfolded protein response and programmed cell death. These alterations have been interpreted in part as the result of a direct effect of DA on mitochondria (*e.g.,* alteration of mitochondrial proteases activity) and in part as the effect of the activation of cellular processes on mitochondria (*e.g.,* regulation of programmed cell death) (Alberio et al., 2014). Moreover, high-resolution proteomic characterization of human SN from PD donors led to the identification of several differentially expressed proteins. The ORA of over-expressed proteins displayed the enrichment of cytoskeletal remodelling. On the other hand, an ORA of under-expressed proteins highlighted several pathways associated to energy metabolism and mitochondrial activities, intracellular transport processes, synaptic activities or translation (Licker et al., 2014).

Amyotrophic lateral sclerosis

ALS is an adult-onset, fatal, neurodegenerative disease, affecting motor neurons of the primary motor cortex, the central trunk and the spinal cord. The typical symptoms of this disease include muscle weakening, with gradual and irreversible loss of voluntary movements control, dysphagia (inability to swallow) and dysarthria (problems with word articulation) (Kiernan et al., 2011). These symptoms are due to the involvement of upper and lower motor neurons (Saccon et al, 2013).

The worldwide annual incidence of ALS is about 1.9 per 100,000, with a relatively similar rate in Caucasian populations and lower rates in African, Asian and Hispanic populations (Arthur et al., 2016). Men have a greater risk of developing ALS than women (Ingre et al., 2015). The death occurs typically after 2-4 years from the pathology onset, due to the impairment in respiratory muscles. Only 5–10% of patients survive beyond 10 years (Chiò et al., 2009).

Two different forms of ALS have been described: sporadic ALS, with an age at onset from 58 and 63 years (Logroscino et al., 2010), and familial ALS, characterized by an earlier onset, approximately around 40 to 55 years (Ingre et al, 2015). About 10-15% of patients have a family history of ALS (Byrne et al., 2011).

The inheritance patterns of ALS vary depending on the mutation, although there is often a Mendelian pattern and high penetrance in familial ALS. The two major genetic contributors known to date are

the Cu,Zn-superoxide dismutase-1 (SOD1) gene and the C9ORF72 gene, even if many other genes have been associated to ALS so far, *e.g.*, TARDBP (encoding for TAR DNA-binding protein 43), FUS (encoding for RNA-binding protein FUS), ANG (encoding for Angiogenin), OPTN (codifying for Optineurin), SETX (encoding for Senatassin) and VAPB (encoding for vesicle associated membrane protein B) (Andersen and Al-Chalabi, 2011; Turner et al., 2013) (Table 1.4).

Table 1.4: Some of the most common ALS-related genes.

Gene	Protein function
SOD1 (ALS1)	destroys radicals which are normally produced within cells.
C9ORF72 (FTDALS1)	is a negative regulator of autophagy initiation, of mTORC1 signalling and endosomal trafficking.
TARDBP (ALS10)	is a regulator of transcription and splicing. It is involved in neuronal plasticity and maintenance of dendritic integrity.
FUS (ALS6)	is involved in neuronal plasticity and maintenance of dendritic integrity, by transporting messenger RNA to dendritic spines for local translation.
ANG (ALS9)	hydrolyses cellular tRNAs, resulting in decreased protein synthesis.
OPTN (ALS12)	interacts with adenovirus E3-14.7K protein and may use tumor necrosis factor-alpha or Fas-ligand pathways to mediate apoptosis, inflammation or vasoconstriction. It is involved in cellular morphogenesis and membrane trafficking, vesicle trafficking, and transcription activation through its interactions with the RAB8, huntingtin, and transcription factor IIIA proteins.
SETX (ALS4)	is involved in both DNA and RNA processing.
VAPB (ALS8)	is a type IV membrane protein, found in plasma and intracellular vesicle membranes. It interacts with VAPA, VAMP1 and VAMP2 and may be involved in vesicle trafficking.
VCP (ALS14)	plays a role in protein degradation, intracellular membrane fusion, DNA repair and replication, regulation of the cell cycle, and activation of the NF-kappa B pathway.
CHMP2B (ALS17)	is a component of the Endosomal Sorting Complex Required for Transport II that functions in the recycling or degradation of cell surface receptors.

Investigations of ALS genes have delineated pathogenic roles for recurring themes. First, the motor neuron death usually entails deposition of aggregated proteins, often ubiquitinated and predominantly cytoplasmic. Second, in ALS, the levels and functions of RNA and RNA-binding proteins are abnormal. Aggregates of protein and RNA are detected both in motor neurons and non-neuronal cells, such as astrocytes and microglia. Third, most cases entail some disturbance of neuronal cytoskeletal architecture and function. Additionally, in almost all cases, motor neuron death is influenced by non-neuronal cells and cells involved in neuroinflammation. A defining feature of motor

neurons is the length of their axons, rendering them highly dependent on intracellular transport mechanisms to maintain normal structure and function. Critical in sustaining this extraordinary architecture is the cytoskeleton and associated molecular scaffolds and motors. Moreover, several processes have been postulated to have a role in ALS pathogenesis, such as, increased nitrative stress, intracellular calcium dysregulation and glutamatergic dysfunction. Glutamate-mediated excitotoxicity is characterized by an over activation of post synaptic receptors (NMDA ionotropic and AMPA receptors) by glutamate, which is the main excitatory neurotransmitter of the central nervous system. The toxic action of glutamate may rise from the permanence of this neurotransmitter in the inter synaptic space, because of a reduction in the expression of glutamate transporters by glial cells (Staats and VanDen Bosch, 2009). Glutamic excitotoxicity can lead to neurodegeneration through the activation of calcium dependent enzymatic pathways, ROS generation and an increase of pro-inflammatory mediators (Hensley et al., 2006).

The discovery of the glutamatergic alteration was the major turning point in the development of the pharmacotherapeutic approach to ALS leading to the introduction of riluzole, a benzothiazole derivative. It inhibits the glutamatergic transmission, either at a presynaptic or post synaptic level, through modulation of the ionotropic glutamate receptors (Cheah et al., 2010) and it can protect neurons, increasing the patients' survival.

ALS diagnosis is based on specific criteria known as El Escorial criteria (Agosta et al., 2015). These criteria are: 1) signs of degeneration of lower motor neurons, which are in the spinal cord and brainstem, by clinical examination or specialized testing; 2) signs of degeneration of upper motor neurons, which are in the brain, by clinical examination; 3) progressive spread of signs within a region to other regions; and 4) the absence of evidence of other disease processes that might explain the observed clinical and electrophysiological signs. If ALS is suspected, the next step is usually an electromyogram (EMG), to highlight signs of suffering of the second motor neuron in the muscles of arms and legs. Additional tests may include Nuclear Magnetic Resonance (NMR), to exclude other brain and spinal cord diseases, and the lumbar puncture, to exclude other neurological illnesses. Finally, to clarify the diagnosis in atypical cases, the muscle and nerve biopsy is adopted.

To recognize the different stages of ALS, several staging scales are utilized: Revised ALS Functional Rating Scale (ALSFRS-R), King's clinical staging and Milano-Torino (MiToS) functional staging (Chiò et al., 2012; Roche et al., 2012). The most commonly used is the ALSFRS, which is a validated questionnaire-based scale. Patient scores (from 4, normal situation, to 0, complete loss of function) are assigned to various tasks (speech, salivation, swallowing, handwriting, cutting food and handling utensils, dressing and hygiene, turning in bed and adjusting bed clothes, walking, climbing stairs,

dyspnoea, orthopnoea and respiratory insufficiency). By using these data, clinicians can evaluate four domains: gross motor tasks, fine motor tasks, bulbar functions and respiratory function.

Proteomics of amyotrophic lateral sclerosis

Deep proteomics characterization and ORA were employed to assess the suitability of several cell lines and primary motor neuron cultures as cell models for ALS, by identifying cellular pathways functionally relevant in motor neurons (Hornburg et al., 2014). Comparative proteomics profiling of cerebrospinal fluid (CSF) from sporadic ALS, healthy control and other neurological disease subjects led to the relative quantification of 1712 CSF proteins. The ORA of proteins up-regulated highlighted the activation of the "acute inflammatory response" and the "regulation of inflammatory response" in sporadic ALS CSF samples, whereas over-expressed proteins were involved in the "synapse organization" and the "extracellular matrix organization" (Collins et al., 2015).

Amyotrophic lateral sclerosis patients with parkinsonian signs

Several evidences support the existence of common pathogenetic mechanisms at the basis of different neurodegenerative disorders. Thus, it is not surprising that the progression of a neurodegenerative disease can lead to the manifestation of other brain pathologies, caused by the same altered processes. This explain why the simultaneous occurrence of more than one neurodegenerative pathology (usually called comorbidity) in the same patient is a quite common phenomenon, especially with the worsening of the cardinal pathology. In some patients with ALS, extrapyramidal symptoms and signs, typical of PD, due to nigrostriatal dysfunction have been reported (ALS-PD patients) (Park et al., 2011; Belin et al., 2015). The association between ALS and parkinsonism, although rare, occurs more frequently than expected by chance. Indeed, the frequency of PD symptoms in ALS patients is significantly higher than in the general population (Körner et al., 2013). Some authors reported that ALS is associated with parkinsonism with a frequency ranging from 5% to 17% (Manno et al., 2013). In addition, epidemiological studies showed a higher prevalence of parkinsonism in family members of ALS patients (Takahashi et al., 1993). The mean age at the onset of this overlapping syndrome is almost 10 years greater than in ALS without parkinsonism (Qureshi et al., 1996). The most common extrapyramidal signs are bradykinesia and rigidity; which usually respond poorly to the levodopa treatment. The clinical course does not differ from that expected in ALS without parkinsonism.

The association between ALS and PD, has been further highlighted by clinical (Belin et al., 2015), genetic (Körner et al., 2013) and neuroimaging (Cistaro et al., 2014) evidences, in humans and in

preclinical models (Ingre et al., 2015). Studies on ALS patients and on animal models of the disease have shown the presence of pathogenetic processes and clinical signs classically found in PD patients, such as intraneuronal inclusions (Desai and Swash, 1999), deficit in the axonal transport, neurotoxic effects due to the radical species (Johri and Beal, 2012) and endoplasmic reticulum (ER) stress (Monti et al., 2016). Insoluble aggregates of disease-related proteins can be deposited as intraneuronal inclusions, which are histopathological hallmarks of both diseases (Roy et al., 2005). Neuropathological evidence of neuronal loss, together with neurofilamentous and Lewy body inclusions in the basal ganglia, has been demonstrated in some ALS patients (Desai and Swash, 1999; Erol et al., 2015). Neuroimaging studies in ALS patients revealed a progressive reduction in the expression of the post-synaptic D2 receptor at the striatum level and a moderate reduction in the DA transporter (DAT) (Vogels et al., 2000). Imaging studies revealed a progressive dopaminergic deficit in ALS patients, even in the absence of extrapyramidal signs (Zoccolella et al., 2002). This suggests that the extrapyramidal system is involved in ALS, too (Park et al., 2011; Fathinia et al., 2012). Furthermore, necropsy studies have shown neuronal loss in the SN and *globus pallidus* of ALS patients (Yokota et al., 2006). In addition, in recent years, positron emission tomography (PET) and single photon emission computed tomography (SPECT) studies revealed a progressive midbrain dopaminergic deficit in ALS patients, even in the absence of extrapyramidal signs (Beal, 1998). Beside toxic proteins, there is overwhelming evidence of impaired mitochondrial dysfunction, axonal transport defects and neurotoxic effects of free radicals as a causative factor (Johri and Beal, 2012).

ALS patients with mutation on TARDBP gene (Seilhean et al., 2009) or with repetition of an esanucleotide of the C9ORF72 gene or patients carrying mutations in the ANG gene developed also PD symptoms (Chiò et al., 2012). In addition, genetic mutations involved in familial forms of PD, for example a missense mutation (E163K) in the PARK7 gene (encoding for DJ-1), has been found also in ALS patients, causing mitochondrial dysfunction and cognitive impairment (Annesi et al., 2005) (Table 1.5).

Table 1.5: Summary of the known ALS-PD related genes.

Gene	Clinical features
FUS (ALS)	Upper and lower motor neuron disorder, with a typical age at onset between 40 and 50 years. Bulbar signs, frontotemporal dementia and parkinsonism.
ANG (ALS)	Upper and lower motor neuron disorder, with a typical age at onset between 30 and 60 years. Bulbar signs and parkinsonism.
TARDBP (ALS)	Upper and lower motor neuron disorder, with a typical age at onset between 40 and 60 years. Bulbar signs, frontotemporal dementia and parkinsonism. Characterized by a good L-dopa responsiveness.
VCP (ALS)	Motor neuron disease, with a typical age at onset between 20 and 40 years. Characterized by myopathy, cardiomyopathy and peripheral neuropathy, but presenting also frontotemporal dementia, pyramidal signs and parkinsonism.
CHMP2B (ALS)	Upper and lower motor neuron disorder, with a typical age at onset between 40 and 60 years. Bulbar signs, respiratory insufficiency and parkinsonism.
C9ORF72 (FTDALS)	Motor neuron disease, with a typical age at onset between 50 and 60 years. Worsened by frontotemporal dementia, cognitive impairment and parkinsonism. Patients do not respond to L-dopa therapy. Routine brain MRI shows prominent frontal lobe atrophy.
SOD1 (ALS)	Upper and lower motor neuron disorder, resulting in fatal paralysis. Presence of ubiquitin-positive inclusions within surviving motor neurons and deposition of pathologic aggregates. Some patients show Parkinsonian traits.
PARK7 (PD)	PD characterized by resting tremor, postural tremor, bradykinesia, muscular rigidity, anxiety and psychotic episodes. Onset before 40 years, slow progression and initial good response to levodopa. Traits reminiscent of ALS-parkinsonism/dementia complex (Guam disease).
LRRK2 (PD)	PD characterized by bradykinesia, rigidity, resting tremor, postural instability, neuronal loss in the SN, and the presence of neurofibrillary MAPT (tau)-positive and Lewy bodies. Some patients show traits that recall ALS.
TRPM7 (ALS-PD dementia complex)	Neurodegenerative disorder characterized by signs and symptoms typical of both PD and ALS. Often associated with dementia.

These findings suggest that PD and ALS share common pathogenic mechanisms. Mitochondrial dysfunction, oxidative stress and neurotoxic effects of free radicals have been supposed to be involved in neuronal death of both diseases. In addition, other pathogenic mechanisms have been proposed in

these disorders, including glutamatergic neuro-excitotoxicity, as well as apoptotic neuronal death (Tatton et al., 1997).

Biomarker discovery of neurodegenerative diseases

The study of central nervous system (CNS) diseases is hampered by the availability of biological models that can recapitulate the pathogenetic process. In neurodegenerative diseases, proteomics analysis of post-mortem tissues is strongly limited by (i) the scarce availability of autoptic specimens, (ii) the fluctuation of protein levels identified in autopsy samples, due to rapid post-mortem changes in the brain and (iii) the advanced stage of the disease normally affecting donors (Plum et al., 2015). More information comes from cellular or animal models of neurodegenerative disorders that can mimic a specific aetiology or a specific pathogenetic mechanism (Plum et al., 2015). Several proteomics studies reported so far in association with neurodegenerative diseases focused on biomarker discovery (Pal et al., 2014). A biomarker is a characteristic that can be objectively measured and evaluated as an indicator of normal biological processes, pathogenic processes, or pharmacological responses to a therapeutic intervention. Biomarkers may help the diagnosis, the correlation with the progression of the disease, the therapy assessment or evidence the susceptibility to a disease. Biomarkers present in body fluids (*e.g.*, saliva, blood) and PBMCs are ideal, because they can be measured by simple, non-invasive and non-expensive tests. CSF is considered the ideal source for identifying biomarkers in neurodegenerative diseases because there is no barrier between CSF and the brain. However, CSF is not as easily accessible as other body fluids, whose collection, unlike CSF, is considered almost non-invasive. This limits large-scale validation studies and thus the introduction into clinical practice. PBMCs are considered an appropriate cellular model for the search of peripheral markers both for diagnostic purposes and for a better understanding of neurodegenerative disorders, like PD and ALS (Nardo et al., 2011). Immune cells may mirror at the periphery dysfunctions occurring at the central level, in particular those due to a genetic background. For instance, mutations in the Parkin gene render PBMCs more susceptible to DA and iron-mediated apoptosis (Fasano et al., 2008). Moreover, the dogma of the immune privilege of CNS has been challenged, based on following observations: i) immune system patrols the CNS through continuous migration of leukocytes, ii) the immune system, through T-Lymphocyte-sustained autoimmune mechanisms, may promote neuroprotective response, iii) the adaptive immune system affects cognitive performances and behaviour and iv) immune system may contribute to neuronal damage, as suggested by the demonstration of chronic neuroinflammatory process in the brain of PD patients (Fasano et al, 2008).

Mitochondria

Mitochondria are double membranes-enclosed cytoplasmic organelles, whose dysfunction is commonly associated to neurodegenerative disorders. The structure of mitochondria can be divided in four components: outer mitochondrial membrane (OMM), intermembrane space (IMS), inner mitochondrial membrane (IMM) and mitochondrial matrix. The inner membrane is highly folded, forming tubular or lamellar structures called cristae, where the complexes of the respiratory chain are embedded. Mitochondria are intimately involved in cellular homeostasis. Indeed, they provide energy in form of ATP to the cell, play a key role in the biosynthesis of several macromolecules (such as nucleotides, lipids, heme, and iron-sulfur clusters) and regulate the intracellular Ca^{2+} homeostasis (Vakifahmetoglu-Norberg et al., 2017). As mitochondria are essential for a plethora of cellular processes, the regulation and the maintenance of mitochondrial function are very important for the cell.

Mitochondrial dynamics

Mitochondria are very dynamic organelles that forms complex networks. The mitochondrial network changes continuously in response to the activation of a specific signalling pathway or the presence of a particular metabolic stimulus. Fusion and fission are involved in the mitochondrial network dynamics.

Mitochondrial fusion allows for the exchange of components between mitochondria, thus enabling the maintenance of their functional state (Chen and Chan, 2006). This process is made possible by three different proteins, Mitofusin 1 (MFN1), Mitofusin 2 (MFN2) and Dynamin-like 120 kDa protein (OPA1) (Figure 1.5). MFN1 and MFN2 are integral OMM proteins with GTPase activity that are responsible for the fusion of the OMM (Dimmer and Scorrano, 2006). The first step of fusion is mediated by the formation of homotypic (MFN1-MFN1 or MFN2-MFN2) or heterotypic (MFN1-MFN2) complexes (Koshiba et al., 2004). The turnover of MFN1 and MFN2 proteins depends on the recruitment of the AAA-ATPase p97 that permits the degradation of the ubiquitinated MFNs through the proteasome (Pallanck, 2010). It has been demonstrated that deletion of MFN1 or MFN2 causes mitochondrial fragmentation and poor mitochondrial function (Perier and Vila, 2012). OPA1 is an integral GTPase protein that is responsible for the fusion of the IMM (Chan, 2006). This protein is imported in the IMS, where it is processed by several proteases, such as PARL, YME1L and OMA1 (MacVicar and Langer, 2016), thus leading to the formation of both long (L-OPA1) and short (S-OPA1) protein forms. In physiological conditions, a correct balance between L-OPA1 and S-OPA1

is maintained to preserve the mitochondrial network morphology (Song et al, 2009). However, mitochondrial depolarization causes the activation of OMA1 protease, which determines the accumulation of the S-OPA1 (Head et al., 2009). This process leads to the inhibition of the IMMs fusion, thus causing mitochondrial fragmentation (Song et al, 2009). OPA1 is also involved in the protection against apoptotic cell death. Indeed, this protein plays a key role in the maintenance of cristae structure and junctions, thus preventing the release of cytochrome c from mitochondria (Ramonet et al., 2013). Moreover, OPA1 knock down leads to Bax translocation, release of cytochrome c and caspase activation (Olichon et al., 2003).

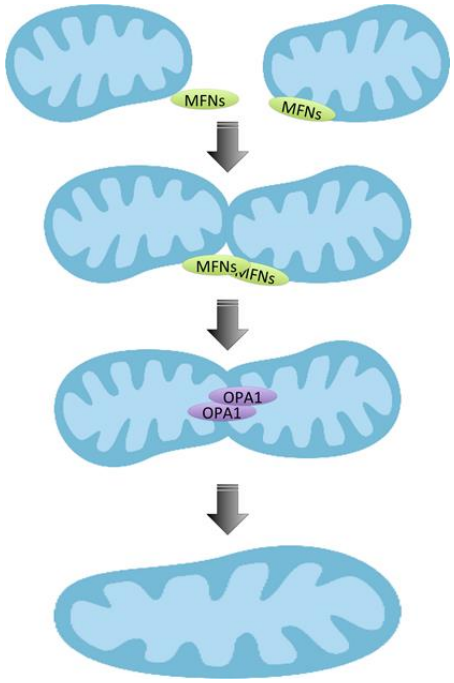

Figure 1.5: Both MFN1 and MFN2 are responsible for the fusion of the OMM, while OPA1 plays a key role in the fusion of the IMM.

Mitochondrial fission is important to allow the proper cellular distribution of these organelles and the degradation of damaged mitochondria through mitophagy (Otera and Mihara, 2011). This process is made possible by the GTPase activity of the cytosolic protein dynamin-1-like protein (DRP1). Indeed, once this GTPase protein localises on mitochondria, DRP1 oligomerizes into ring-like structures and constricts mitochondria thanks to GTP hydrolysis (Ingerman et al., 2005). The recruitment of DRP1 to the OMM depends on specific post-translational modifications. For example, fission is triggered when calcineurin dephosporilates DRP1 protein, while is prevented when PKA phosphorylates the conserved residue Ser-637 of DRP1. The recruitment of DRP1 on the OMM requires also the presence of specific mitochondrial receptors (Parone et al., 2008). The most characterized receptor

that interacts with DRP1 is Mitochondrial fission 1 protein (FIS1) (Karren et al., 2005) (Figure 1.6). There are also other mitochondrial membrane proteins that interact with DRP1, thus contributing to the fission process. For example, MFF proteins can recruit DRP1 independently for Fis1 and its overexpression determines mitochondrial fragmentation (Otera et al., 2010). Eventually, MiD49 and MiD51 are involved in the fission process through their capacity to recruit DRP1 on the OMM (Palmer et al., 2011).

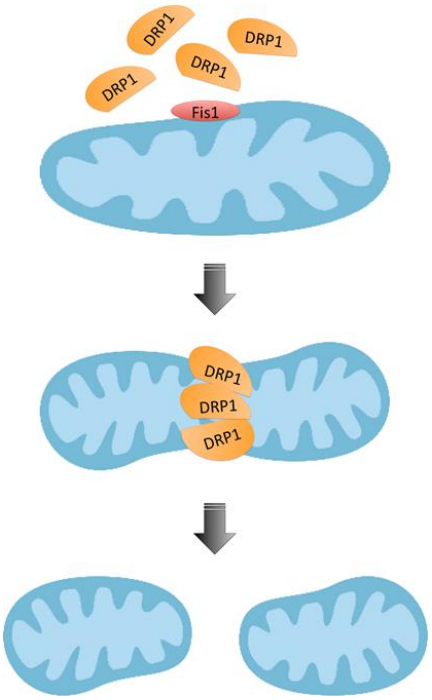

Figure 1.6: FIS1 is a mitochondrial membrane receptor involved in the recruitment of DRP1 protein. Once DRP1 localizes and oligomerizes on the OMM, it constricts mitochondria thanks to the hydrolysis of GTP molecules.

Mitophagy is an important quality control process that allows for the recognition and the consequent lysosomal degradation of damaged mitochondria (Youle and Narendra, 2011). The missed mitochondrial disposal causes the accumulation of dysfunctional mitochondria (Egan et al., 2011) that can lead to cell death. The most characterized mitophagy mechanism is the PINK1/Parkin pathway. Under basal conditions, the precursor of PINK1 is synthesized in the cytosol and imported into the OMM via translocase of outer mitochondrial membrane complex (TOM). Full-length PINK1 is further transferred into the IMM through the translocase of inner mitochondrial membrane (TIM) complex in a membrane potential dependent manner. Here, PINK1 is processed by the mitochondrial processing peptidase (MPP), that cleaves the MTS sequence, resulting in a ~60-kDa PINK1 form. This MPP-cleaved form of PINK1, which spans the IMM, is then further cleaved by the rhomboid protease of the IMM, presenilin associated rhomboid-like protease (PARL), to give rise to the 52-kDa

mature form. PINK1 is then degraded through the proteasome. This pathway keeps endogenous PINK1 levels very low in polarized mitochondria to prevent mitophagy of healthy mitochondria (Eiyama and Okamoto, 2015) (Figure 1.7).

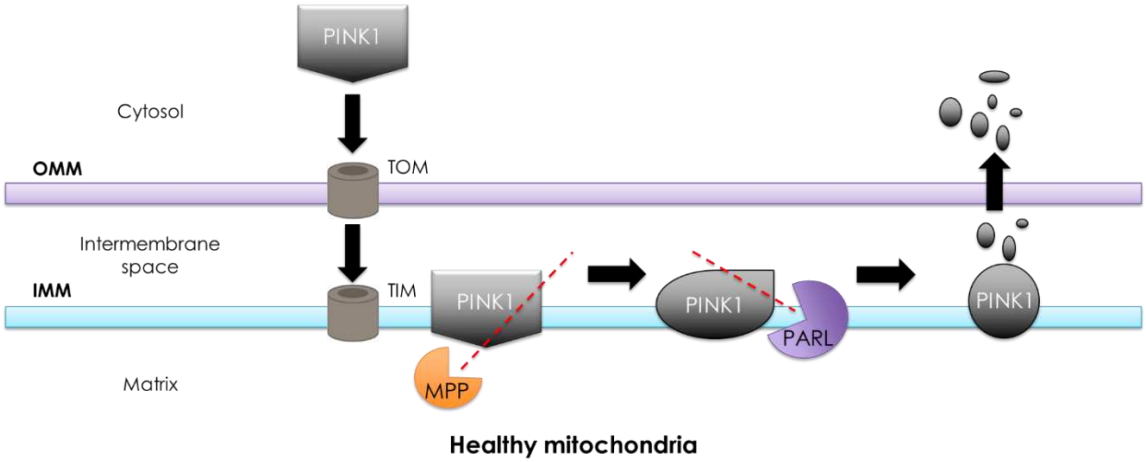

Figure 1.7: In healthy mitochondria, the precursor of PINK1 (64 kDa) is imported into the OMM via TOM and further transferred into IMM through TIM complex in a membrane potential dependent manner. Here, 64-kDa PINK1 is processed by the MPP. This form of PINK1 is then cleaved by PARL, to give rise to the 52-kDa mature form, and subsequently degraded by mitochondrial peptidases and by the proteasome.

On the contrary, the import of PINK1 and its proteasomal degradation are inhibited, when mitochondria are damaged and lose their membrane potential (*e.g.,* after treatment with protonophors as Carbonyl cyanide m-chlorophenyl hydrazine (CCCP)). The inhibition of PINK1 degradation causes the accumulation of this protein onto the OMM. This process leads to the mitochondrial recruitment of the E3-ubiquitin ligase Parkin, which catalyses the covalent attachment of ubiquitin moieties onto specific mitochondrial proteins (*e.g.* MFNs, VDACs, Miro and TOMM70) (Pickrell and Youle, 2015) (Figure 1.8). The recruitment of Parkin to mitochondria depends on the phosphorylation and consequent activation of this protein by PINK1 (Ordureau et al., 2014), on VDAC proteins (Sun et al., 2012) and on MFN2 (Chen and Dorn, 2013). Once the OMM proteins are ubiquitylated, several autophagy receptors are recruited to damaged mitochondria, to bind the ubiquitin-tagged OMM proteins (Figure 1.8). The impairment of PINK1/Parkin mitophagy axis could lead to the accumulation of dysfunctional mitochondria that may contribute to dopaminergic cell death, due to the increased production of ROS and the enhanced release of mitochondrial apoptogenic factors (Fernández-Moriano et al., 2015).

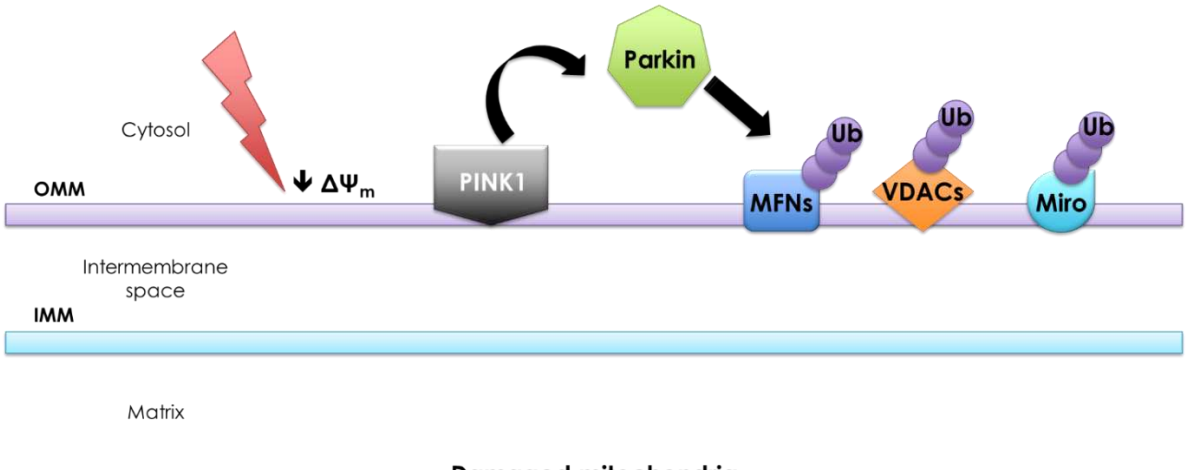

Figure 1.8: In depolarized mitochondria, PINK1 accumulates onto the OMM, thus recruiting Parkin. Parkin catalyzes the covalent attachment of ubiquitin moieties onto specific mitochondrial proteins. This process leads to the selective engulfment of damaged organelles by the autophagosome.

Mitochondrial proteome

The majority of mitochondrial proteins are encoded by nuclear genes, synthesized in the cytosol and eventually imported to the appropriate mitochondrial sub-compartment through several multimeric translocation machines (*e.g.* TOM and TIM) (Kang et al., 2017). The mitochondrial DNA (mt-DNA) has 37 genes that encode subunits of the respiratory chain, tRNAs and rRNAs (Scarpulla et al., 2012). Several human diseases are associated with mutations of mitochondrial proteins encoded by mitochondrial genome, or by nuclear chromosomes, or mutation in proteins that, interacting with mitochondria, regulate mitochondrial homeostasis (Gorman et al., 2015; Su et al., 2018). Therefore, the study of the mitochondrial proteome associated with specific physiological or pathological conditions increased. Indeed, the detection of the molecular landscape underlying mitochondrial dysfunction could represent new opportunities to investigate the pathogenesis of several diseases (Picard et al., 2016). The Human Proteome Organization (HUPO) has promoted in recent years the mitochondrial human proteome project (mt-HPP), whose main goal is to understand the function of the mitochondrial proteome and its crosstalk with the proteome of other organelles. By combining proteomics and computational biology, it would be possible to systematically consider mitochondrial proteins encoded by the mt-DNA, by nuclear DNA and protein imported into mitochondria or simply associated to them (Monti et al., 2018). The simultaneous consideration of all mitochondrial proteins and their first interactors led to the generation of the functional mitochondrial human proteome network (Fasano et al., 2016) that can be used to map proteins derived from proteomics studies. In particular, the mapping of proteome alterations related to diseases where mitochondrial dysfunctions are involved (*e.g.,* PD) may evidence the driver mitochondrial molecular factors and pathways.

1.2

Scope of the thesis

AD, PD and ALS are complex neurodegenerative disorders, whose aetiology and pathogenesis have not completely characterized. Many biochemical, environmental and genetic mechanisms have been proposed to play a role in the neuronal damage and loss in both diseases. Moreover, PD and ALS share common pathogenetic mechanisms. Indeed, the frequency of extrapyramidal symptoms in ALS patients is significantly higher than in the general population. Due to the complexity of these diseases, a systems biology approach would be appropriate to dissect their pathogenesis. By combining bioinformatics tools and proteomics analysis, it would be possible to highlight biochemical processes shared by neurodegenerative diseases and disease-specific pathways, which may justify the degeneration of different neuron populations. Finally, a focus on the mitochondrial interactome and proteome may elucidate important steps of PD degenerative process.

To this purpose, in the first project (**Meta-Neuro project**, Meta-analysis of Neurodegenerative diseases) developed in the present thesis, a meta-analysis of the literature of all the proteomic investigations of neuronal alterations in PD, ALS and AD as control (non-motor neurodegenerative disease) was performed. The main objective was to obtain a comprehensive snapshot of molecular factors involved in PD by the analysis of proteomics and genetics data. Moreover, with the aid of the over-representation analysis, we wanted to highlight biochemical pathways specifically involved in PD pathogenetic process. Eventually, protein networks were generated, based on physical or functional interactions, in order to identify cellular components and macro-complexes involved in PD pathogenesis only.

To further develop the results obtained by the first project, we decided to characterize differences in the PBMCs proteome of patients with ALS, PD and ALS patients with parkinsonian signs (ALS-PD) (**ProLyPALS project**, Proteomics of Lymphocytes in Parkinson's disease and Amyotrophic Lateral Sclerosis). The main goals were the verification of the outcome of the Meta-Neuro project and the discovery of novel molecular factors specifically involved in one of the two pathologies. Indeed, the

characterization of ALS-PD patients may evidence proteins and pathways, which lead to the manifestation of both diseases. To this purpose, a 2-DE analysis of PBMCs samples was used to identify proteins that are specifically involved in PD or ALS, and proteins that are altered by both pathogenetic processes. To interpret these data and solve false positive and false negative issues, a systems biology approach was used to unravel the involvement of biochemical pathways responsible for the degeneration of different neuron populations.

Several molecular pathways implicated in PD aetiology converge on mitochondria. Mitochondrial dysfunction could affect neuronal survival. To focus on the main mitochondrial processes involved in PD, an updated version of the functional mitochondrial human proteome network was generated and used to map PD-specific proteins obtained by the meta-analysis (**MitoNet project,** Mitochondrial Network). All the high-quality information collected in the neXtProt database (the reference database for the HPP) were used to visualize the mitochondrial interactome. PD-specific proteins mapped on the network were used to identify pathways altered at the mitochondrial level.

The last project developed in this thesis (**DynaMoParD project**, Dynamic Model of Parkinson's Disease) is focused on the characterization of mitochondrial state and dynamics in cellular models of mitochondrial impairment in PD. To this purpose, SH-SY5Y human neuroblastoma cells treated with several mitochondrial toxins (*i.e.,* DA, rotenone or MPP^+) at different time points were used to retrieve data about key molecular factors involved in mitochondrial dynamics, with the final goal of generating a dynamic mathematical model of the "PD mitochondrion". Altered DA homeostasis seems to be an important cellular pathogenetic mechanism involved in neurodegeneration in PD. In this context, it is possible to use the SH-SY5Y neuroblastoma cell line to mimic the improper handling of this neurotransmitter by the administration of exogenous DA in the culture medium. Moreover, rotenone and MPP^+ are commonly used toxins in PD research due to their ability to induce parkinsonism through the inhibition of complex I. As a reference model of mitophagy induction, the treatment with the uncoupler CCCP was used in all experimental designs as a positive control.

.

PART II

Meta-Neuro

Meta-analysis of Neurodegenerative diseases

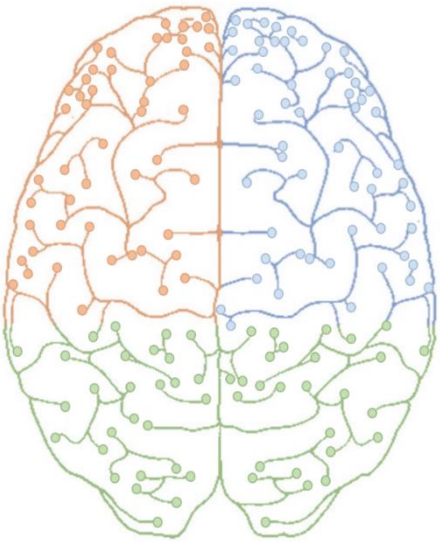

2.1

Materials and Methods

Input lists generation

A meta-analysis of the literature was performed and all quantitative proteomic studies of neuronal alterations in PD, ALS, and AD were retrieved. The search was conducted in PubMed database (https://www.ncbi.nlm.nih.gov/pubmed/), using the following query: "proteom* [Title/Abstract] AND Parkinson* [Title/Abstract]), ("proteom* [Title/Abstract] AND Amyotrophic lateral Sclerosis* [Title/Abstract]) ("proteom* [Title/Abstract] AND Alzheimer* [Title/Abstract]". We included all English language investigations found in the database and published within the end of 2015. All papers about therapies and biomarkers in peripheral fluids (such as: saliva, plasma, blood) were manually filtered out and only full-text original articles focused on the development of diseases in the CNS were considered. All protein IDs found to be differentially abundant in the disease state were retrieved manually and three input lists were generated ("PD_Proteins", "ALS_Proteins" and "AD_Proteins"). No further filtering of results was applied by our analysis. For proteins obtained from non-human organisms (such as *D. melanogaster* and *C. elegans*), their orthologs, as reported in the Uniprot database (www.uniprot.org), were considered for the further analysis. Furthermore, the proteins IDs were converted to the corresponding gene symbol, as annotated in Uniprot database.

Genetic information was taken from the curated DisGeNET database (http://disgenet.org, v4 released April 15th 2016) (Piñero et al., 2015), using the following search terms: PD (umls:C0030567), ALS (umls:C0002736), and AD (umls:C0002395). All genes involved in the three diseases were retrieved and three input lists generated ("PD_Genes", "ALS_Genes" and "AD_Genes").

Bioinformatics analysis

Venn diagram (http://bioinformatics.psb.ugent.be/webtools/Venn/) was used to compare the protein input lists ("PD_Proteins", "ALS_Proteins" and "AD_Proteins"). Therefore, proteins were divided into two groups, "disease-specific" proteins (only-PD_Proteins, only- ALS_Proteins, and only-AD_Proteins) and "in common among different diseases" proteins. To compare the protein and gene input lists, InteractiVenn (http://www.interactivenn.net/) (Heberle et al., 2015) was used and PD specific genes and proteins (PD_Proteins-Genes) were identified.

An ORA of "only-PD_Proteins" list and of "PD_Proteins", "ALS_Proteins" and "AD_Proteins" lists was performed using the "Analyze tool" in Reactome (http://www.reactome.org/) (Fabregat et al., 2018) and Panther in GO BP (http://www.geneontology.org/) (The GO Consortium, 2017) database. For both analyses only, categories with a p value <0.05 were considered as significant. In order to compare the results obtained after the analysis of the input lists, we used GOView (http://www.webgestalt.org/GOView/) (Wang et al., 2017). GOView is a web-based application, which allows users to compare and visualize multiple GO term lists in a directed acyclic graph (DAG), able to reveal relationships among the terms.

The web portal BioProfiling.de was used to build networks (http://www.bioprofiling.de) (Antonov 2011). This tool covers almost all the available information about signalling and metabolic pathways (databases: Reactome and KEGG) and physical PPI (database: IntAct). Accordingly, the protein input lists previously generated ("_Proteins") were analysed with the PPI spider tool (Antonov et al., 2009). The p value provided, computed by Monte Carlo simulation, refers to the probability to get a model of the same quality for a random gene list of the same size (Antonov 2011). The significant D1 networks (all nodes belong to the input list), $p < 0.01$, were considered to further interpret and discuss proteomics results. The direct interactor networks were exported as .xgmml files and edited using Cytoscape 3.2.0 (http://www.cytoscape.org/) (Shannon et al., 2003). Then, the three networks were merged to exclude nodes shared by different diseases and to identify "only-PD_Nodes", later extracted in a new interaction network. To perform network topology analysis of the enriched networks, we used the NetworkAnalyzer Cytoscape application. It performs analysis of biological networks providing distributions of more complex network parameters, including node degrees, average clustering coefficients, topological coefficients, and shortest path lengths. Several network topology parameters such as the diameter of a network, the average number of neighbours, and the number of connected pairs of nodes were also computed (Assenov et al., 2008). Again, the GO Consortium was used to perform the ORA (GO terms).

Western blot analysis of *Substantia Nigra* samples

Mesencephalic tissues from five sporadic PD patients and five age-matched controls (defined by the Brain Bank as non-demented, since they did not show any sign of dementia at the time of death) (Table 2.1) were obtained from the Netherlands Brain Bank (NBB), Netherlands Institute for Neuroscience, Amsterdam. A written consent for a brain autopsy was obtained from all donors. Eventually, clinical information for each subject was obtained from the NBB.

Table 2.1: Characteristics of PD patients and gender and age-related control subjects (CTRL).

NBB number	Sex	Age	Diagnosis
2007-013	M	61	PD
2009-003	M	62	CTRL
2007-029	M	67	PD
1999-116	M	78	CTRL
2006-062	M	87	PD
2009-001	M	88	CTRL
2009-045	F	59	PD
2001-004	F	64	CTRL
2009-078	F	88	PD
1999-111	F	88	CTRL

Notes: NBB: Netherlands Brain Bank; M: Male, F: Female; CTRL: control subjects, PD: Parkinson's disease

The tissue specimens (approximately 12 mg) were lysed in 500 µl of tissue lysis buffer (50 mM Tris-HCl pH 7.4, 150 mM NaCl, 1% Triton, 2 mM ethylenediaminetetraacetic acid (EDTA) 1 mM 1,4-dithiothreitol (DTT), 1x phosphatase inhibitors (Roche), 1× phenylmethylsulfonyl fluoride (PMSF), 1× protease inhibitor cocktails (PIC). The tissues were manually lysed using a Potter homogenizer and then incubated on ice for 30 minutes. The samples were sonicated on ice (0.5 cycles, 15 pulses, twice). After this procedure, the lysates were centrifuged at 18000×g for 15 minutes at 4°C in order to collect the supernatants in new tubes.

Total protein concentration was quantified using the bicinchoninic acid (BCA) method (Thermo Fisher Scientific). Equal amounts of proteins, previously incubated in Laemmli loading buffer, were resolved in 10% sodium dodecyl sulfate PAGE (SDS, TGX Stain-Free FastCast Acrylamide Kit, 10%, BioRad). The fluorescent stain was activated by UV light, following manufacturer's instructions.

Then, proteins were transferred to polyvinylidene difluoride (PVDF) membranes (Millipore) at 1.0 mA/cm^2, 1.5 hours (TE77pwr, Hoefer) and the fluorescent signal acquired (GelDoc-Ite Imaging System; UVP). Membranes were then saturated for 2 hours at room temperature (RT) in tris-buffered saline with 0.05% tween 20 (TBST) containing 5% skimmed milk powder. Eventually, blots were probed with antibodies against: TALDO1 (Abcam ab67467,1:500) and β-actin (GeneTex GTX23280,

1:8000) in 5% milk-TBST overnight at 4°C. Blots were incubated with anti-mouse (Millipore 12-349, 1:1500) peroxidase-conjugated secondary antibody in 5% milk-TBST. Enhanced chemiluminescence substrate (Millipore Corporation) was used in order to visualize the peroxidase signals. Images (16 bit grayscale) were acquired with the G:BOXChemi XT4 (Syngene) system and analysed using the ImageJ software (https://imagej.nih.gov/ij/) (Schneider et al., 2012), normalizing each TALDO1 signal for the β-actin signal.

2.2

Results

Protein lists generation

All the proteomics investigations of PD, AD and ALS disease models were collected performing a meta-analysis of the literature. The input lists were generated using all information about proteins altered by the three diseases extracted from full-texts of selected articles (Table 2.2). 762, 420 and 139 papers were identified in PubMed about proteomics investigations in AD, PD and ALS, respectively. The studies retained (healthy/disease comparisons and quantitative proteomics studies) were 40 for AD, 46 for PD and only nine for ALS (Supplementary Table 2.1). The three input lists generated were AD_Proteins (928 proteins), PD_Proteins (1155 proteins) and ALS_Proteins (387 proteins) (Table 2.2).

Table 2.2: Number of PubMed hits and selected articles obtained by the meta-analysis procedure and number of proteins in each input list.

	PubMed hits	**Healthy/disease comparisons and quantitative proteomic studies**	**_Proteins**
AD	762	40	928
PD	420	46	1155
ALS	139	9	387

Over-representation analysis of "_Protein" lists

In order to understand which cellular pathways were mainly affected by the three diseases examined, an ORA was performed on the "_Proteins" input lists using the GO BP enrichment tool of the GO consortium. Only significant categories (p value <0.05) were considered information (Tables 2.3). The "apoptotic process" served as an internal control, since alterations in the apoptotic pathway resulted to be present in all the three conditions (PD, AD, and ALS), as expected for neurodegenerative

disorders. Similarly, the ORA revealed the alteration of protein transport as a pathway involved in the three diseases ("protein targeting" and "regulation of protein transport"). On the other hand, disease-specific pathways were identified. Indeed, pathways converging on mitochondria ("mitophagy" and "mitochondria localization"), on the proteasome system ("proteolysis involved in cellular protein catabolic process") and on the production of oxidative stress ("response to oxygen radical") seemed to play a pivotal role in the pathogenesis of PD (Table 2.3). By contrast, cytoskeleton organization, ion homeostasis and lipid biosynthetic process resulted to be altered in AD, while aberrant RNA processing appeared to be mainly involved in ALS pathogenesis ("rRNA metabolic process", "ncRNA metabolic process" and "mRNA splicing via splicesome") (Table 2.3).

Table 2.3: Summary table of the most significant results of the GO Biological Processes analysis of "_Proteins" input lists, after GoView filtering.for the further analysis. Given the huge amount of results obtained, GOView was used to select and sum up the most relevant

<table>
<tr><th>AD_Proteins</th><th>PD_Proteins</th><th>ALS_Proteins</th></tr>
<tr><td colspan="3">Apoptotic process
Electron transport chain
Axon guidance
Intracellular protein transport
Protein targeting
Signalling pathway (Fc receptor, NIK/NF-kappaB)</td></tr>
<tr><td></td><td colspan="2">Cell cycle phase
Establishment of protein localization to endoplasmic reticulum
DNA damage response
Nuclear-transcribed mRNA catabolic process, nonsense-mediated decay</td></tr>
<tr><td colspan="2">Negative regulation of neuron apoptotic process
Establishment of synaptic vesicle localization
Mitochondrial membrane organization
Mitochondrial transport
Signalling pathway (ERBB, Fc epsilon, fibroblast growth factor receptor, insulin receptor, epidermal growth factor receptor)</td><td></td></tr>
<tr><td>G2/M transition of mitotic cell cycle</td><td></td><td>G2/M transition of mitotic cell cycle</td></tr>
<tr><td>Cellular potassium and sodium ion homeostasis
Microtubule cytoskeleton organization</td><td>Proteolysis involved in cellular protein catabolic process
Mitochondrion localization
Mitophagy
Signalling pathway (ephrin receptor, tumor necrosis factor, canonical Wnt)</td><td>rRNA metabolic process
ncRNA metabolic process
Nuclear transport
RNA transport</td></tr>
</table>

Physical interaction network

Starting from the protein input lists, direct interactor networks were generated (Supplementary Figure. 2.1). Then, the three networks were merged (Supplementary Figure 2.2) and "only-PD_Nodes" (129 nodes) were extracted in a new network shown in Figure 2.1. This network highlights the alteration

of proteins involved in the regulation of proteolysis (light blue nodes), a process mainly guided by the proteasome complex.

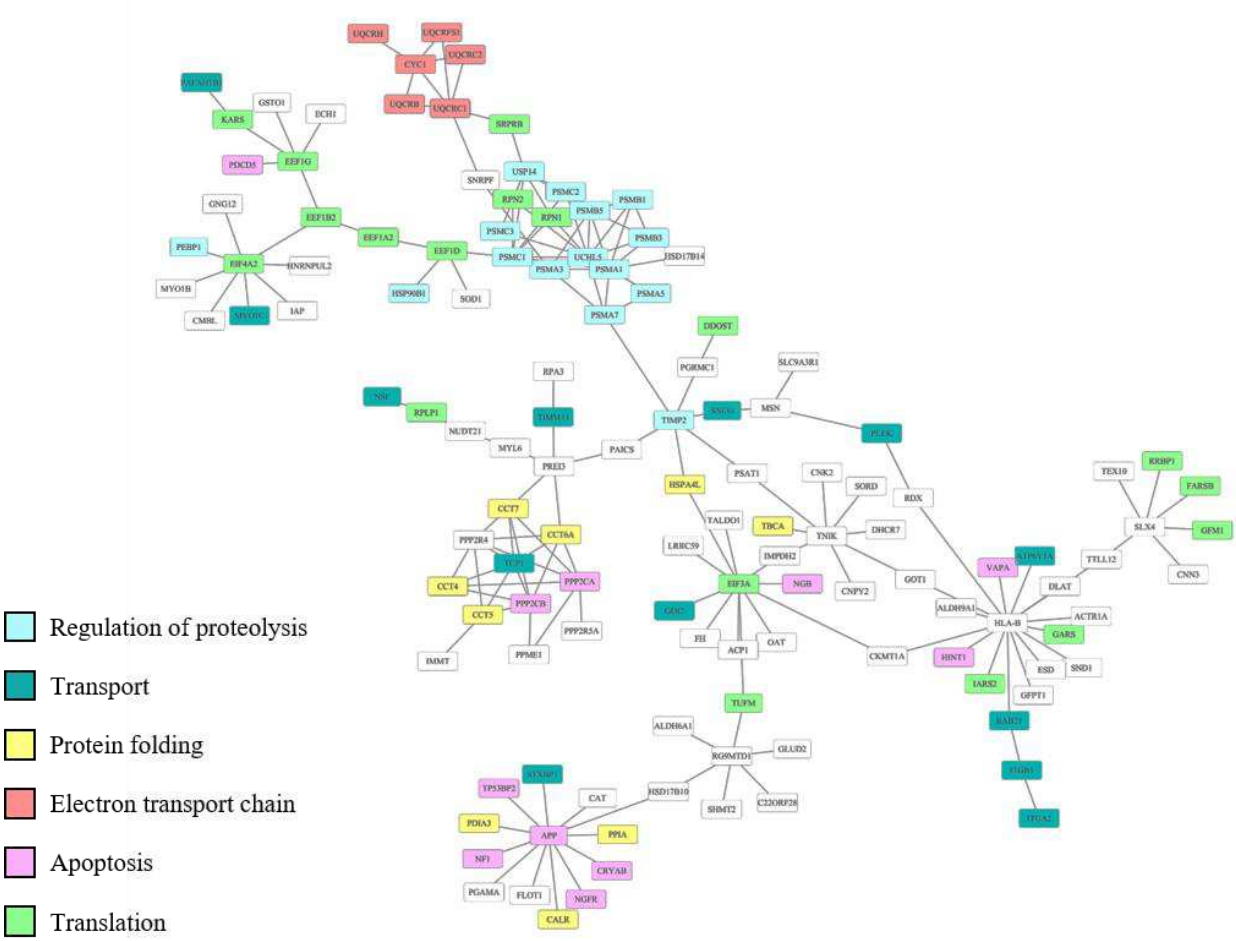

Figure 2.1: Significant networks built by PPI spider ($p < 0.01$), using IntAct database as the reference set. D1 model of only-PD_Nodes. Colours indicate gene functional roles according to the GO classification.

In order to investigate which cellular macro complexes were involved in PD, NetworkAnalyzer was used. The size of nodes was adjusted according to their degree: the bigger the node, the higher the number of edges (Figure 2.2). At the same time, to identify the cellular localization of the complexes, an ORA was performed using the category CC of the GO Consortium. Three complexes included in the network are highlighted in Figure 2.2: "respiratory chain complex", "proteasome complex" and "chaperonin containing T complex" (CCT complex) together with "protein phosphatase 2a complex" (PPP2A complex).

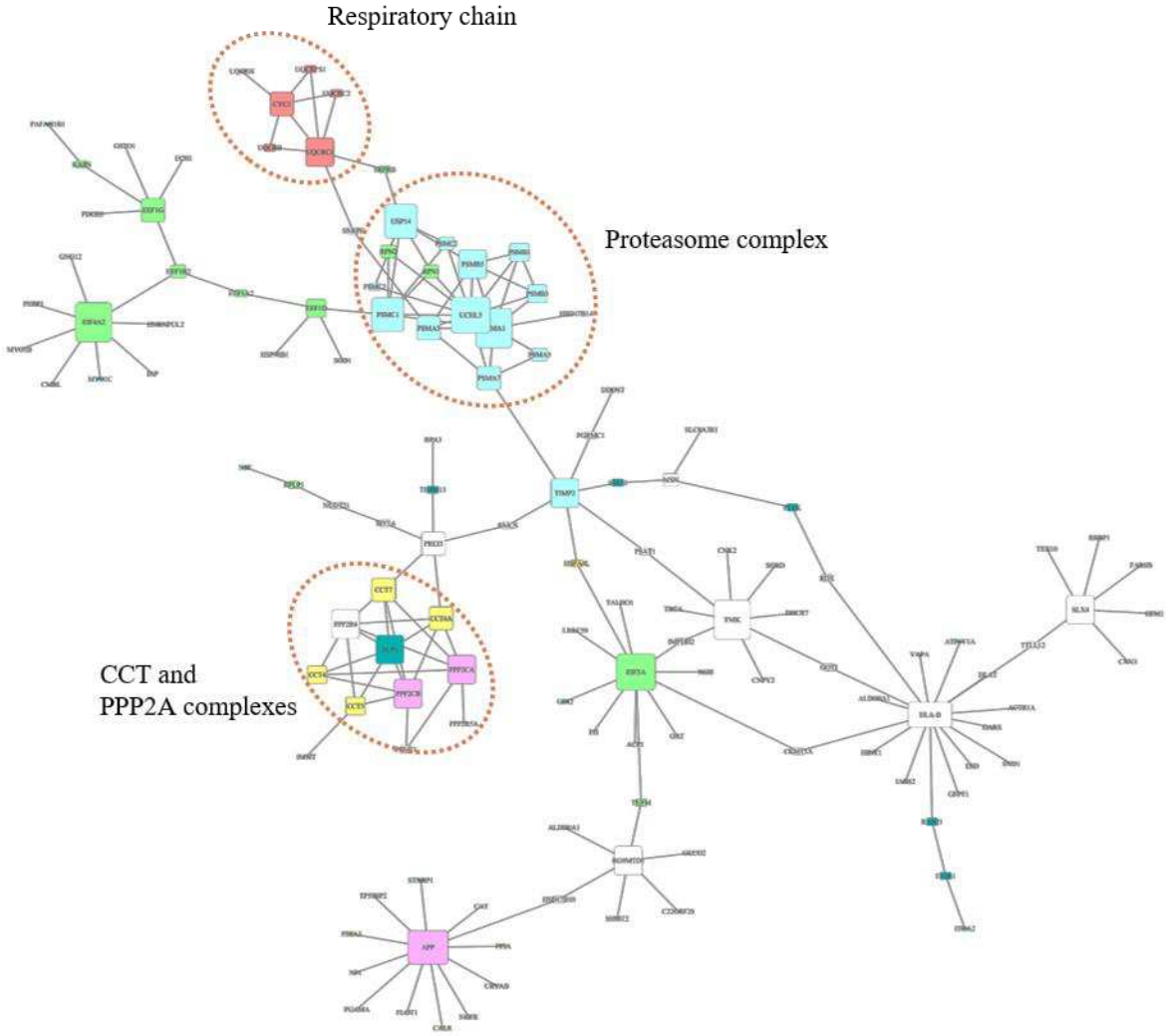

Figure 2.2: D1 model of only-PD_nodes after analysis with NetworkAnalyzer and ORA, using GO consortium CC.

Analysis of macro complexes

Eventually, to assess how complexes were involved in PD pathogenesis, they were separately analysed. Quantitative information on each protein were retrieved from original papers. Since it was impossible to compare papers using different scales and normalization methods, all quantitative data reported in the paper were used to categorize variations as up- or down-regulations. Proteins reported as consistently up-regulated in PD are the red nodes of the network, while down-regulated ones are green nodes. Yellow nodes represent contradictory results (different studies showed opposite variations) (Figure 2.3). Alterations in protein levels are reported in Supplementary Table 2.2. Figure 2.3A shows two closely related complexes, the chaperonins CCT complex and the phosphatases PPP2A complex. In the CCT complex, all the chaperonins were found to be down-regulated, except for CCT5. This protein is down-regulated when SNCA is over-expressed (Gui et al., 2012) as well as in MPTP-treated mice (Jin et al., 2005). Conversely, it is up-regulated in mouse neuroblastoma cell lines (Burté et al.,

2011) and in PINK1 knockout mice (Triplett et al., 2015). With reference to the respiratory chain (Figure 2.3B), the components were altered in different directions, depending on the disease model considered (three yellow nodes: UQCRH, CYC1, and UQCRC1). Furthermore, the components of the regulatory (19S) subunit of the proteasome complex (Figure 2.3C) were all down-regulated, while members of the catalytic (20S) subunit were all up-regulated.

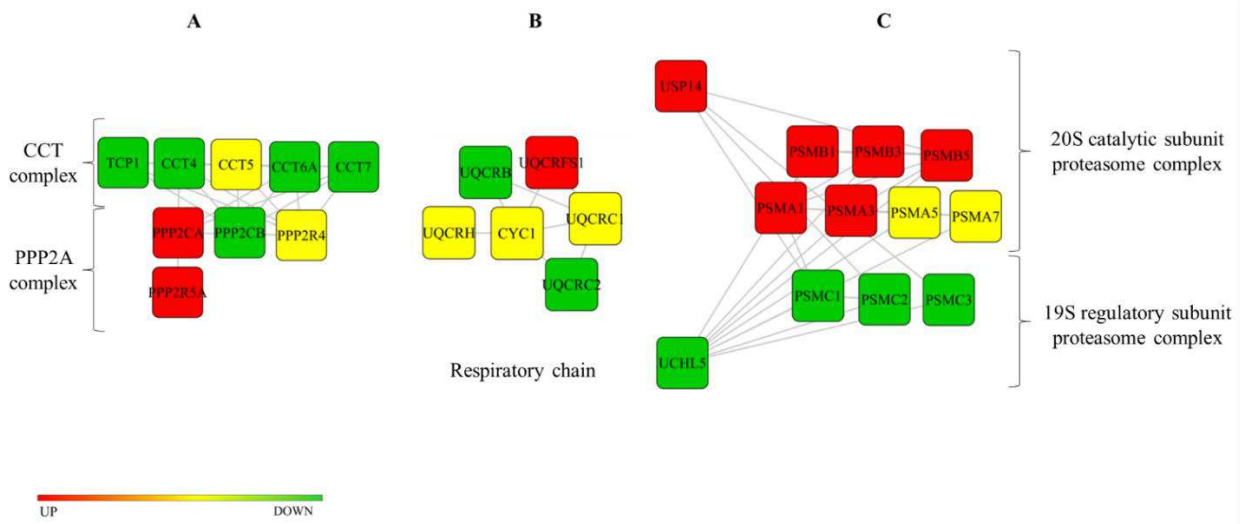

Figure 2.3: Protein complexes specifically involved in PD. Nodes are coloured based on their confidence of being up- (red) or down-regulated (green) in the disease state. Yellow nodes are proteins whose level is presented as down-regulated in some papers and up-regulated in others. (A) shows the chaperonins CCT complex and the phosphatases PPP2A complex, (B) shows the complex III of the respiratory chain and (C) represents the proteasome complex.

Parkinson's disease-specific biochemical pathways and gene ontologies

In order to identify proteins that were unique to a specific disease, the three "_Proteins" lists were analysed (Figure 2.4). 675 proteins resulted to be altered in PD only (only-PD_Proteins input list). On the other hand, PD and ALS shared 69 proteins, while AD and ALS showed only 29 proteins in common.

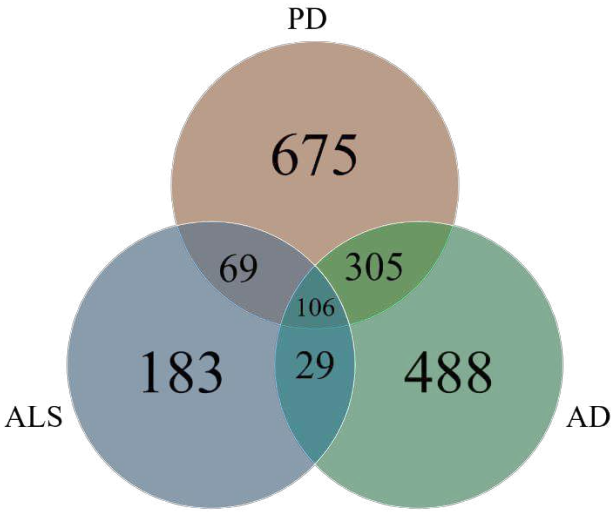

Figure 2.4: Venn diagram of the three input lists. Venn diagram showing the number of disease-specific proteins and proteins shared by more than one disease.

To identify the over-represented pathways when only PD-specific proteins were considered, an ORA of only-PD_Proteins input list (675 IDs) was performed. To this purpose, GO BP and Reactome were used as reference databases. Again, "mitophagy" and apoptotic process ("regulation of apoptosis") were found to be over-represented. Moreover, "translation" and "metabolism of amino acid and derivates" were significant ORA results (Table 2.4).

Table 2.4: Summary table of the most significant results of the GO Biological Processes and Reactome analysis of "only PD_Proteins" input list.

Go Consortium Biological Process	Reactome
Vesicle-mediated transport, Regulation of apoptotic process, Regulation of cell motility, Protein complex assembly, Signalling pathways (*e.g.* MAPK cascade, NIK/NF-kappaB signalling, Wnt signalling pathway), Regulation of protein catabolic process, Actin cytoskeleton organization, Modulation of synaptic transmission, Mitochondrion organization, Translation, Nuclear-transcribed mRNA catabolic process nonsense-mediated decay, SRP-dependent cotranslational protein targeting to membrane	Cellular response to heat stress, DNA replication, Laminin interactions, Nonsense-Mediated Decay (NMD), Mitophagy (PINK1/Parkin mediated Mitophagy), Metabolism of aminoacid and derivates, Translation, Regulation of apoptosis, Signalling pathway (*e.g.* MAPK family signalling cascade, signalling by Wnt, signalling by Hedgehog), Membrane trafficking

Identification of Parkinson's disease-specific proteins and genes

In order to identify both proteins and genes exclusively associated to PD, genetic information was extracted from the curated database DisGeNET, and three additional input lists called AD_Genes, PD_Genes, and ALS_Genes were obtained (Table 2.5).

Table 2.5: Numbers of IDs of "_Proteins" and "_Genes" input lists. "_Genes" input lists were obtained using DisGeNET as reference database.

	Input lists	
	"_Proteins"	**"_Genes"**
AD	928	1663
PD	1155	766
ALS	387	799

The "_Proteins" and the "_Genes" input lists were compared using the InteractiVenn tool (Figure 2.5).

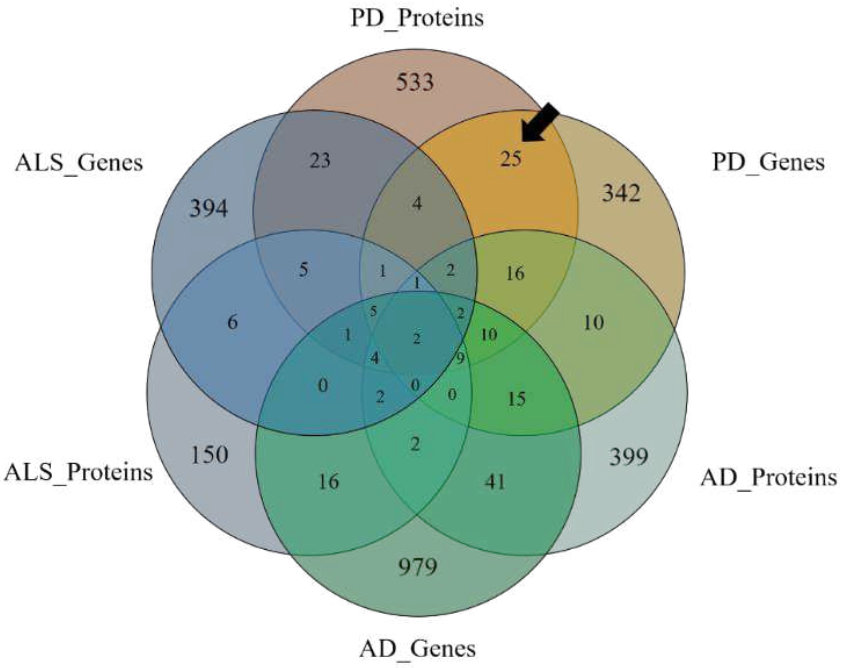

Figure 2.5: Venn diagram showing disease-specific genes and proteins and those shared by different diseases. The arrow shows the overlap between the PD_Proteins list and the PD_Genes list.

As a result, 25 IDs were present in both "PD_Proteins" and "PD_Genes" input lists and not present in any other protein or gene list (Table 2.6). Therefore, these IDs have been associated to PD both by genetics and proteomics analyses.

Table 2.6: Gene Symbol and description of 25 IDs that were present both in "PD_Proteins" and "PD_Genes" input lists.

Gene Symbol	Description
ALDH1A1	Retinal dehydrogenase 1
AP1M1	AP-1 complex subunit mu-1
B2M	Beta-2-microglobulin
CD200	OX-2 membrane glycoprotein
DDC	Aromatic-L-amino-acid decarboxylase
DLG2	Disks large homolog 2
FBN1	Fibrillin-1
FBP1	Fructose-1,6-bisphosphatase 1
GAD1	Glutamate decarboxylase 1
GCH1	GTP cyclohydrolase 1
GLUD2	Glutamate dehydrogenase 2, mitochondrial
HSPA1L	Heat shock 70 kDa protein 1-like
MANF	Mesencephalic astrocyte-derived neurotrophic factor
NOD2	Nucleotide-binding oligomerization domain-containing protein 2
NQO2	Ribosyldihydronicotinamide dehydrogenase [quinone]
PDXK	Pyridoxal kinase
RPL14	60S ribosomal protein L14
RPL23A	60S ribosomal protein L23a
RPL6	60S ribosomal protein L6
RPS8	40S ribosomal protein S8
SFXN2	Sideroflexin-2
SNRPF	Small nuclear ribonucleoprotein F
TALDO1	Transaldolase 1
UBE2S	Ubiquitin-conjugating enzyme E2 S
WFS1	Wolframin

Verification of Transaldolase 1 as a Parkinson's disease protein

As a proof of principle, one protein in the list of the 25 PD unique IDs was selected to verify its up-regulation in PD affected tissues, as suggested by the bioinformatic analysis.

Transaldolase 1 (TALDO1) abundance was checked in SN samples obtained from five sporadic PD patients and five matched control subjects (CTRL). Western blot analysis revealed that protein level of TALDO1 were higher in the affected tissue of sporadic PD patients, as reported in the literature (Alberio et al., 2012; Licker et al., 2014) (Figure 2.6).

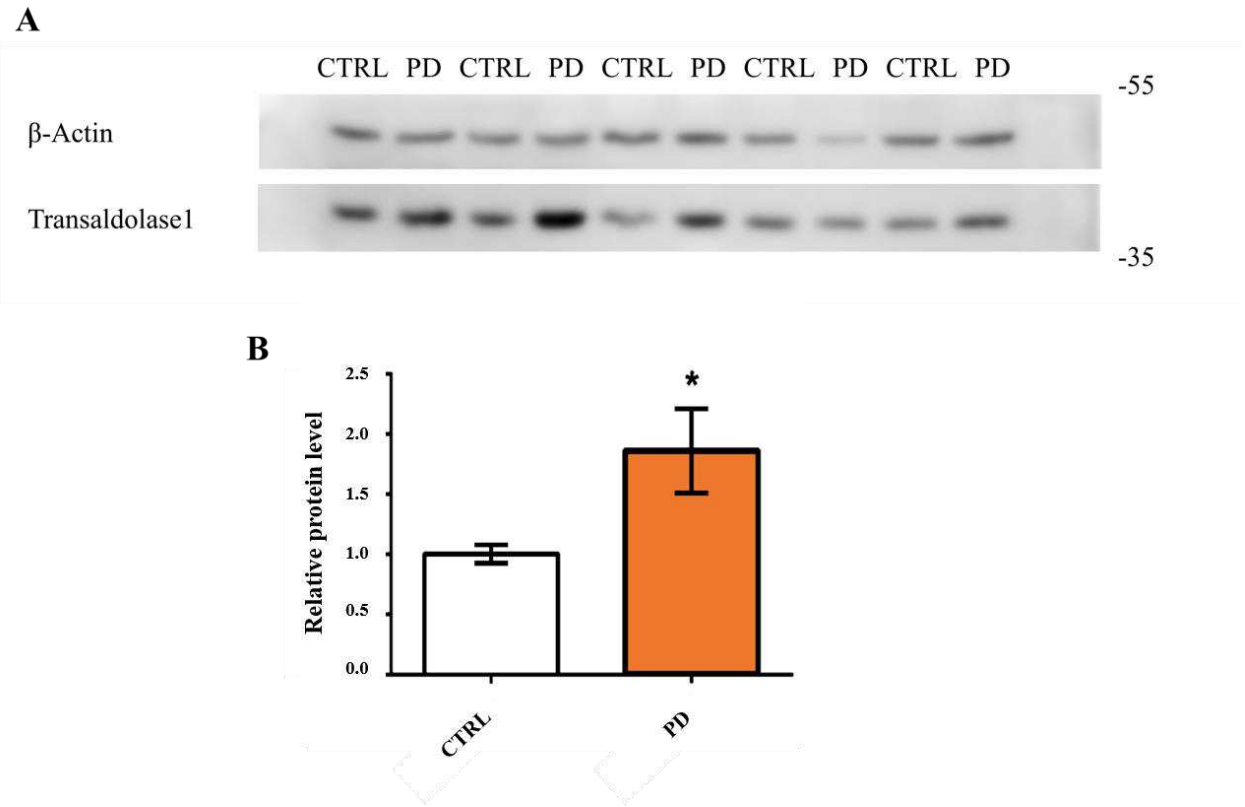

Figure 2.6: Western blot analysis of 10 SN samples (five PD patients and five control subjects (CTRL)). (A) A representative Western blot, showing Transaldolase 1 and β-Actin, used as a loading control. (B) Bars report the relative change of Transaldolase 1 signals (normalized to the related β-actin signal) in PD patients with respect to control subjects, arbitrarily set to 1. Values are the mean ± SEM of three technical replicates (*, $p < 0.05$).

PART III

ProLyPALS

Proteomics of Lymphocytes in Parkinson's disease and Amyotrophic Lateral Sclerosis

3.1

Materials and Methods

Study subjects

Sixty-nine subjects were enrolled by the Parkinson's Disease and Amyotrophic Lateral Sclerosis Centres at the Department of Neuroscience, University of Torino, and by the Neurology Division at the Department of Translational Medicine, University of Eastern Piedmont. Every subject was associated to an alphanumeric code to ensure that his/her identity was not disclosed to investigators.

Among the patients enrolled for the study, 20 subjects were newly diagnosed (de-novo) PD patients, while 49 were ALS patients. Among them, 20 subjects were de-novo ALS patients (ALS), 20 were ALS patients already under riluzole treatment (ALS_r) without parkinsonian signs, while nine patients were ALS patients with parkinsonian symptoms and signs (ALS-PD), usually under riluzole treatment. MDS-UPDRS was used for PD diagnosis, while ALS diagnosis was evaluated using the ALSFRS system (Table 3.1).

Table 3.1: Summary of the clinical information collected.

<table>
<tr><th>PD</th><th>ALS</th><th>ALS_r</th><th>ALS-PD</th></tr>
<tr><td rowspan="2">Clinical neurological examination
MDS-UPDRS
MR encephalopathy
SPECT with DAT scan</td><td colspan="3">Clinical neurological examination
ALSFRS
DNA analysis for the major known genes involved in ALS
(SOD1, FUS, TARDBP, C9ORF72)</td></tr>
<tr><td></td><td colspan="2">Dose of riluzole</td></tr>
<tr><td colspan="4">For each subject, information about age, sex, height and weight (at the time of blood collection), smoke or alcohol use, work and physical activity, diagnosis, familiarity with other neurologic pathologies, therapies, exposition to substances or environment particularly dangerous and any other recent pathologies were also collected.</td></tr>
</table>

Note: MDS-UPDRS: Movement Disorder Society (MDS) of the Unified Parkinson's Disease Rating Scale; MR: Magnetic Resonance; SPECT: Single Photon Emission Computed Tomography; ALSFRS-R: ALS Functional Rating Scale-Revised.

Gender and age distributions were similar in different groups. Supplemental Table 3.1 reports demographic and clinical data for all enrolled subjects (for a summary see Table 3.2). Subjects suffering from inflammatory or infectious diseases and subjects that took drugs capable of interfering with

PBMCs at the time of enrolment were excluded from the study. All patients signed an informed consent before being recruited for the present study, following approval by the Institutional Review Boards of the University Hospitals where subjects were enrolled.

Table 3.2: Summary of enrolled patients in the study.

		PD (20)	ALS (20)	ALS_r (20)	ALS-PD (9)
Age at the withdrawal ± SD (years)		63.3±10.1	67.4±10.4	64.8±9.8	69.8±7.7
Male%		45%	65%	50%	67%
Unmedicated		20	20	0	3
Riluzole	**50 mg/d**	0	0	4	0
	50 mgx2/d	0	0	16	6
ALSFRS score		0	37.6±7.3	30.3±8.4	29.2±7.5
Motor MDS-UPDRS score		36.3±10.4	0	0	0

Note: d: daily.

Peripheral blood mononuclear cells isolation

All subjects underwent a venous blood sampling (16 ml) from the antecubital vein, between 9 a.m. and 10 a.m., after an overnight fast.

Blood was collected into a CPT-tube with sodium citrate (BD Bioscience) and it was centrifuged (1500 g, 20 minutes, RT) to separate plasma, PBMCs (layer over the gel barrier) and erythrocytes/neutrophils (layer under the gel barrier). Then, the PBMCs layer was transferred into a new tube and centrifuged again (10 minutes at 600 g, RT).

The resulting pellet was washed twice with 10 mL of PBS (w/o Ca^{2+} and Mg^{2+}). Lastly, samples have been divided into 4 aliquots of 1 mL each and then pelleted at 500-1000 g for 10 minutes. Pellets were immediately frozen and stored at -80°C.

Two-dimensional electrophoresis and image analysis

PBMCs were resuspended in 100 µl UTC (7M urea, 2M thiourea and 4% 3-[(3-cholamidopropyl) dimethylammonio]-1-propanesulfonate (CHAPS)) with a protease/phosphatase inhibitors cocktail (Sigma-Aldrich). Cells were left in this solution for 30 minutes to allow a complete cell lysis, sonicated (10 pulses at 0.5 cycle and 80 amplitude, and 10 pulses at 0.5 cycle and 100 amplitude) and centrifuged (13000 g for 30 minutes, RT) to precipitate cellular debris.

Protein concentration was determined according to Bradford. Total proteins (500 μg) were separated through 2-DE using 18 cm IPG DryStrips with a nonlinear 3–10 pH gradient (GE Healthcare) followed by 12.5% SDS-PAGE. The resulting maps were stained with Ru(II) tris(bathophenanthroline disulfonate) (Serva). Images were acquired (12-bit grayscale) with the GelDoc-It Imaging System (UVP) and analysed with ImageMaster 2D Platinum (GE Healthcare). A total of about 400 spots were detected in gels and included in the analysis.

Statistical analysis

Spot volumes were normalized over the sum of the volume of those spots present in all gels. The spots present in less than 65% of the gels were excluded from the further analysis. Then, the biological variability of the subjects in each group was assessed by Pearson linear correlation and Q-Q plots. After a logarithmic transformation data were processed to eliminate confounding factors: gender (Wilcoxon test, p value < 0.01), age at the withdrawal (Pearson test, p value < 0.01) and riluzole-sensitivity (Student's T-test, p value < 0.01), controlling that riluzole-sensitivity was not correlated to disease severity (ALSFRS score). We generated a single group (ALS_all) with all ALS patients (ALS and ALS_r).

For the feature selection, relative volumes were analysed by the non-parametric Wilcoxon test to find differences ($p < 0.2$) in patients with PD with respect to ALS subjects (ALS_all).

Predictive model for the classification of PD patients with respect to ALS subjects was built by linear discriminant analysis (LDA) of the spots identified as described above. In this case, missing values were replaced by the mean value of the spot volume of the group or, if the mean was lower than the 98th percentile, by the minimum value observed in the group.

For each subject that has to be predicted by the model, a likelihood score (Predscore) was calculated by linear combination of relative spot volumes according to the following equation:

$$Predscore = \sum_i c_i * Vol_i$$

Simplified models were obtained by progressively removing spots with the lowest discriminating weight (W), calculated according to the equation:

$$W = |c_i * (\overline{Vol_{i,ALS\_all}} - \overline{Vol_{i,PD)}}|$$

where c_i is the LDA coefficient for spot i and $\overline{Vol_{i,ALS\_all}} - \overline{Vol_{i,PD}}$ is the absolute separation of the mean values of spot i in ALS subjects (ALS_all) and PD. Each predictive model has been tested with

the leave-one-out (predicting one subject excluded from the model construction) and K-fold methods (testing the prediction of 10 patients, randomly eliminated before the construction of the model (k = 6)). The performance of predictive models has been quantified by measuring the area under the ROC curve.

Finally, the LDA model which allowed us to predict subject groups with the best sensitivity and specificity was chosen as reference model to predict the ALS-PD patients. The spots deriving from that model were selected to be excised for protein identification. Eventually, we used them to discriminate groups of ALS-PD patients by a principal component analysis (PCA) and classify them as ALS or PD.

All procedures for data analysis and graphics were written in R, an open-source environment for statistical computing (Figure 3.1).

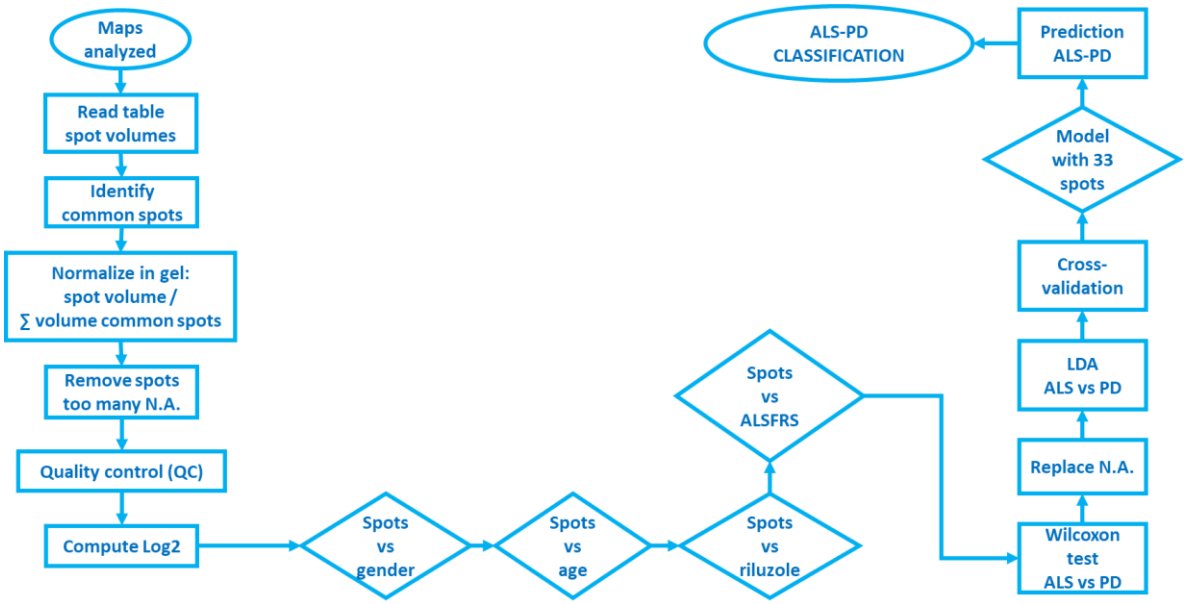

Figure 3.1: Summary of statistical analysis steps.

In-gel digestion, mass spectrometry and protein identification

Spots corresponding to proteins of interest were excised manually. Spots were reduced (10 mM DTT in 100 mM NH_4HCO_3 for 45 minutes at 56°C) and then alkylated (55 mM IAA in 100 mM NH_4HCO_3 for 30 minutes at RT). Spots were dehydrated using CH_3CN for 5 minutes. Dry spots were reswollen with a solution of 10 ng/µL trypsin (Modified Porcine Trypsin, sequencing Grade, Promega, Madisonin in 100 mM NH_4CO_3) and digested overnight at 37°C. Upon digestion, peptides obtained

from each spot were extracted with a solution of Trifluoroacetic acid (TFA) and CH_3CN. The supernatants were collected in a fresh tube and vacuum dried.

The peptide mixtures were analysed by LC-MS/MS, using LTQ XL-Orbitrap ETD equipped with a HPLC NanoEasy-PROXEON (Thermo Fisher Scientific). Protein identification was manually performed by searching the National Centre for Biotechnology Information non-redundant database using the Mascot Ion Search program (http://www.matrixscience.com). The following parameters were set: specific trypsin digestion, up to one missed cleavage; fixed carbamidomethylation of cysteines, partial oxidation of methionines, partial protein N-terminal acetylation, partial N-terminal pyro-carbamidomethylation, peptide mass tolerance ± 10 ppm, fragment mass tolerance ± 0.6 Da, 2+ to 3+ peptide charge, species restriction to human. All identified proteins had a Mascot score corresponding to a statistically significant ($p < 0.05$) confident identification according to Fisher's test. At least 2 different peptides had to be assigned. Peptide and protein identifications corresponding to keratins or trypsin were not considered.

Bioinformatics analysis

The web portal String (https://string-db.org/) (Szklarczyk et al., 2017) was used to build networks. The database covers most of the available information regarding signalling and metabolic pathways (Biocarta, BioCyc, GO, KEGG, and Reactome) and physical protein-protein interactions (BIND, DIP, GRID, HPRD, IntAct, MINT, and PID). Accordingly, the spots deriving from the LDA model were used to generate the network. The provided PPI enriched p value is a major of the connectivity of nodes and verifies whether the proteins of the input list have more interactions among themselves than what would be expected for a random set of proteins of similar size, drawn from the genome. Such an enrichment indicates that the proteins are at least partially biologically connected, as a group. The significant network ($p < 0.01$) was further considered to interpret and discuss proteomics results. The network was exported as a. txt file and visualized and modified by Cytoscape 3.6.1 (http://www.cytoscape.org/) (Shannon et al., 2003). The ORA of nodes of the network was carried out using the Reactome database (http://www.reactome.org/) (Fabregat et al., 2018).

3.2

Results

Two-dimensional electrophoresis profiling of PBMCs proteins

Human PBMCs expression profiles of patients (PD, ALS, ALS_r and ALS-PD) were obtained by 2-DE. A total of about 400 spots were detected in gels and 50 of them were present in all gels.

The sum of these common spots was plotted (Supplemental Figure 3.1) to verify a normal distribution, which allows for the use of this value for normalization purposes. A total of 324 spots were detected in 65% of gels and included in the analysis. After the visualization of the distribution of missing values (Supplemental Figure 3.2), a threshold of 24, as the maximum number of gels in which a spot was not detected, was considered acceptable. This corresponds to the presence of each spot in at least 65% of the gels. Then, the biological variability of the subjects in each group was evaluated. Pairs of 2-DE gels from different subjects in the same group were compared by Pearson linear correlation of corresponding spot volumes after logarithmic transformation (Supplemental Figure 3.3). All comparisons between gel pairs showed a linear behavior. Therefore, all gels were retained, and spot volumes used for the analysis.

69 maps were screened to identify proteins whose changes were linked to possible confounding factors, as gender, age and drug treatments. 7 spots showed significant differences by the Wilcoxon test ($p<0.01$) between male and female patients (Supplemental Figure 3.4). 21 spots presented significant ($p<0.01$) Pearson linear correlation between spots volume and age of patients at the withdrawal (Supplemental Figure 3.5). Both groups of spots were eliminated from further analysis. Then, 13 spots showed significant differences by the Student' T test ($p<0.01$) between ALS patients treated (ALS_r) or not (ALS) with riluzole (Supplemental Figure 3.6). The level of these spots did not correlate with the ALSFRS score (Supplemental Table 3.2). Thus, all riluzole-sensitive spots were

excluded from further analyses. Thus, it was possible to merge ALS and ALS_r groups into a new category (ALS_all).

Features (spots) selection

By comparing 2-DE maps from 20 PD patients and 40 ALS subjects (ALS_all), 54 protein spots (Wilcoxon test, $p<0.2$) were selected as the emergent properties and considered for the subsequent analysis (grey and black dots in Figure 3.2). The nine black dots represent protein spots showing different levels in the two groups, with a p value lower than 0.05 (Wilcoxon test, $p<0.05$).

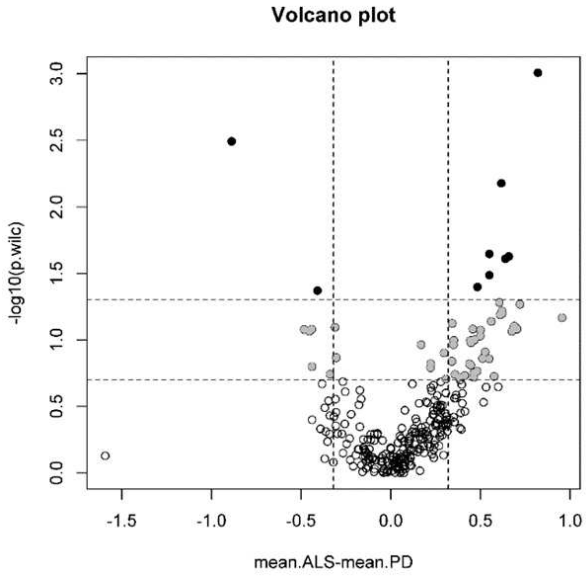

Figure 3.2: Volcano plot of all the spots. White dots have a p value (Wilcoxon test) higher than 0.2. Gray dots have a p value comprised between 0.2 and 0.05. Black dots are significant for the Wilcoxon test with a p value lower than 0.05. The two vertical lines evidence differences of 2 folds between ALS_all and PD.

54 spots were used to construct a LDA between ALS_all and PD groups. 50 iterative models were generated, in which the spot with the lowest weight was eliminated. The cross-validation of the model was performed in two different ways: the leave-one-out process (Supplemental Figure 3.7) and the K-fold process (Supplemental Figure 3 .8). The model which permitted to predict patients of the test set with the best sensitivity and specificity (sensitivity = 95% and specificity = 100%) was chosen as the reference one (Figure 3.3), and the 33 spots used to generate the model were selected.

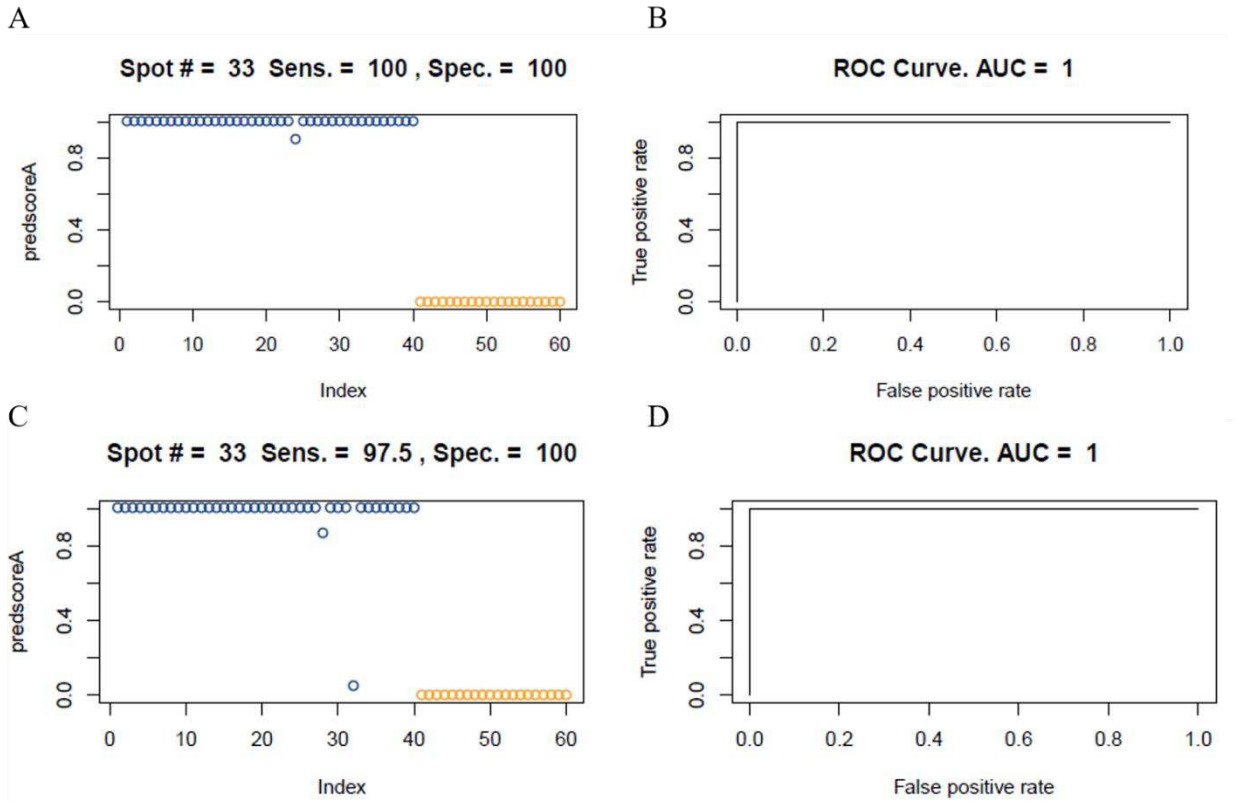

Figure 3.3: Leave-one-out (A, B) and K-fold (C, D) cross-validation of the selected model (33 spots). A and C represent graphs of prediction scores of each patient. B and C represent the ROC curve. In "blue" ALS_all patients and in "orange" PD patients.

The Predscore (based on the linear combination of 33 spots) was used to predict ALS-PD patients (Figure 3.4; Table 3.3). This model classified 4 subjects as ALS patients and 5 subjects as PD patients.

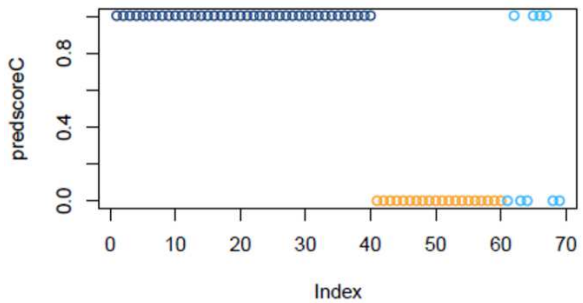

Figure 3.4: Prediction of the ALS-PD patients, based on the selected model of 33 spots validated through K-fold method. ALS_all patients in "blue", PD in "orange" and ALS-PD patients in "light blue".

Table 3.3: Classification of the ALS-PD patients.

Patient ID	Classified as:
ALS-PD 1	PD
ALS-PD 2	ALS
ALS-PD 3	PD
ALS-PD 4	PD
ALS-PD 5	ALS
ALS-PD 6	ALS
ALS-PD 7	ALS
ALS-PD 8	PD
ALS-PD 9	PD

Proteins identification

Proteins corresponding to the 33 selected spots were excised (Figure 3.5) and identified by LC-MS/MS as reported in Table 3.4.

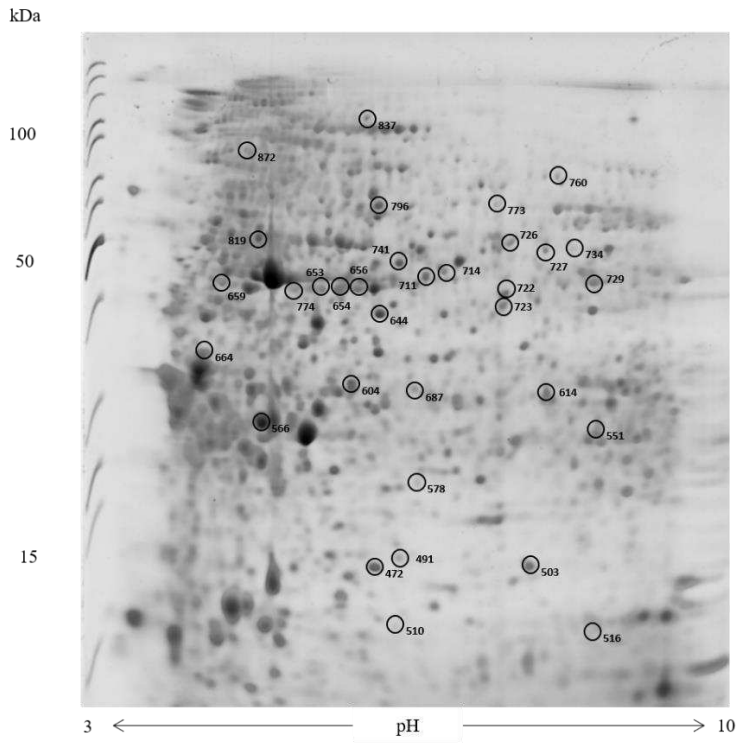

Figure 3.5: Spots excised for MS analysis are evidenced on a representative 2-DE map.

Table 3.4: Identification of protein spots.

SPOTS N°	GENE	UNIPROT ID	PROTEIN	KDa	PI
472	SOD1	P00441	Superoxide dismutase [Cu-Zn]	15.9	5.7
491	**NME1**	**P15531**	**Nucleoside diphosphate kinase A**	**17.2**	**5.8**
503	**HSPA8**	**P11142**	**Heat shock cognate 71 kDa protein (fragment)**	**70.9**	**5.4**
510	PFDN5	Q99471	Prefoldin subunit 5	17.3	5.9
516	FGA	P02671	Fibrinogen alpha chain (fragment)	95	5.7
551	**PGAM1**	**P18669**	**Phosphoglycerate mutase 1**	**28.8**	**6.7**
566	ACTB	P60709	Actin, cytoplasmic 1	41.7	5.29
578	**PRDX3**	**P30048**	**Thioredoxin-dependent peroxide reductase, mitochondrial**	**27.7**	**7.7**
604	CAPZB	P47756	F-actin-capping protein subunit beta	31.3	5.4
614	**PNP**	**P23492**	**Purine nucleoside phosphorylase**	**32.1**	**6.5**
644	TUBB2A	Q13885	Tubulin beta chain	49.7	4.8
653	MSN	P26038	Moesin	67.8	6.1
654	MSN	P26038	Moesin	67.8	6.1
656	MSN	P26038	Moesin	67.8	6.1
659	**LMNB1**	**P20700**	**Lamin-B1**	**66.4**	**5.1**
664	**ACTB**	**P60709**	**Actin, cytoplasmic 1 (fragment)**	**41.7**	**5.29**
687	PKM	P14618	Pyruvate kinase PKM (fragment)	57.9	7.9
711	**PKM**	**P14618**	**Pyruvate kinase PKM**	**57.9**	**7.9**
714	FGG	P02679	Fibrinogen gamma chain	51.5	5.4
722	PKM	P14618	Pyruvate kinase PKM (fragment)	57.9	7.9
723	TUBB1	Q9H4B7	Tubulin beta-1 chain	50.3	5
726	**VCL**	**P18206**	**Vinculin (fragment)**	**124**	**5.5**
727	FGB	P02675	Fibrinogen beta chain	56	8.5
729	SERPINB1	P30740	Leukocyte elastase inhibitor (fragment)	42.7	5.9
734	ENO1	P06733	Alpha-enolase	47.2	7
741	TUBA1C	Q9BQE3	Tubulin alpha-1C chain	49.9	4.9
760	WDR1	O75083	WD repeat-containing protein 1	69.2	6.2
773	FGB	P02675	Fibrinogen beta chain	55.9	8.5
774	MSN	P26038	Moesin	67.8	6.1
796	PDIA3	P30101	Protein disulfide-isomerase A3	56.8	5.9
819	TUBB1	Q9H4B7	Tubulin beta-1 chain	50.3	5
837	TLN1	Q9Y490	Talin-1 (fragment)	269.8	5.8
872	ACTN1	P12814	Alpha-actinin-1	103	5.5

In bold/blue, protein spots showing different levels in the two groups with a p value lower than 0.05 (Wilcoxon test, $p<0.05$).

A focus on amyotrophic lateral sclerosis patients with parkinsonian signs

Using 33 spots, a PCA was performed to verify whether ALS-PD patients were classified as ALS or PD by our model. The first component (PC1) accounted for 25.4% of variance (Supplemental Figure 3.8). To focus on more relevant spots in determining the classification of ALS-PD patients, we considered the PC1 value of the 33 spots. We arbitrarily decided to consider spots with |PC1|>0.2 (see Table 3.5.) and verify in which direction they influenced the classification of ALS-PD patients.

Table 3.5: Spots with |PC1|>0.2.

SPOTS N°	GENE	UNIPROT ID	|PC1|	SIMILAR TO
516	FGA	P02671	0.220329	ALS
551	**PGAM1**	**P18669**	**0.26505**	**PD**
614	**PNP**	**P23492**	**0.31735**	**PD**
664	**ACTB**	**P60709**	**0.219239**	**ALS**
687	PKM	P14618	0.27921	PD
729	SERPINB1	P30740	0.24897	ALS
734	ENO1	P06733	0.303292	PD
741	TUBA1C	Q9BQE3	0.21397	ALS
760	WDR1	O75083	0.27932	PD
773	FGB	P02675	0.290507	PD
872	ACTN1	P12814	0.23861	PD

In bold/blue, protein spots showing different levels in the two groups with a p value lower than 0.05 (Wilcoxon test, $p<0.05$).

Starting from the 33 proteins previously identified, a network-based analysis was performed, using the String database as a reference set. With this approach, a direct interactor network was generated (Figure 3.6), including 23 proteins.

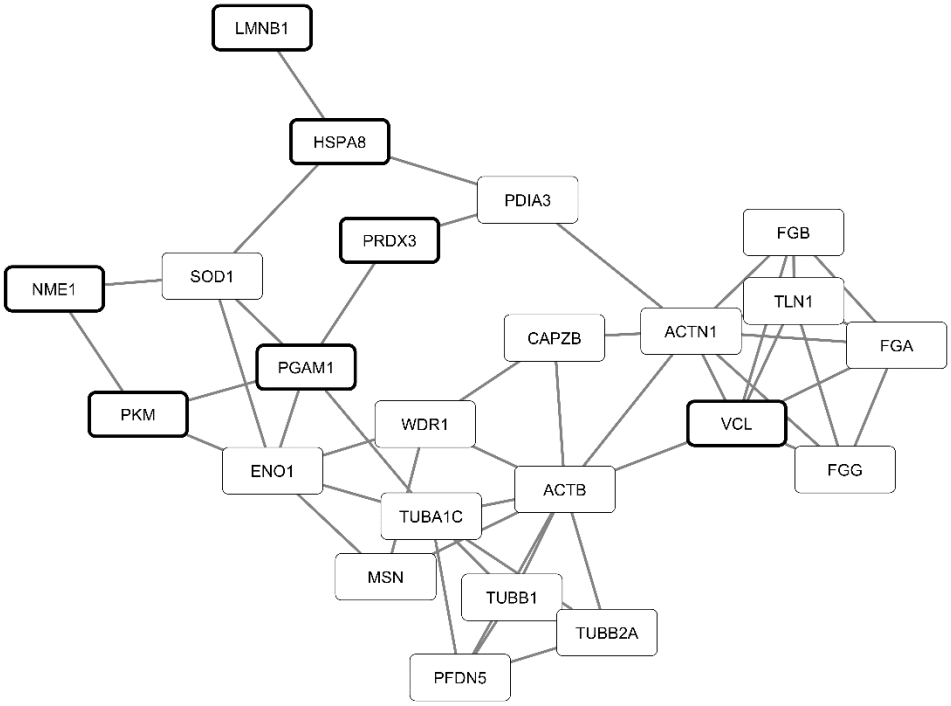

Figure 3.6: Direct interactor network obtained using String as reference database. Nodes with thicker border represent proteins showing different levels in the two groups with a p value lower than 0.05.

Since ALS-PD patients are primarily ALS patients, we wanted to visualize which protein signature determined their difference with ALS patients with no extrapyramidal signs and caused the classification of some of them as PD. To this purpose, ALS-PD classified as ALS or as PD were compared with ALS patients (ALS_all). The results are reported on the network in Figure 3.7. PGAM1, ENO1, FGA, FGB, ACTN1, PKM, WDR1 and TUBA1C (bigger nodes, Figure 3.7A) were proteins that contributed the most to the classification ($|PC1|>0.2$). In Figure 3.7A, it is possible to visualize data of ALS-PD patients classified as ALS. ACTN1, PKM, WDR1 and TUBA1C probably contributed the most for the classification of this group as ALS, since their levels are homogenous with respect to the ALS group. Conversely, PGAM1, ENO1, FGB, FGA, PDIA3, TUBB1 (yellow or blue nodes, Figure 3.7A) represent proteins that showed the greatest difference of expression with respect to ALS patients (fold change (ALS-PD vs. ALS) >1.5), witnessing the difference of comorbid patients also at the molecular level. For ALS-PD patients classified as PD, PGAM1 and WDR1 had $|PC1|>0.2$ and a fold change <0.5 (Figure 3.7B), again contributing the most to the classification model.

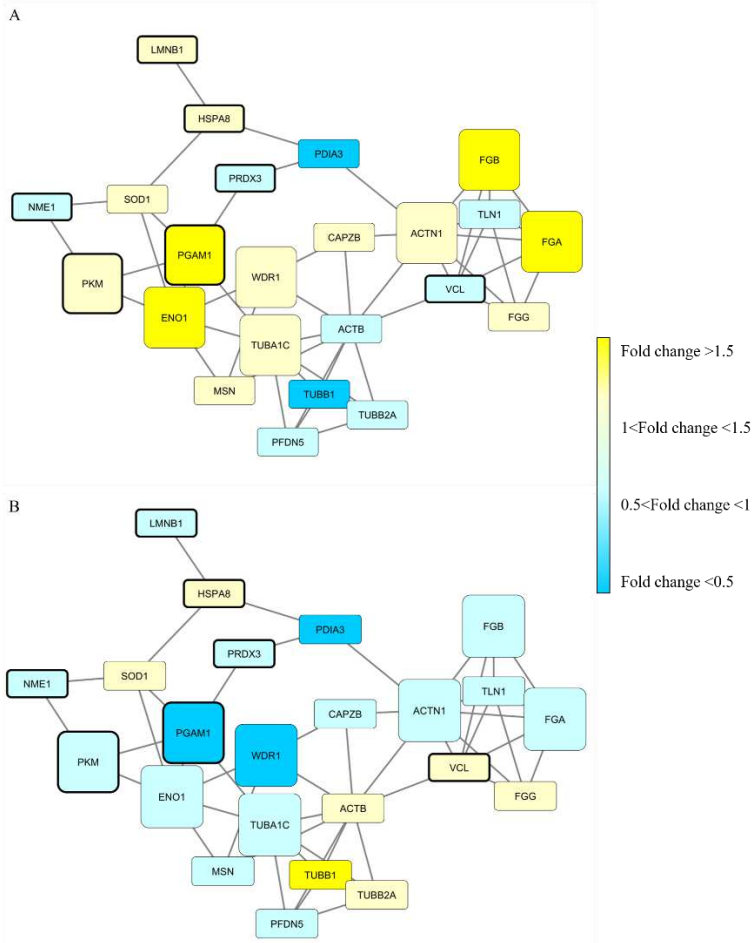

Figure 3.7: Direct interactor network, obtained using String as reference database. Nodes with thicker borders represent proteins showing different levels in the ALS and PD groups, with a p value lower than 0.05. Bigger nodes represent proteins with |PC1| >0.2. Color code is correlated with protein abundance and indicates the fold change in the comparison ALS-PD vs. ALS. (A) ALS-PD patients classified as ALS, (B) ALS-PD patients classified as PD.

Afterwards, the IDs list of the network nodes was used to perform an ORA, using Reactome as reference database. In Table 3.6, the top 25 over-represented pathways are reported. All pathways significantly (FRD<0.001) over-represented were reported in Supplemental Table 3.3.

Table 3.6. the top 25 over-represented pathways, using Reactome as reference database.

Pathway Name	Entities				Reactions
	Found	Total	Pvalue	FDR	Ratio
Prefoldin mediated transfer of substrate to CCT/TriC	6	28	1.25E-10	2.58E-08	1.72E-04
Cooperation of Prefoldin and TriC/CCT in actin and tubulin folding	6	36	5.57E-10	5.74E-08	5.15E-04
Platelet degranulation	8	137	2.14E-09	8.65E-08	9.45E-04
Signalling by high-kinase activity BRAF mutants	6	46	2.38E-09	8.65E-08	5.15E-04
MAP2K and MAPK activation	6	47	2.70E-09	8.65E-08	6.87E-04
Signalling by moderate kinase activity BRAF mutants	6	48	3.06E-09	8.65E-08	6.01E-04
Response to elevated platelet cytosolic Ca2+	8	144	3.15E-09	8.65E-08	0.001202
Paradoxical activation of RAF signalling by kinase inactive BRAF	6	49	3.46E-09	8.65E-08	6.01E-04
Hemostasis	14	806	5.60E-09	1.23E-07	0.028086
Recycling pathway of L1	6	54	6.14E-09	1.23E-07	0.001202
Signalling by RAS mutants	6	61	1.26E-08	2.27E-07	6.87E-04
Signalling by BRAF and RAF fusions	6	68	2.39E-08	3.90E-07	4.29E-04
HSP90 chaperone cycle for steroid hormone receptors (SHR)	6	69	2.60E-08	3.90E-07	0.001031
Immune System	22	2638	3.20E-08	4.48E-07	0.126256
RHO GTPases activate IQGAPs	5	35	3.62E-08	4.70E-07	4.29E-04
Gene and protein expression by JAK-STAT signalling after Interleukin-12 stimulation	6	74	3.92E-08	4.70E-07	0.003092
L1CAM interactions	7	129	3.97E-08	4.76E-07	0.004638
Cellular responses to stress	11	511	4.33E-08	4.77E-07	0.015803
Interleukin-12 signalling	6	85	8.82E-08	8.82E-07	0.00481
Oncogenic MAPK signalling	6	87	1.01E-07	1.01E-06	0.00292
Interleukin-12 family signalling	6	97	1.90E-07	1.69E-06	0.009791
Gap junction trafficking	5	50	2.09E-07	1.69E-06	0.001718
Cellular responses to external stimuli	11	598	2.11E-07	1.69E-06	0.021816

PART IV

MitoNet

Mitochondrial Network

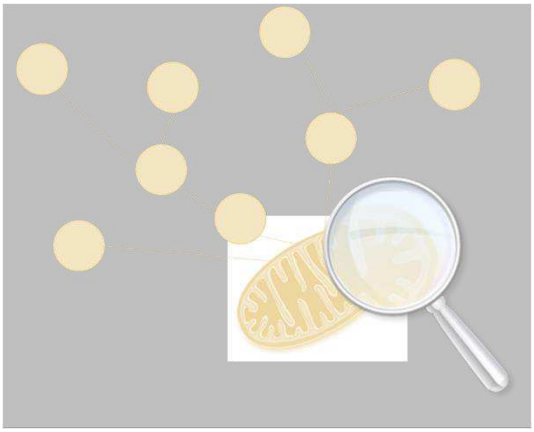

4.1

Materials and Methods

Input list generation

All proteins with high quality (gold label) annotated as mitochondrial in subcellular location and/or GO Cellular Component sections of the neXtProt database (https://www.nextprot.org/ release 2018-01-17) were collected and two input lists were generated (SUB_LOC list and GO_CC list). SUB_LOC list and GO_CC list were compared using Venn diagram (http://bioinformatics.psb.ugent.be/cgi-bin/liste/Venn/calculate_venn.htpl). MITO list was created unifying the SUB_LOC list and the GO_CC list.

Identification of mitochondrial missing proteins

To highlight missing proteins, MITO list was analysed using Protein Evidence (PE) information retrieved from the neXtProt database. Proteins with evidence at transcript level (PE2), evidence for homology (PE3) and predicted (PE4) were collected and the MISSING list was generated. To demonstrate the existence of missing proteins (IDs of MISSING list) PubMed and the Global Proteome Machine database GPMdb (gpmdb.thegpm.org) (Craig et al., 2004) were used.

The functional mitochondrial human proteome network generation

To obtain a comprehensive mitochondrial network, data were extracted from neXtProt, using the advanced search functionality based on SPARQL language on the neXtProt SNORQL interface (http://snorql.nextprot.org/) (as detailed in Supplemental data 4.1). All gold protein-protein interactions for proteins in the MITO list were retrieved in the protein interaction section

(Supplemental data 4.2). Moreover, binary interactions were manually retrieved from the free text annotations and reported in the network table.

The functional mitochondrial human proteome network (MITO network) was generated using Cytoscape 3.6.1 (http://www.cytoscape.org/) (Shannon et al., 2003). In this network, nodes represent proteins (mitochondrial proteins and their first interactors), while edges represent high quality protein-protein interaction data.

Bioinformatics analysis

Sub-cellular and sub-mitochondrial location

To classify other cellular localizations (Table 4.1) and the sub-mitochondrial localization (Table 4.2) of mitochondrial proteins of the MITO network, the advanced search of the neXtProt database was used. All gold data of the subcellular location and GO Cellular Component sections were retrieved (Supplemental data 4.3).

Table 4.1: Uniprot and GO Cellular Component code of sub-cellular locations.

Sub-cellular localization	Uniprot code	GO Cellular Component code
Cytoplasm	SL-0086	GO_0005737
Endoplasmic reticulum	SL-0095	GO_0005783
Golgi apparatus	SL-0132	GO_0005794
Lysosome	SL-0158	GO_0005764
Nucleus	SL-0191	GO_0005634
Mitochondrion	SL-0173	GO_0005739

Table 4.2: Uniprot and GO Cellular Component code of sub-mitochondrial locations

Sub-mitochondrial localization	Uniprot code	GO Cellular Component code
Inner membrane	SL-0168	GO_0005743
Inter membrane space	SL-0169	GO_0005758
Matrix	SL-0170	GO_0005759
Membrane	SL-0171	GO_0031966
Outer membrane	SL-0172	GO_0005741

Proteins relevant for a particular condition

Using the MITO network, it is possible to highlight mitochondrial proteome alterations involved in a specific disease. To find biochemical pathways specifically involved in PD, only-PD_Proteins input

list (see Chapter 2.2, paragraph Physical Interaction Network) (Monti et al., 2018) was mapped on the MITO network. Mapped nodes were extracted and an over-representation analysis was performed using the "Analyze tool" in Reactome (Fabregat et al., 2018) and Panther in GO BP (http://www.geneontology.org/) (The GO Consortium, 2017) database. Arbitrarily, only GO Biological Processes with fold enrichment > 5 were considered (Macron et al., 2018). These limits allowed us to focus on specific ontologies (end nodes of ontology trees) and eliminate more general macro GO. For both analyses only, categories with FDR<0.001 were considered as significant.

4.2

Results

Generation of the MITO list

All gold proteins annotated as mitochondrial in subcellular location and GO Cellular Component sections of the neXtProt database were retrieved. Uncertain protein (PE5, 12 mitochondrial proteins) were neglected from the further analysis. Mitochondrial sub-cellular location list (SUB_LOC list, 1219 IDs) and mitochondrial GO Cellular Component list (GO_CC list, 1193 IDs) were generated. The SUB_LOC list and GO_CC list shared 999 mitochondrial proteins, while 194 proteins were present only in GO_CC list and 220 mitochondrial proteins were SUB_LOC list-specific (Figure 4.1). All mitochondrial proteins annotated as such in neXtProt database were used to generate a new input list, the MITO list (SUB_LOC list U GO_CC list, 1413 IDs).

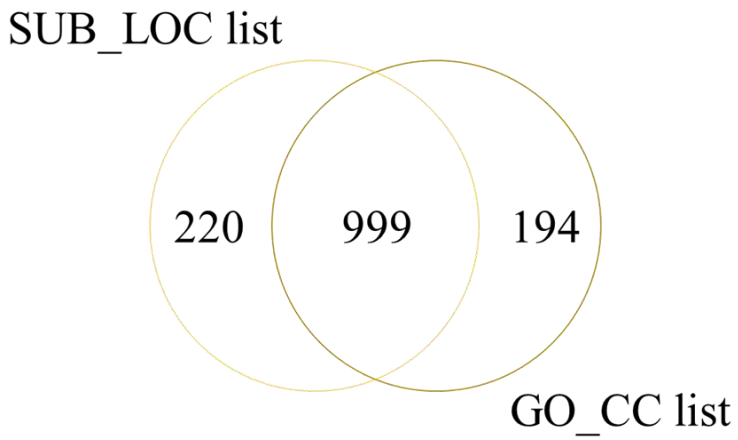

Figure 4.1: Mitochondrial IDs Venn diagrams. The Venn diagram shows the source of mitochondrial IDs in the MITO list (retrieved by neXtProt database) and the number of proteins shared by the SUB_LOC list (retrieved by the sublocation section) and the GO_CC list (retrieved by the GO Cellular Component section).

Protein evidence level of mitochondrial proteins

Using Protein Evidence (PE) data retrieved from the neXtProt database, proteins of the MITO list were classified (Table 4.3) in order to identify "missing proteins". "Missing proteins" as defined by the HUPO HPP consortium are neXtProt PE2-4 entries. Proteins of MITO lists annotated as PE2 (evidence at the transcript level) or PE3 (inferred from homology) or PE4 (predicted) were used to generate a new list called MISSING list (containing 23 IDs) (Table 4.3).

Table 4.3: PE2, PE3 proteins of the MITO list. All data were collected from neXtProt database (release 2018-01-17).

Entries in the neXtProt database	**PE2** (evidence at transcript level) 1660	**PE3** (Inferred from homology) 452	**PE4** (Predicted) 74
MITO list (1413 IDs)	20	3	0
Gene Name	ACSM4, ACSM6, ANKRD37, ATP5G2, ATP5G3, COX7B2, COX8C, GDF5OS, MCCD1, METTL12, MTRNR2L5, PRELID2, SIAH3, SLC25A34, SLC25A45, SLC25A47, SLC25A52, TDH	ATP5EP2, KIF28P, UQCRHL	

The proteins of the MISSING list were examined. Using data retrieved from the literature, it was possible to identify the existence of Methyltransferase-like protein 12 (METTL12). METTL12 is a protein involved in the regulation of citrate synthase activity. Indeed, the methylation of Lys 395 inhibits citrate synthase (Małecki et al., 2017). This post-translational modification is blocked by oxaloacetate and by S-adenosylhomocysteine. Moreover, the methylation of Lys-368 of citrate synthase by METTL12 probably influences protein-protein interactions in the metabolism of the citric acid cycle (Małecki et al., 2017; Rhein et al., 207). Due to these new data, the PE status of this protein has been updated by UniProtKB (2018_01 release) and its status will be upgraded to PE1 in the next neXtProt release. As concerns PE3 proteins, Kinesin-like protein KIF28P (KIF28P) was inferred from mouse and rat, while Cytochrome b-c1 complex subunit 6-like, mitochondrial (UQCRHL) was inferred from yeast and mouse. On the other hand, ATP synthase subunit epsilon-like protein, mitochondrial (ATP5EP2) was defined as a pseudogene but one of its peptides was identified by MS in the context of a phosphoproteome analysis in human samples (Yu et al., 2007).

The functional mitochondrial human proteome network

Starting from the MITO list, using the high-quality (gold) protein-protein interaction information from neXtProt, a network was generated. The resulting functional mitochondrial human proteome

network (MITO network) had 3395 nodes: mitochondrial proteins (yellow nodes) were 825, while 2570 nodes were first non-mitochondrial interactors (blue nodes) (Figure 4.2).

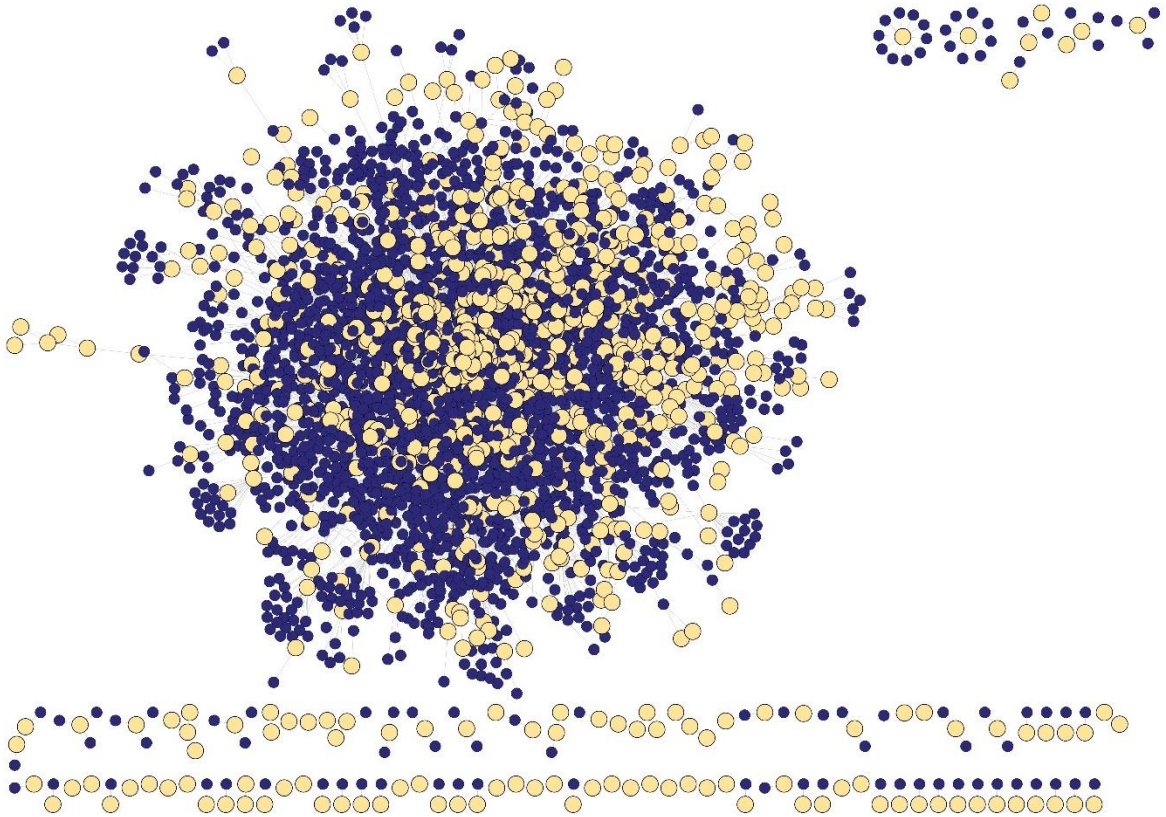

Figure 4.2: The functional mitochondrial human proteome network. Yellow nodes represent mitochondrial proteins (encoded by the mitochondrial genome or translocated to the mitochondrion, if indicated as mitochondrial in the sub location and/or GO Cellular Component sections of the neXtProt database). Blue nodes represent gold interactors of the mitochondrial proteins, as obtained by querying the protein interaction sections of the neXtProt database.

Sub-cellular and sub-mitochondrial location of mitochondrial nodes

All the mitochondrial nodes (yellow nodes in Figure 4.2) of the MITO network were analysed in terms of other sub-cellular locations, in order to understand how many mitochondrial proteins were exclusively mitochondrial. Only the six most represented cellular components (Cytoplasm, Golgi Apparatus, Lysosome, Endoplasmic Reticulum, Mitochondrion, Nucleus) were considered and all gold data were retrieved in the same sections of the neXtProt database. 36 proteins (4%) were exclusively mitochondrial, whereas the majority of the proteins had other cellular locations (Figure 4.3). Cytoplasm (93% of mitochondrial proteins were also localized in the cytoplasm) and nucleus (41% of mitochondrial proteins were also localized in the nucleus) were the most represented other cellular locations for mitochondrial proteins (Figure 4.3).

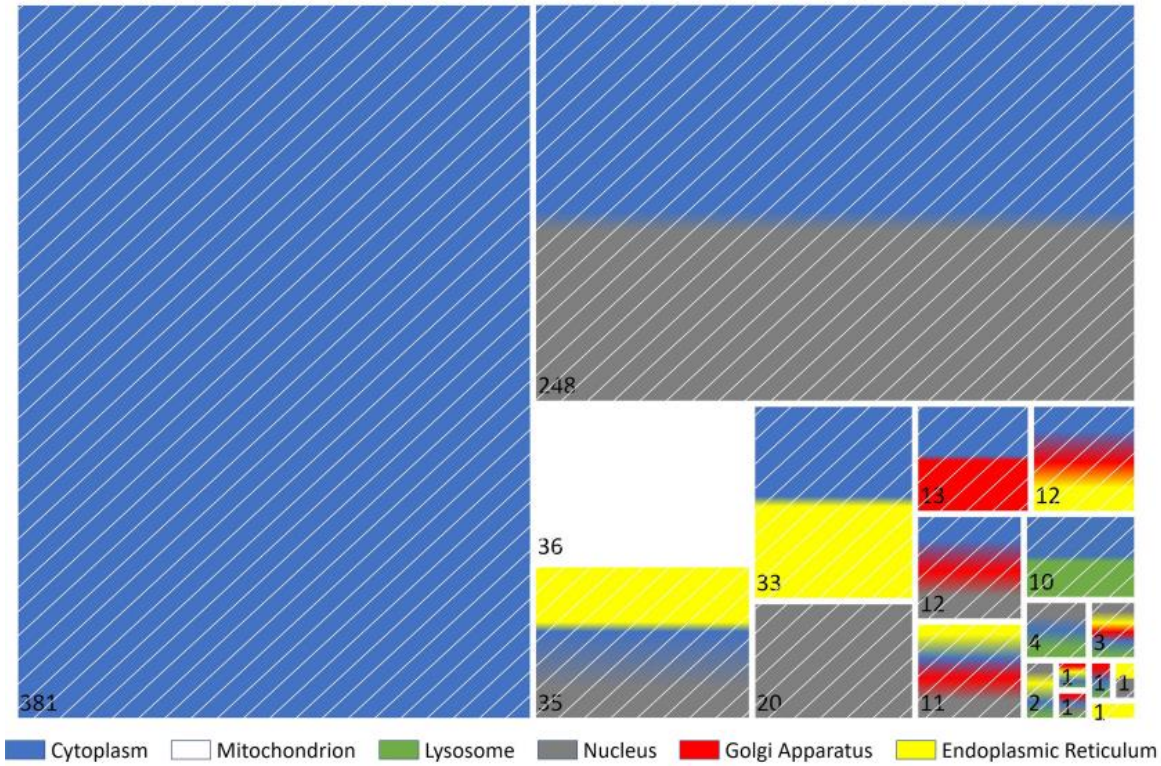

Figure 4.3: Graphical representation of multiple sub-cellular locations. Colour code is explained at the bottom. The size of the category square is proportional to the number of proteins in that group, which is written inside each square. Rectangles are placed progressively from the largest and more represented category on the left to the smallest and less represented one on the bottom-right. Category squares describing multiple locations are filled with white (mitochondrion) and coloured stripes (other location).

Moreover, 376 proteins had a "generic mitochondrion" annotation in neXtProt subcellular location or GO Cellular Component sections, while 449 other mitochondrial nodes had more precise sub-mitochondrial annotations: 138 proteins were localized in the mitochondrial matrix, 103 were inner membrane mitochondrial proteins, 92 were localized in the outer membrane and 16 were localized in the inter membrane space (Figure 4.4).

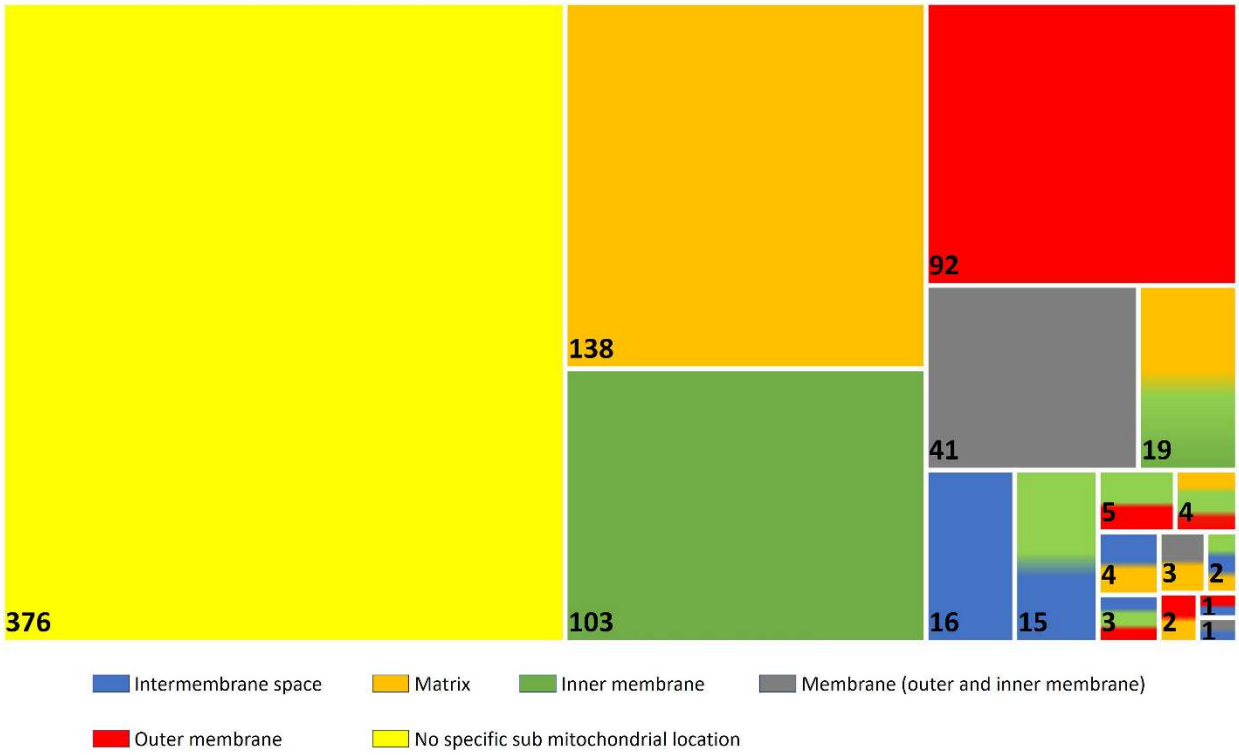

Figure 4.4: Graphical representation of sub-mitochondrial locations. Colour code is explained at the bottom. The size of the category square is proportional to the number of proteins in that group, which is written inside each square. Category squares describing multiple locations are filled with different colours. Rectangles are placed progressively from the largest and more represented category on the left to the smallest and less represented one on the bottom-right.

Focus on the mitochondrial impairment in Parkinson's Disease

675 proteins of the only-PD_Proteins list (see Chapter 2.2, Physical Interaction Network) (Monti et al., 2018) were analysed using the MITO network (Figure 4.5).

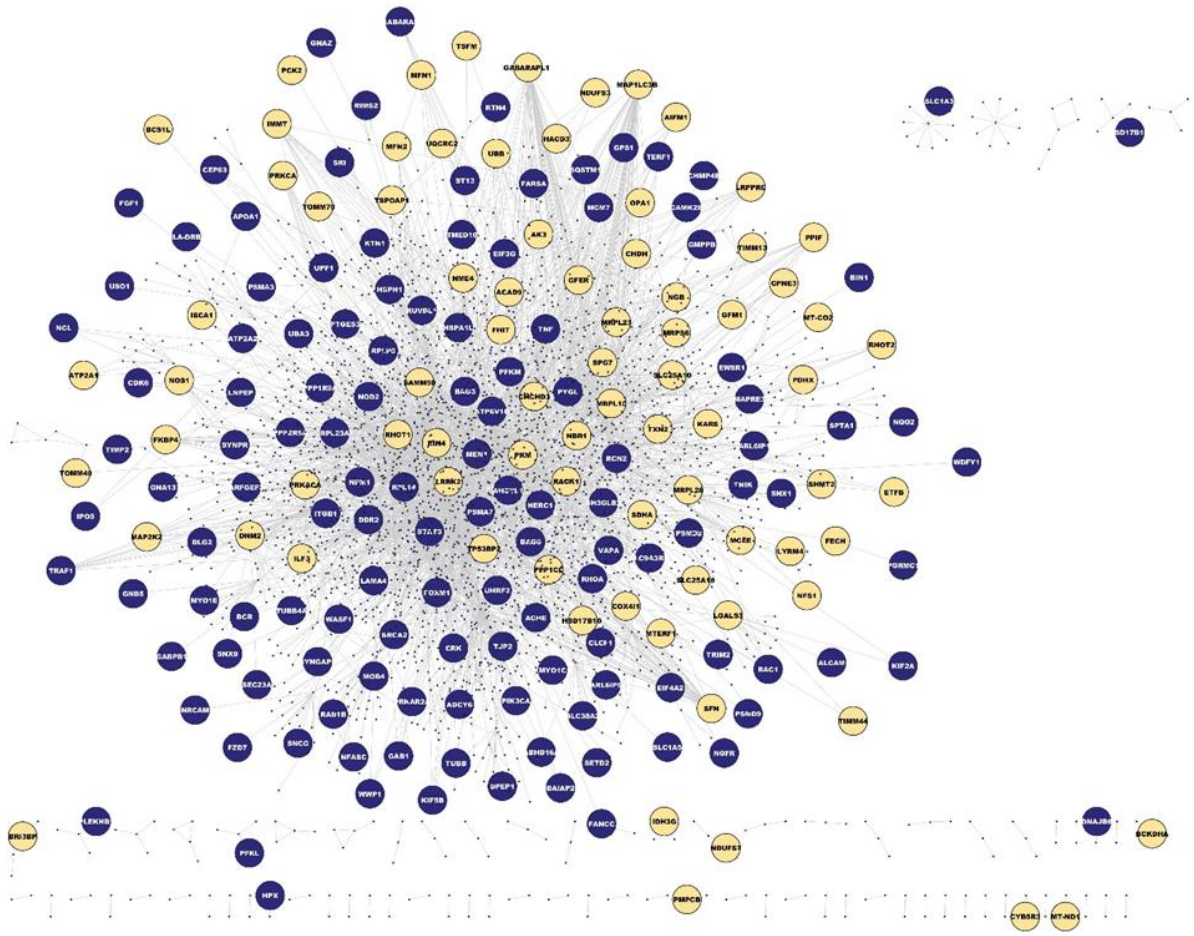

Figure 4.5: PD specific proteins mapped onto the MITO network. Yellow nodes encode for mitochondrial proteins, while blue nodes encode for first interactors.

208 PD-related proteins (31%) were mapped on the network, highlighting the central role of mitochondria in this pathology. An ORA was performed using Reactome and GO BP as reference databases. Reactome results highlighted the central role of mitophagy ("Pink/Parkin Mediated Mitophagy", FDR 3.92×10-4 and "Mitophagy", FDR 8.02×10-4) and of "mitochondrial protein import" (FDR 5.24×10-4) (Supplemental Table 4.1). On the other hand, the GO BP mainly involved was "mitochondrial transport" (FDR 1.94×10-8, Fold Enrichment 8.81). An interesting result was the over-representation of the GO BP "regulation of neurotransmitter transport" (FDR 7.08×10-4, Fold Enrichment 6.91) (Supplemental Table 4.1).

PART V

DynaMoParD
Dynamic Model of Parkinson's Disease

5.1

Materials and Methods

Cell culture and treatments

The human neuroblastoma SH-SY5Y cells (ECACC, Cat No. 94030304; Lot No. 11C016) were maintained at 37°C under humidified conditions and 5% CO2 in high glucose Dulbecco's Modified Eagle's Medium (DMEM) (Euroclone) supplemented with 10% Fetal Bovine Serum (FBS) (Euroclone), 100 U/mL penicillin (Euroclone), 100 g/mL streptomycin (Euroclone) and 2 mM L-glutamine (Euroclone). Cells were seeded 24 hours before treatments. Cells were then treated with mitochondrial toxins (Table 5.1) for 3, 6, 9 and 24 hours (time-course).

To eliminate the peroxide dioxide spontaneously generated in the extra-cellular milieu, catalase (700 U/ml) was added to DMEM in treatments with dopamine (DA (CAT)) or with MPP^+ (MPP^+ (CAT)). A treatment with MPP^+ alone was added to verify that catalase did not influence cellular and molecular responses. Eventually, SH-SY5Y cells were treated with CCCP, or ROT or an equal volume of vehicle, DMSO.

Table 5.1: Experimental conditions.

Treatments	Concentration
SH-SY5Y (control)	-
1-methyl-4-phenylpyridinium (MPP^+)	2.5 mM
Catalase (CAT)	700 U/mL
Dopamine and Catalase (DA (CAT))	250 μM (700 U/mL)
1-methyl-4-phenylpyridinium and catalase (MPP^+(CAT))	2.5 mM (700 U/mL)
Dimethyl sulfoxide (DMSO)	20 μM
Rotenone and Dimethyl sulfoxide (ROT (DMSO))	500 nM (20 μM)
Carbonyl cyanide m-chlorophenyl hydrazine and Dimethyl sulfoxide (CCCP (DMSO))	20 μM (20 μM)

Citotoxicity assay

Cell viability was investigated using the neutral red (NR) uptake assay. Cells were seeded in 24-well plates at 10^5 cells per well and cultured for 24 hours at 37 °C before the assay. Cells were exposed to different experimental conditions (Table 5.1), for several time points, 3, 6, 9 and 24 hours. At the end of the treatment, the conditioned medium was removed, and cells were incubated with freshly prepared NR solution (50 µg NR/ml in culture medium) for 3 hours at 37 °C. Then cells were rapidly washed with a fixative (1% CaCl2 and 1.3 % formaldehyde) and subsequently lysed with the extraction solution (50% ethanol and 1% acetic acid). After 30 minutes incubation at RT, aliquots of the resulting solutions were transferred to cuvettes and the absorbance was recorded at 540 nm. Results were expressed as a percentage of control. All experiments were run in triplicate. Statistical significance was assessed by the Welch-corrected t test.

Quantitative Western blot analysis

1×10^5 SH-SY5Y cells were seeded in T25 flasks and cultured for 24 hours at 37 °C before treatments. At the end of the treatments, cells were detached with trypsin-EDTA, collected by centrifugation (300 × g, 4 °C, 7 minutes) and washed with ice-cold PBS. Cells were lysed using RIPA buffer (0.1% SDS 50 mM Tris-HCl pH 7.6, 150 mM NaCl, 1% sodium desoxycholate, 1% NP-40) and incubated on ice for 30 minutes. Afterwards, lysates were centrifuged at 15000 × g for 40 minutes at 4°C and supernatants collected. 60 µg of proteins were incubated in Laemmli loading buffer and then resolved by 10% or 16% SDS-PAGE. Then, proteins were transferred to PVDF membranes at 1.0 mA/cm^2, 1.5 hours (TE77pwr, Hoefer). Membranes were then saturated for 2 hours at RT in TBST containing 5% skimmed milk powder. Eventually, blots were probed with antibodies against several proteins (Table 5.2) in 5% milk-TBST overnight at 4°C.

Table 5.2: Primary and secondary antibody used in quantitative Western blot analysis.

Protein	Primary antibody dilution	Secondary antibody	Secondary antibody dilution
OPA1	1:250 (HPA036927, Sigma Aldrich)	Anti-rabbit	1:2500 (#AP132P, Millipore Corporation)
MFN1	1:1000 (sc-50330, Santa Cruz Biotechnology)		
PINK1	1:1000 (#6946, Cell Signaling)		
VDAC1	1:1000 (ab15895, Abcam)		
COX5β	1:1000 (#C4498, Sigma-Aldrich)		
ACT	1:10000 (GTX23280, GeneTex)	Anti-mouse	1:10000 (12-349, Millipore Corporation)

Blots were incubated with peroxidase-conjugated secondary antibodies, as reported in Table 5.2, in 5% milk-TBST. Enhanced chemiluminescence substrate (Millipore Corporation) was used in order to visualize the peroxidase signals. Images (16 bit grayscale) were acquired with the G:BOXChemi XT4 (Syngene) system and analysed using the ImageJ software (https://imagej.nih.gov/ij/) (Schneider et al., 2012), normalizing each protein signal for the β-actin signal.

Results were expressed as a percentage of control. All experiments were run in triplicate. Statistical significance was assessed by the Welch-corrected t test.

Measurement of mitochondrial membrane potential (Δψm)

SH-SY5Y cells were seeded in 24-well plates (1×10^5 cells/well) and cultured for 24 hours at 37 °C before treatments. Cells were treated for 24 hours. To evaluate the mitochondrial membrane potential, medium was removed and replaced with fresh DMEM with 100 nM Mitotracker Red CMXRos (chloromethyl-X-rosamine, Life Technologies), which accumulates into the matrix of mitochondria with intact mitochondrial membrane potential. After 20 minutes of incubation at 37 °C, medium containing Mitotracker was replaced with fresh PBS and cells were fixed with 4% paraformaldehyde for 20 minutes. Nuclei were stained with 300 nM 4',6-diamidino-2- phenylindole (DAPI) for 5 minutes (Life Technologies). Coverslips were mounted with ProLong Gold Antifade mountant (Thermo Fisher Scientific) and cells imaged using a laser-scanning confocal microscope (Leica TCS SP5) through a 63×/1.40 NA oil-immersion objective (HCX PL APO lambda blue). Z-stacks with 0.2 µm step size were acquired with sequential excitation at 1024 x 1024 pixels resolution and 1.5× or 2× magnification, 2 frames average. Eventually, image processing and analysis were performed using the ImageJ software. For each whole field of view (fov), Mitotracker signal intensities were calculated

measuring integrated density values after a reduction of background signal by rolling ball algorithm (200 pixel radius). The corrected intensity was normalized with respect to the number of cells, as defined by nuclear staining with DAPI.

5.2

Results

Cytotoxicity assays

To evaluate the effect of mitochondrial toxins (see Table 5.1) on SH-SY5Y cells, a cytotoxicity assay was performed using NR. Results are reported as the mean percentage of viable cells, obtained by the ratio of the absorbance at 540 nm of treated cells with respect to the related control, in at least three independent experiments. From 6 hours of treatment on, dopamine (DA(CAT)), MPP^+ (MPP^+ and MPP^+ (CAT)), Rotenone (ROT(DMSO)), and CCCP (CCCP(DMSO)) caused a significant decrease of cell viability (about 40%) (Figure 5.1). On the contrary, exposure to catalase (CAT) for 3 and 6 hours induced a slight increase of cell viability (Figure 5.1)

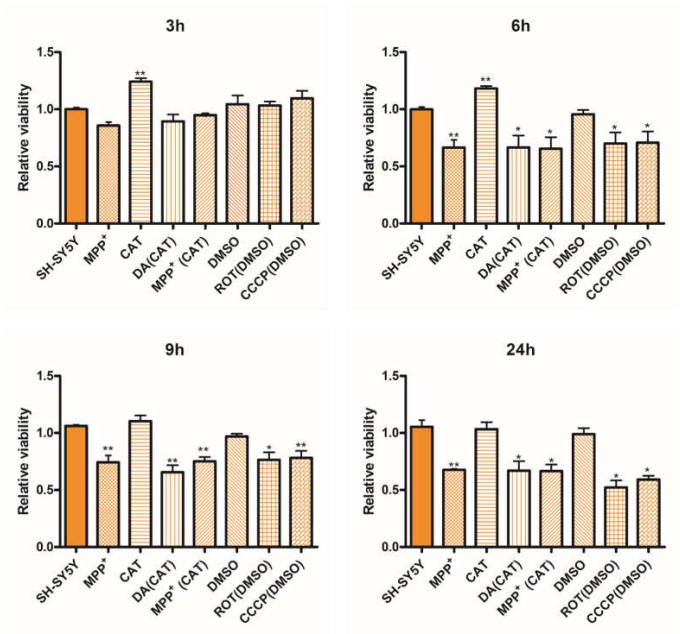

Figure 5.1: Cell viability of SH-SY5Y cells. Relative cell viability after 3, 6, 9 and 24 hours of treatments with several mitochondrial toxins. *, $p<0.05$; **, $p<0.01$.

Molecular characterization of mitochondrial network alterations

To evaluate protein level of OPA1, MFN1, PINK1, VDAC1 and COX5β, SH-SY5Y cells were treated with several mitochondrial toxins (see Table 5.1) and quantitative Western blot analysis was performed.

In order to evaluate whether mitophagy was impaired by DA, MPP^+ and rotenone, PINK1 protein levels were evaluated. As shown in Figure 5.2, PINK1 protein was detectable only in SH-SY5Y cells treated with CCCP treatment (from 6 hours of treatment and subsequent time points), used as a positive control.

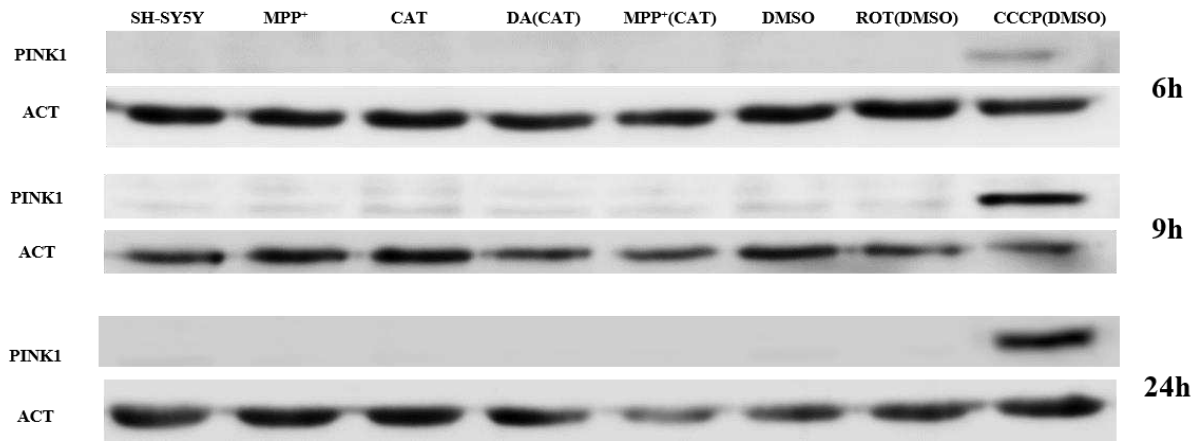

Figure 5.2: Representative Western blot of the effect of DA, MPP^+, rotenone and CCCP treatments on PINK1 accumulation at different time points.

To investigate effects on the mitochondrial mass induced by toxic treatments, Western blot quantification of cytochrome c oxidase subunit 5 β (COX5β), localized in the inner mitochondrial membrane, and voltage-dependent anion-selective channel protein 1 (VDAC1), localized in the outer mitochondrial membrane, was carried out.

As COX5β is concerned, no significant variation was highlighted after rotenone and MPP^+ treatments (MPP^+ with or without catalase). Conversely, after 24 hours of DA treatment, samples showed reduced levels of COX5β. Also, CCCP treatment reduced COX5β level (≈50 % reduction after 6 hours and subsequent time points) (Figure 5.3).

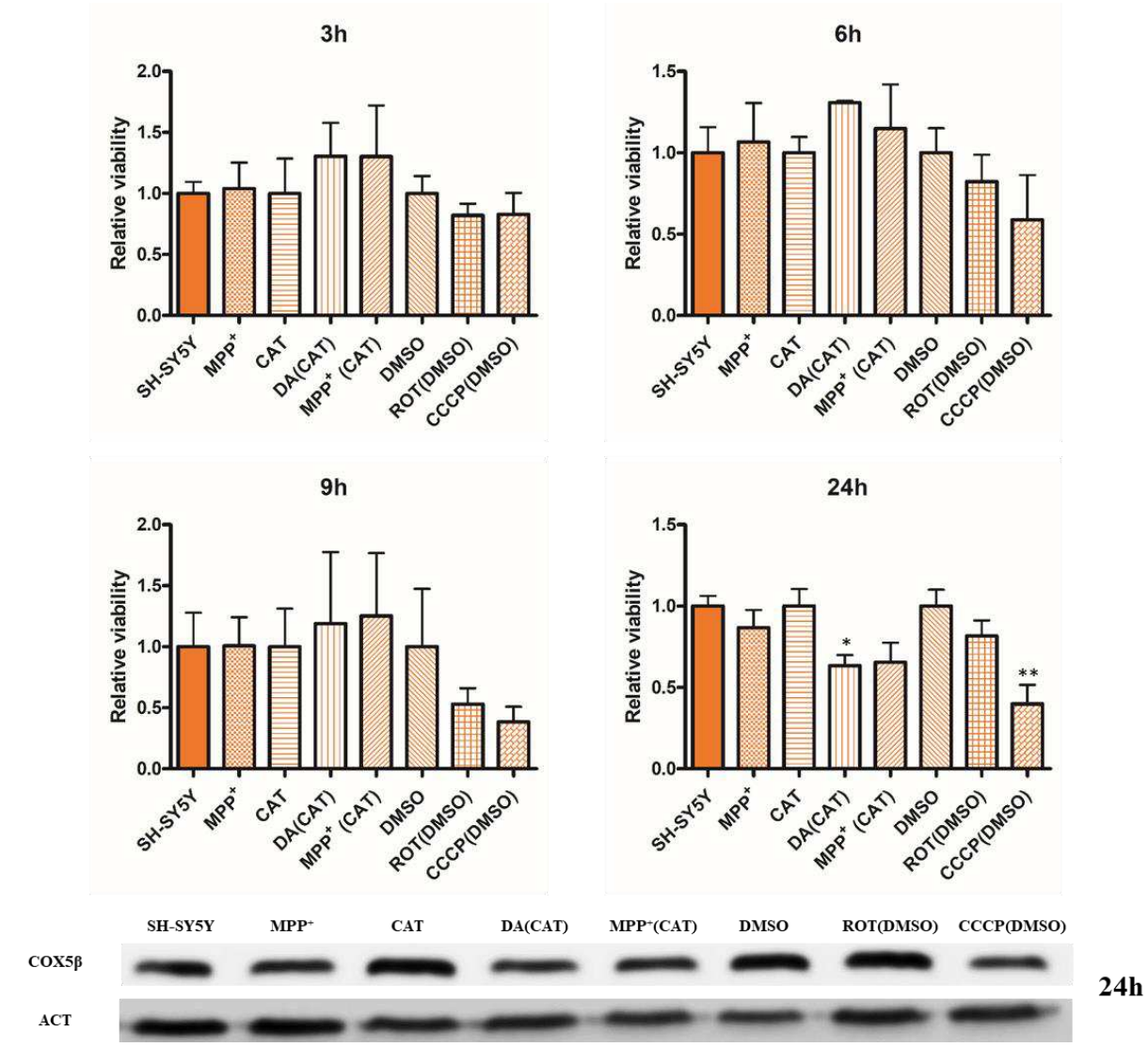

Figure 5.3: Effect of treatments on COX5β. Top: Relative quantification of COX5β. Bars represent the mean of three independent experiments on SH-SY5Y cells treated for 3,6, 9 and 24 hours. Error bars represent SEM of three experiments. *, $p<0.05$; **, $p<0.01$. Bottom: Representative Western blot of the effect of DA, MPP^+, rotenone and CCCP treatments on COX5β at 24 hours.

As VDAC1 is concerned, 24 hours DA treatment caused the reduction of its levels of approximately 60%. On the other hand, 24 hours MPP^+ treatments induced an increase of VDAC1 level (Figure 5.4).

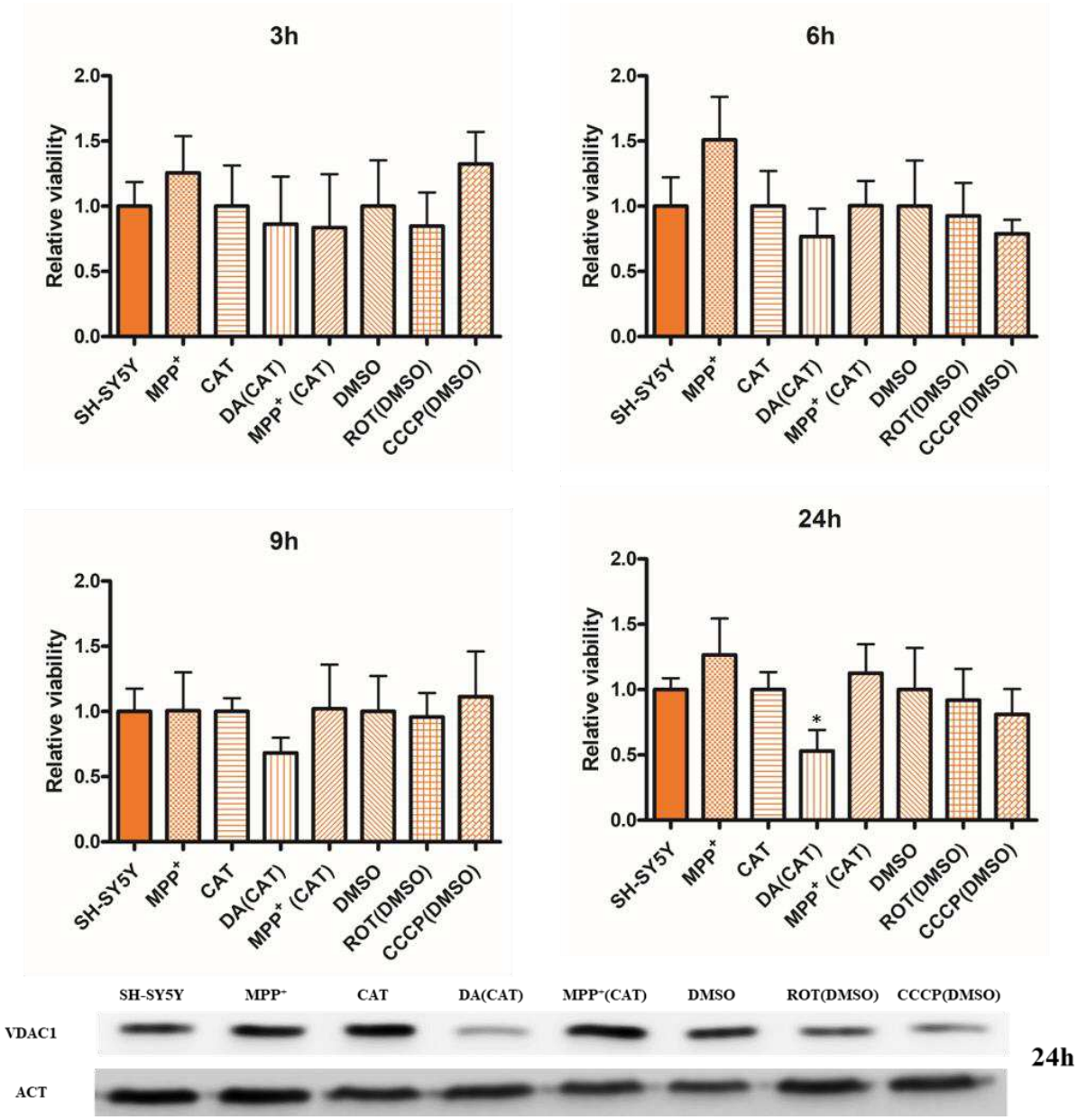

Figure 5.4: Effect of treatments on VDAC1. Top: Relative quantification of VDAC1. Bars represent the mean of three independent experiments on SH-SY5Y cells treated for 3,6, 9 and 24 hours. Error bars represent SEM of three experiments. *, $p<0.05$; **, $p<0.01$. Bottom: Representative Western blot of the effect of DA, MPP^+, rotenone and CCCP treatments on VDAC1 at 24 hours.

Abundance and modifications of OPA1 and MFN1 in all experimental conditions were considered, since their role in influencing mitochondrial dynamics. After CCCP treatment, down-regulation of MFN1 was observed. Three hours of CCCP treatment induced a reduction of 50% of MFN1 protein level. Conversely, other treatments did not have any effect on MFN1 (Figure 5.5).

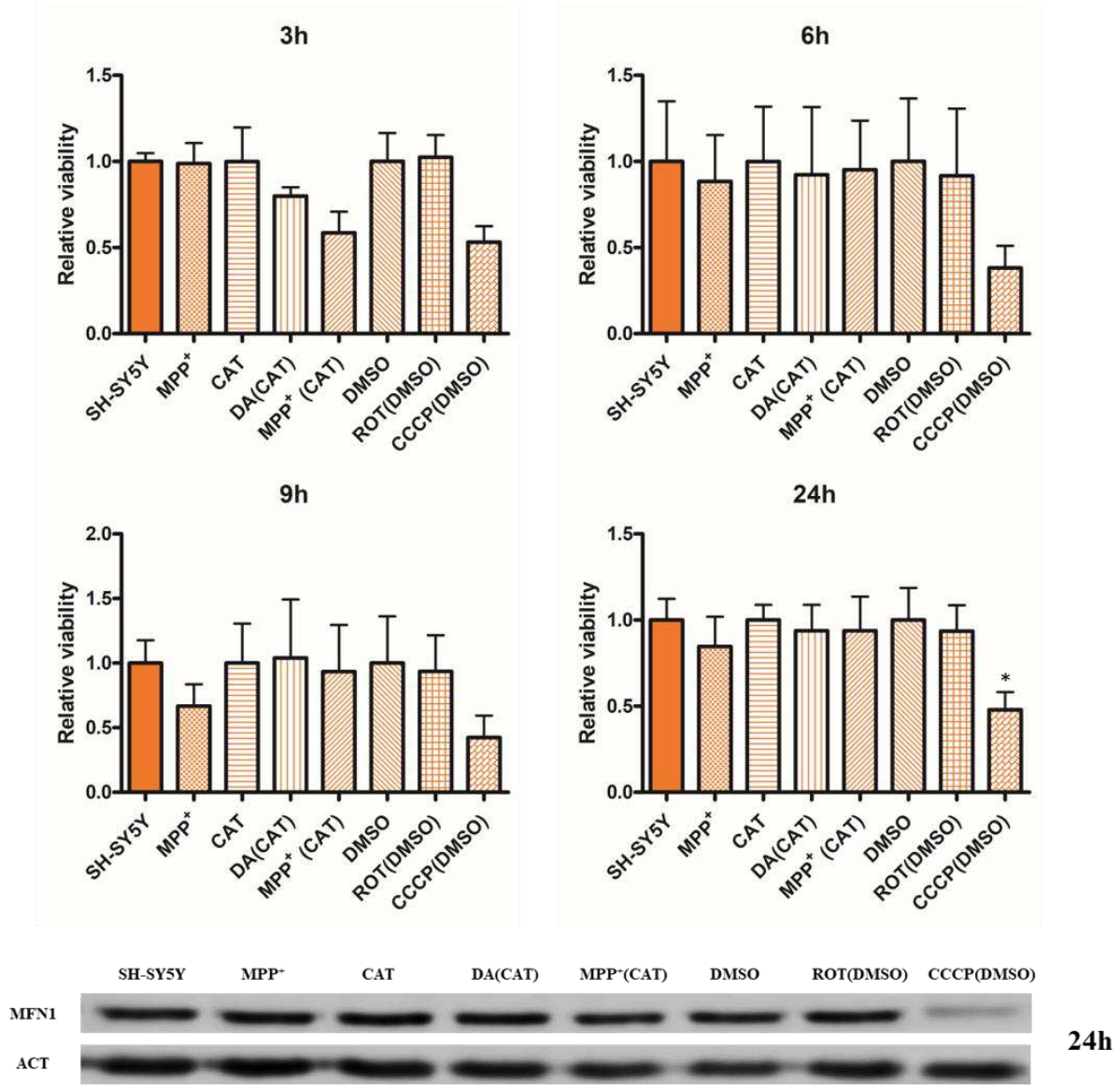

Figure 5.5: Effect of treatments on MFN1. Top: Relative quantification of MFN1. Bars represent the mean of three independent experiments on SH-SY5Y cells treated for 3,6, 9 and 24 hours. Error bars represent SEM of three experiments. *, $p<0.05$; **, $p<0.01$. Bottom: Representative Western blot of the effect of DA, MPP^+, rotenone and CCCP treatments on MFN1 at 24 hours.

As OPA1 is concerned, from 9 hours on, DA and MPP^+ treatments lowered its levels (50% reduction of both the long L-OPA1 and the short S-OPA1 forms at 24 hours; Figure 5.6). On the other hand, CCCP induced the disappearance of L-OPA1 (Figure 5.6).

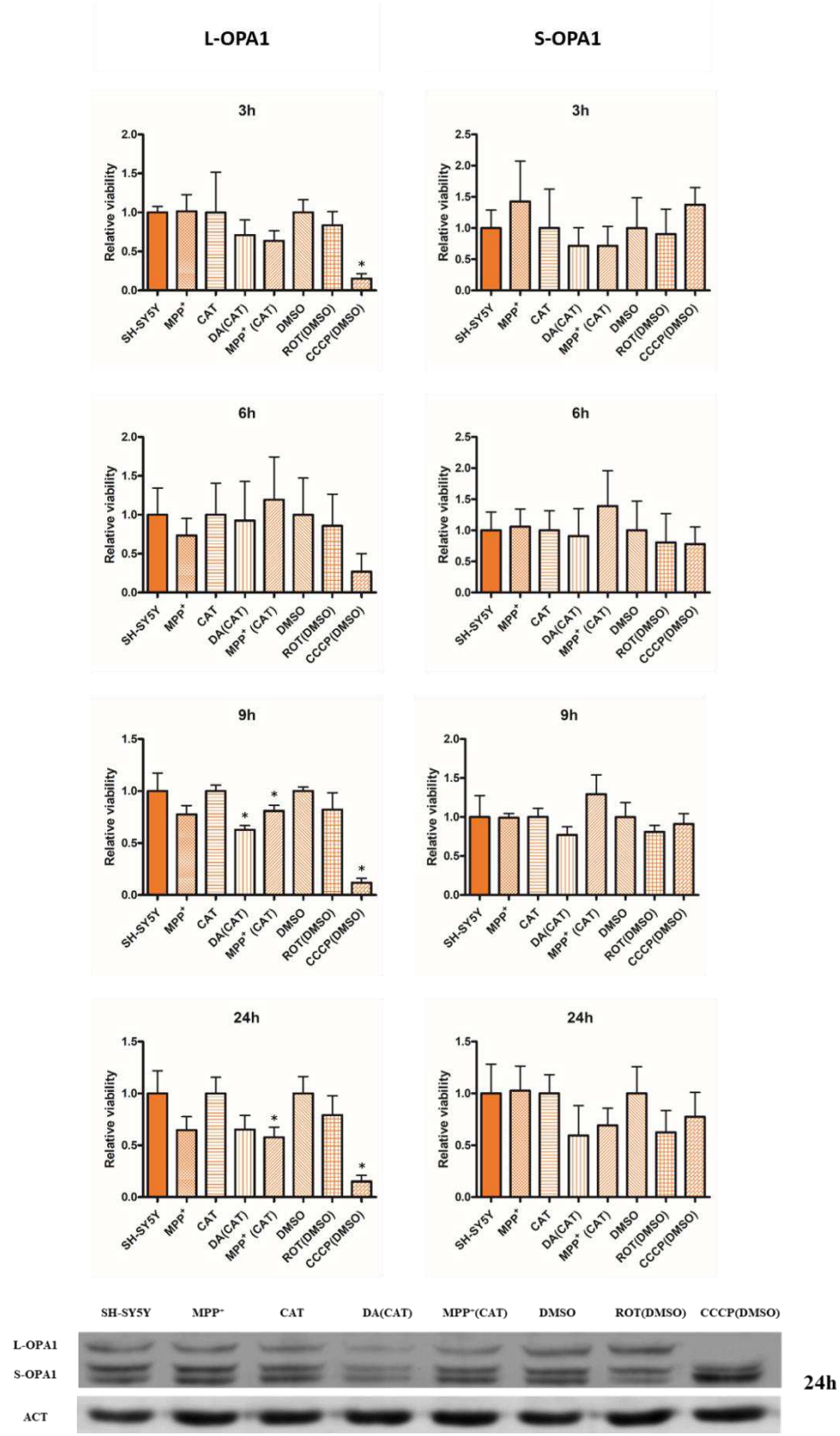

Figure 5.6: Effect of treatments on OPA1. Top: Bars represent the mean of three independent experiments on SH-SY5Y cells treated for 3, 6, 9 and 24 hours. Error bars represent SEM of three experiments. *, $p<0.05$; **, $p<0.01$. Bottom: Representative Western blot of the effect of DA, MPP^+, rotenone and CCCP treatments on OPA1 at 24 hours. Two forms are visible, the longest form (L-OPA1) and the shortest (S-OPA1).

Effect on mitochondrial membrane potential (Δψm) after treatments

In order to determine the effect of treatments on mitochondrial function, living cells were stained with Mitotracker Red CMXRos, which accumulates in mitochondria with an intact membrane potential. Treatment of SH-SY5Y cells with DA, MPP^+, rotenone and CCCP for 24 hours induced a comparable loss of the mitochondrial membrane potential (≈50-60% reduction) (Figure 5.7, Supplemental Figure 5.1)

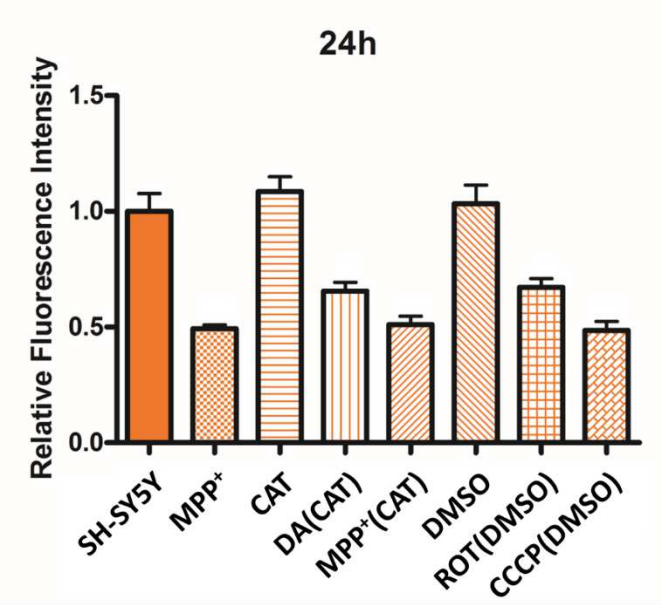

Figure 5.7: Effect of treatments on Δψm. Bars represent the mean of seven fields of SH-SY5Y cells treated for 24 hours. Error bars represent SEM of seven fields of view. Statistical test will be performed after data collection from at least three biological replicates.

PART VI

Discussion and Conclusion

6.1

Discussion

Neurodegenerative disorders, such as AD, PD and ALS are multi-factorial in nature, involving several genetic mutations (in coding or regulatory regions) and epigenetic and environmental factors (Landgrave-Gómez et al., 2015). The main clinical manifestation (movement disorders, cognitive impairment and/or psychiatric disturbances) depends on the neuron population being primarily affected. Complex and multifactorial neurodegenerative diseases can be investigated using a holistic approach that can give a global view about the pathogenetic process and shed light on specific and generic pathways of neurodegeneration (Fasano et al., 2017). Proteomics offers a global molecular snapshot of proteins and consequently of processes that may influence neuronal death. The proteome in fact provides a dynamic view of what is happening in the system under investigation, because the expression of proteins, their abundance, their localization in tissues or cells, the type and amount of their post-translational changes depend from the environment and from the cellular physiological state (Santos and Lindner, 2017). Therefore, all the projects presented in this thesis, by combining bioinformatics tools with proteomics, aimed at highlighting biochemical processes shared by different neurodegenerative diseases and disease-specific pathways, which may justify the degeneration of dopaminergic neurons in PD. Finally, a focus on the mitochondrial interactome and proteome intended to elucidate important specific steps of the degenerative process in PD.

The Meta-Neuro Project

To identify specific biochemical processes involved in the loss of dopaminergic neurons in PD, all papers containing proteomics experiments about neuronal modifications in PD, ALS (motor disorder caused by motor neurons death), and AD (non-motor neurodegenerative disease, used as control) were considered, including papers on human tissues, animal models and cellular models, and excluding

papers about pharmacological effects of particular molecules or peripheral biomarkers. The strength of the meta-analysis approach is to consider at the same time the results of many studies, derived from different models, thus filtering out experimental bias and highlighting really relevant mechanisms. However, this approach has some shortcomings. First, only quantitative proteomics studies were included (post-translational modifications were excluded from the analysis). To solve this issue, proteomics data were merged with information coming from a genetic database (DisGeNET). Another weakness is the few proteomics information about ALS (9 papers) compared to those of PD (46 papers) and AD (40 papers). Consequently, the molecular snapshot obtained for ALS was more incomplete than those generated for PD and AD.

To identify disease-specific pathways and biochemical processes shared by the three neurodegenerative diseases, an ORA on the "_Proteins" input lists was performed, using the GO consortium. By the comparison of over-represented pathways, it was possible to identify processes common to all three diseases that were general hallmarks of cell death. Indeed, the ORA underlined the over-representation of the apoptotic process (used as a kind of positive control), oxidative stress and ROS damage and electron transport chain (ETC). The respiratory chain, especially in pathological conditions, can be a source of ROS. A high level of ROS causes a damage to various cellular components and ultimately results in the activation of apoptosis (Li et al., 2013). Regarding ALS specific-pathways, the involvement of RNA processing was particularly evident. Metabolism ("rRNA metabolic process", "ncRNA metabolic process"), transport ("nuclear transport", "Nuclear import", and "RNA transport") and splicing ("mRNA splicing") were ALS specific over-represented GO. Alteration of RNA metabolism in ALS was already described. First of all, the majority of the genetic mutations observed in familial ALS (TARDBP, FUS, ANG and SETX) can impact directly on either gene transcription, pre-mRNA splicing, ribonucleoprotein complex formation, transport, RNA translation or degradation (Strong, 2010). Moreover, it was observed that neurofilament aggregates are due to a selective disturbance in the steady state levels of their mRNA. Indeed, mRNA of low molecular weight neurofilament proteins (68 kDa) is suppressed, while the mRNA of intermediate molecular weight (160 kDa, NFM) or high molecular weight neurofilaments (200 kDa, NFH) are more stabilized. NFM and NFH generate aggregates (Menzies et al., 2002).

By contrast, cytoskeleton organization, ion homeostasis and lipid biosynthetic process resulted to be altered only in AD. Although alteration at the mitochondrial level (membrane organization and mitochondrial transport) were over-represented in AD and PD, notably, "mitophagy" was involved in PD only. Alteration of the mitochondrial quality control and the consequent mitochondrial impairment have been widely associated to apoptosis directly triggered by these organelles ("apoptotic mitochondrial changes") (Perkins et al., 2009).

The analysis of the three "_Proteins" lists displayed a major overlap between PD and ALS compared to the comparison of AD and ALS. There is an extensive evidence that supports the close relationship between ALS and PD at the clinical (Belin et al., 2015), genetic (Körner et al., 2013) and neuroimaging (Cistaro et al., 2014) levels, in humans and in preclinical models (Ingre et al., 2015). On the contrary, ALS and AD comorbidity has never been reported. Indeed, the molecular overlapping in our analysis resulted to be scarce.

To identify PD-specific proteins, all the proteins shared by AD and ALS were eliminated and an "only-PD_Proteins" list was generated. Twentyfive of these proteins were also found in the DisGeNET database. They probably constitute major molecular hallmarks of PD, since they were never found to be altered in the other two pathologies and were reported both at the proteomic and the genetic levels. Among these PD hallmarks, transaldolase was identified. Transaldolase has already been identified in T-lymphocytes as part of a protein signature, able to discriminate PD patients from control subjects and patients affected by atypical parkinsonism (Alberio et al., 2012). Therefore, this protein may mirror at the peripheral level an alteration occurring in the CNS (Licker et al., 2014). Moreover, since this evidence was only based on one paper in the literature (Licker et al., 2014), the up-regulation of the protein was verified in five SN specimens of PD patients, with respect to five control subjects. As a proof-of-principle of our bioinformatics analysis, the increased level of the protein was confirmed in the experimental analysis. Although it is difficult to speculate about the link between a single protein and a complex, multifactorial disease, transaldolase is involved in the pentose phosphate pathway that regulates mitochondrial homeostasis in the presence of enhanced oxidative stress (Perl et al., 2011). The ORA of the "only- PD_Proteins" list highlighted the importance of mitophagy (GO pathways analysis) and some signal transduction cascades, such as the Wnt signalling pathway (L'Episcopo et al., 2014).

Eventually, PD-specific protein complexes were unravelled. The analysis of PD specific networks evidenced four protein complexes: the proteasome 26S, the ETC complex III, the CCT complex, and the PPP2A complex. Quantitative information about proteins of these complexes were retrieved from original papers. Since it was impossible to compare papers using different scales and normalization methods, variations were categorized as up- or down-regulations. In the proteasome complex, it was possible to identify a different action of the PD pathogenetic process on the expression of members of the catalytic subunit (proteasome 20S, all up-regulated) and of the regulatory subunit (proteasome 19S, all down-regulated). The involvement of the ETC dysfunction in PD has always been related to complex I (Amo et al., 2014), nevertheless, considering all the results together it was possible to highlight also the role of complex III. In the ETC complex III, proteins were reported to be regulated in different directions by the original papers, probably because of the use of different models (Morais

et al., 2014). This may indicate different alterations in the respiratory chain due to different perturbations. Another PD-specific complex was composed by chaperonins (CCT complex) that play an active role in the protection of dopaminergic neurons (Imai et al., 2003). All the proteins of the CCT complex were reported as down-regulated in the papers considered in the meta- analysis, probably indicating an overwhelming of their re-folding/protective capacities. Some of these chaperonins are direct interactors of the PPP2A complex. PPP2A is a protein complex composed by structural (A), regulatory/targeting (B), and catalytic (C) subunits. This phosphatase controls Akt phosphorylation and thus macro autophagy (Klionsky et al., 2016), the activity of tyrosine hydroxylase (Hua et al., 2015) and α-syn aggregation (Wu et al., 2012).

The ProLyPALS Project

PD and ALS probably share common pathways of neurodegeneration even though occurring in different cell types, as evidenced in the literature and by the meta-analysis of the Meta-Neuro project discussed above. As a matter of fact, the frequency of extrapyramidal symptoms in ALS patients is significantly higher than in the general population. ALS patients showing parkinsonian signs and symptoms (ALS-PD) may evidence altered protein levels and pathways, responsible of the manifestation of both diseases. From a genetic point of view, they may present mutations in genes previously linked with ALS or PD only (Körner et al., 2013). It has been demonstrated that the mutation of several genes (VCP, CHMP2B, PFN1, and C9ORF72 for example) induced high susceptibility to develop forms of comorbidity between ALS and PD (Seilhean et al., 2009; Chiò et al., 2012; Gilbert et al., 2010). Thus, there are several commonly altered mechanisms between these two pathologies and ALS-PD patients demonstrate this strong association.

To verify alterations retrieved by the meta-analysis and to find new potential molecular factors specifically involved in comorbidity of these two pathologies, a 2-DE analysis of PBMCs samples of patients with ALS, PD and ALS patients with parkinsonian signs (ALS-PD) was performed and a systems biology approach was used to unravel the involvement of biochemical pathways responsible for the degeneration of different neuronal populations.

2- DE analysis allowed to investigate hundreds of proteins simultaneously, providing information about molecular weight, pI, quantity, and possible post-translational modifications. In particular, protein hydrolysis was highlighted and the change in abundance of several proteins was attributed to an increase in their degradation. For example, FGA molecular weight is 95 kDa, whereas in our study a spot corresponding to a fragment of this protein was identified at 10 kDa.

The cellular source exploited in the present project were PBMCs. Their easiness of sampling permits large-scale validation studies for biomarkers search. They are mainly composed by T-lymphocytes, which patrol what is happening at the central level (Fasano et al., 2008). T-lymphocyte proteome changes may be a valid tool to classify PD and ALS patients. In fact, it has been demonstrated that they reflect the functional impairment of SN dopaminergic neurons (Pacheco et al., 2009) and the same alterations in the level of enzymes involved in the oxidative phosphorylation reported in the spinal cord of PD patients (Ladd et al., 2014). In addition, they have also been used as reporters of pathogenetic events involved in ALS (Nardo et al., 2009). Indeed, PBMCs displayed traits such as intracellular calcium dysregulation (Curti et al., 1996) and glutamatergic dysfunction (Poulopoulou et al., 2005) typical of ALS patients. For these reasons, PBMCs were the best cellular model that could be recovered from patients without invasive samplings. However, the particular sensitivity of circulating cells to other inflammatory states and drug therapies needs a word of caution during patients enrolment and in interpreting results. In fact, only subjects who did not report an inflammatory pathology in the 15 days before the blood collection were enrolled.

The pharmacological therapy is a confounding factor and therefore its effect was eliminated and carefully consider in recruitment criteria. ALS-PD subjects at the time of withdrawal were either in treatment or not with riluzole. This is the reason why both ALS patients under drug treatment (ALS_r) and subjects newly diagnosed and not yet in treatment with riluzole (ALS) were recruited. The effect of drug treatment on lymphocytes' proteome was largely demonstrated in the literature. For example, L-DOPA and DA agonists induce modifications in the proteome of T-lymphocytes (Alberio et al., 2012). No one of the ALS-PD subjects enrolled were in treatment with drugs for PD and therefore only PD patients recently diagnosed and not yet under pharmacological treatment were recruited. Once the effect due to riluzole was eliminated, all ALS patients were considered as a homogeneous group (ALS_all). As a consequence, the group resulted more comparable with the ALS-PD group for the categories "years from the diagnosis" and "severity of the pathology".

A power analysis was performed to decide the correct number of subjects to be enrolled for each group, in order to highlight differences of 65% in protein levels. Considering the variability among subjects, 20 patients were recruited for each group. However, the comorbidity between ALS and PD is quite a rare pathology. Therefore, all the patients visited in the last year at the PD and ALS Centres of the Department of Neuroscience of the University of Torino have been enrolled. The small number of ALS-PD patients was overcome by our analysis, because we used ALS and PD patients for the construction of a discriminating model and ALS-PD patients as a test set. A supervised analysis was used to classify the enrolled subjects. However, the Wilcoxon test with a permissive p value ($p<0.2$) and without the correction for multiple testing was used to select features to be used in the

construction of a discriminating model (LDA). In addition, the substitution of missing values of the spots selected was performed only after the univariate test, to avoid data manipulation and the introduction of biases. Final model, constructed with the spot selected by the Wilcoxon test, was validated by the k-fold method (the more robust one) in an iterative way. The model that demonstrated the best sensibility and specificity (sensibility = 97.5% and specificity = 100%) in the cross-validation was chosen as the reference one, and the 33 spots used to generate the model were selected.

The prediction classified five ALS-PD patients as PD and four subjects as ALS patients. This was quite surprising since ALS-PD patients are subjects that firstly present ALS and develop PD signs only in a second moment. However, their classification as PD subjects can be due to several factors: early appearance of parkinsonism, severity of parkinsonian signs, familiarity with PD, mutations in genes commonly involved in PD. To this purpose, the results of the analysis will be merged with other data from patients (such as the genetic screening for the classical PD genes, DATscan analysis of ALS-PD patients and MDS-UPDRS score), in order to better justify the ALS-PD classification.

In addition, several features were analysed in detail. For example, it is largely known that mutations in Cu,Zn-superoxide dismutase-1 (SOD1) are causative for familial forms of ALS (Saccon et al., 2013). Anyway, it is quite surprising that the levels of this protein contributed to the multivariate classification of ALS patients in PBMCs samples, even in comparison with another neurodegenerative disease. Several selected spots resulted to correspond to fibrinogen. In a proteomics study on total lymphocytes from PD patients, it was demonstrated that two different isoforms of gamma fibrinogen either correlated with the disease state or with the disease duration (Mila et al., 2009). Instead, total beta fibrinogen levels were found to be reduced in T-lymphocytes of PD patients (Alberio et al., 2012). Again, all forms of fibrinogen were down-represented in PBMCs of PD patients (down-regulation of beta and gamma fibrinogen and up-regulation of a cleaved form of alpha-fibrinogen), even if compared with ALS patients' samples. Another interesting result is the involvement of several glycolytic enzymes, Phosphoglycerate mutase 1, Alpha-enolase and Pyruvate kinase, in the classification of ALS-PD patients. Also, ORA highlighted the involvement of glycolysis (Reactome pathway analysis). It has recently been demonstrated that in PD patient PBMCs, mitochondrial dysfunction is associated with a concomitant increase in the glycolytic flux, independently for the glucose uptake or the monocyte activation (Smith et al., 2018). Moreover, others selected spots were proteins of the cytoskeleton (TUBB1, TUBB2A, ACTB, TUBA1C) or proteins associated to cytoskeleton (MSN, VCL, ACTN1, CAPZB and WDR1). An altered expression of cytoskeletal proteins was recently reported also by a RNA-seq analysis of PBMCs of sporadic and familiar ALS patients (Gagliardi et al., 2018).

The MitoNet Project

All data obtained from previously discussed projects highlighted that several molecular pathways implicated in PD aetiology converge on mitochondria. To focus on the main mitochondrial processes involved in PD, an updated version of the functional mitochondrial human proteome network was generated and used to map PD-specific proteins obtained by the meta-analysis. The neXtProt database (official HPP database) was used as reference to retrieve all high-quality proteins annotated as mitochondrial in subcellular location and GO Cellular Component sections. Only gold annotations were considered, in order to be more robust in the definition of mitochondrial proteins. In this way, proteins synthesized in mitochondria, proteins imported into the mitochondrion and proteins transiently associated or imported only in particular conditions were considered. NeXtProt PE5 entries were neglected from the analysis because they are uncertain protein predictions that may correspond to erroneous translations of pseudogenes, long non-coding RNA or other kinds of non-coding elements. 1413 IDs were annotated as "Gold" mitochondrial proteins in neXtProt database and were used to generate the updated version of the functional mitochondrial human proteome network (Fasano et al., 2016). To create this tool, a network-based analysis was performed, using the high-quality protein-protein interaction information from neXtProt (Lane et al., 2014). Mitochondrial proteins that were retrieved thanks to annotations in subcellular location and GO Cellular Component sections may not be exclusively mitochondrial, since other cellular locations may be reported. Indeed, according to the Human Protein Atlas, more than half of the human proteome has multiple subcellular localizations, either simultaneously occurring within a cell or alternatively occurring at different stages of the cell cycle (Thul et al., 2017). Indeed only 4% (36) of proteins were exclusively mitochondrial, whereas the majority of them had other cellular locations (93% of mitochondrial proteins were also localized in the cytoplasm and 41% of mitochondrial proteins were also localized in the nucleus). These localizations may also be due to the fact that nuclei and cytoplasm are the major contaminants when isolating mitochondria (Alberio et al., 2017). Nevertheless, it is well known that many proteins translocate from the nucleus to mitochondria and viceversa following several stimuli, contributing, for example, to mitochondrial biogenesis and functionality during stress and aging (Lionaki et al., 2016). The functional mitochondrial human proteome network was used to focus on mitochondrial protein complexes or biochemical pathways potentially involved in PD. 675 proteins have already been related specifically to PD ("only-PD_Proteins" list of the Meta-Neuro project). 31% of PD-related proteins mapped on the functional mitochondrial human proteome network, highlighting the central role of mitochondria in this pathology. Moreover, using this approach, it was possible to eliminate all proteins that were not mitochondrial (or associated with this organelle) and identify only mitochondrial pathways altered by PD pathogenesis. To this purpose, an ORA was performed. Mitophagy

("Pink/Parkin Mediated Mitophagy" and "Mitophagy") and "mitochondrial protein import" were over-represented. Mutations in PINK1 and Parkin genes have been associated with familial forms of PD. Nevertheless, several pieces of evidence suggest that dysfunctional, depolarized mitochondria are not properly disposed also in the sporadic forms of the disease, thereby contributing to bioenergetic failure and oxidative stress (Bondi et al., 2015; Zilocchi et al., 2018). Moreover, the alteration of proteins involved in the protein import into the mitochondrion is probably due to mitochondrial membrane potential loss (Pickles et al., 2018). An interesting result was the over-representation of the "regulation of neurotransmitter transport" (using as reference GO BP database). It has already been proposed that synapse dysfunction is an early and leading event in determining neuronal degeneration and loss in PD (Monti et al., 2015).

The DynaMoParD Project

The final aim of the present project will be the generation of a dynamic model of the "PD mitochondrion", to describe mathematically what happens in mitochondria of PD patients. The proposed model will focus on a particular type of cellular model of PD (human neuroblastoma cells treated with mitochondrial toxins). The model will adopt a fuzzy logic-based formalism that will provide a temporal simulation of the system. To this purpose, preliminary data were collected about several proteins involved in mitochondrial dynamics, such as mitophagy, fusion and fission. Next steps will be the generation of many other wet results and their integration, to generate membership functions of the fuzzy-model, with the final aim to use the virtual "PD mitochondrion" as a simulation platform.

Mitochondria play important roles in many cellular activities (*e.g.,* energy production, metabolism, aging and cell death) (Itoh et al., 2013). Neurons contain many mitochondria to satisfy their high request of ATP (Kageyama et al., 2013). Mitochondria are maintained as short tubular structures, which are highly dynamic and move, divide, and fuse by fission and fusion pathways. Mitochondrial fission is mediated by DRP1, a soluble cytosolic protein that assembles into spiral filaments around mitochondrial tubules. MFF, FIS1 are OMM proteins and have been proposed as DRP1 receptors. Several different post-translational modifications, including phosphorylation, ubiquitination and sumoylation of DRP1 regulate its interactions with mitochondria (Wilson et al., 2013). The Drp1 spiral has been proposed to constrict mitochondrial tubules through conformational changes, driven by GTP hydrolysis (Wilson et al., 2013). Mitochondrial fusion is mediated by MFNs (MFN1 and MFN2) and OPA1. MFNs are localized in the OMM, fuse the mitochondrial membranes of adjacent tubules through homotypic and heterotypic interactions (Song et al., 2009). OPA1 is localized in the IMM and interacts with MFNs to form intermembrane protein complexes that couple the fusion of outer

membranes to that of the inner membranes (Song et al., 2009). Loss of either MFNs or OPA1 leads to a similar mitochondrial fragmentation phenotype, suggesting that both outer and inner membrane fusion processes are affected. The dynamic behaviour of mitochondria allows the segregation of damaged mitochondria via the fission process and exchange of material between healthy mitochondria via the fusion process (van der Bliek et al., 2013). Additionally, mitophagy is triggered in the presence of severely damaged or superfluous mitochondria. Damaged mitochondria are isolated from the mitochondrial network and sequestered in autophagosomes to be delivered to lysosomes for degradation (Youle and Narendra, 2011). One of the most studied mechanisms for mitophagy in mammalian cells is the PINK1/Parkin-mediated mitophagy pathway. Briefly, a loss of $\Delta\psi m$ is thought to be sufficient to induce PINK1 accumulation in the OMM, PINK1-induced phosphorylation of ubiquitin and parkin, and parkin-mediated ubiquitination of OMM proteins (including VDAC1) (Gao et al., 2015).

Many neurodegenerative diseases are associated with alterations in the fission and fusion of mitochondria (Cho et al., 2009). However, the impairment of the mitochondrial quality control could be the primary cause of the PD pathogenesis (Polyzos and McMurray, 2017).

To retrieve data about molecular factors involved in mitochondrial dynamics (fusion and fission) and mitophagy, different cellular models of mitochondrial impairment were used. In particular, human neuroblastoma cells (SH-SY5Y) were treated i) with inhibitors of ETC complex I (500 nM rotenone and 2.5 mM MPP^+) (Langston et al., 1984), ii) by the administration of exogenous DA (250 μM) in the culture medium to mimic the altered DA homeostasis that seems to be an important cellular pathogenetic mechanism involved in PD (Alberio et al.,2014; Bondi et al., 2015); and iii) with the uncoupler CCCP (20 μM), used as a reference model of PINK1/Parkin mitophagic pathway induction (Narendra et al., 2010). The optimal concentration of toxins (DA, MPP^+, rotenone and CCCP) was determined by the neutral red assay, in order to obtain comparable levels of cell death after 24 hours exposure to all toxins.

SH-SY5Y treated with CCCP for 24 hours showed depolarized mitochondria. Moreover, all molecular alterations observed can be explained in light of inhibited fusion and induced mitophagy. Indeed, MFN1 was down- regulated, thus preventing the fusion of the OMMs (Bondi et al., 2015), PINK1 was accumulated and several mitochondrial proteins (such as COX5β) were reduced, as a consequence of mitochondrial elimination by mitophagy. Transmission electron microscope (TEM) images of this toxic model confirmed this view, showing the presence of many vacuoles and mitochondria fused with phagosomes (Zilocchi et al., 2018).

On the other hand, SH-SY5Y treated for 24 hours with DA, MPP^+ or Rotenone showed a different behaviour. A similar mitochondrial depolarization was observed, comparable to the Δψm loss induced by CCCP, however, this event seemed not to be followed by a proper disposal of depolarized mitochondria. Indeed, the number of mitochondria was not lowered. Moreover, human neuroblastoma cells treated with DA or MPP^+ or rotenone did not show significant alterations in MFN1 protein levels, thus suggesting that fusion of the OMM was not blocked. Moreover, both long and short forms of OPA1 decreased. These data suggest an impairment of the IMM fusion. Moreover, PINK1 did not accumulate on the OMM (impairment of mitophagy). As concerns COX5β levels, a protein of the IMM normally used as mitochondrial marker, was reduced after MPP^+ and DA treatments (Bondi et al., 2015; Zilocchi et al., 2018). Levels of the OMM protein VDAC1 were analyzed. Indeed, besides its role in energetic metabolism, VDAC1 is also involved in the regulation of calcium homeostasis and in the mitochondria-mediated apoptosis (Naghdi and Hajnóczky, 2016). Moreover, it has been proposed that VDACs play an essential role in recruiting Parkin to defective mitochondria, in order to eliminate them through mitophagy, even if their actual role in triggering this process seems to be controversial (Narendra et al., 2010). VDAC1 protein level was decreased after DA treatment (Alberio et al., 2014), probably degraded by mitochondrial proteases, as already suggested (Di Pierro et al., 2016). By contrast, MPP^+ treatment caused an increase of VDAC1 level.

Taken together, these data provide a static snapshot of cellular events activated or inhibited after toxic treatments. To overcome this drawback, a fuzzy model was constructed (Figure 6.1).

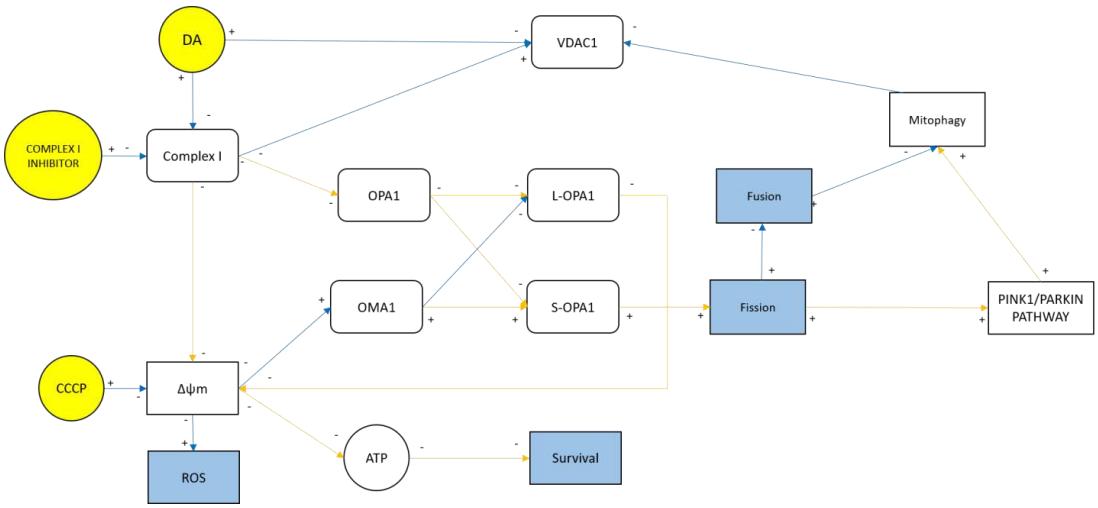

Figure 6.1: Network map of the model of mitochondrial dynamics (fusion and fission) and mitophagy. Circles represent metabolites and ions, rounded rectangles represent proteins and rectangles represent pathways or cellular processes. Blue nodes represent model's output, while yellow nodes represent model's input.

The fuzzy model of mitochondrial dynamics and mitophagy was formalized as a graph (represented in Figure 6.1) composed of 17 nodes. The components were divided in 3 categories: molecules and ions (circles in Figure 6.1), pathway and cellular processes (rectangles in Figure 6.1), and proteins (rounded rectangle in Figure 6.1). - while edges represented the known positive and negative regulations among these components. Associated with each node, a set of membership functions was defined to represent multiple states of the nodes; in order to describe the interactions existing among them, a set of fuzzy logic rules was also defined for each node. The input nodes of the model are Complex I inhibitor (MPP^+ and rotenone), DA and CCCP. These nodes were not regulated by any other node and their value must be specified by the user for each simulation.

At this moment only preliminary data were collected and this information is not enough to define membership functions (IF <antecedent> THEN <consequent>). Thus, it will be necessary to collect many other experimental data after the different mitochondrial insults (*i.e.,* DA, rotenone, MPP^+ and CCCP) at different time points (3, 6, 9 and 24 hours). In particular, for each time point, it will be necessary to obtain experimental information about protein level of VDAC1, COX5β, MFN1, OPA1-L, OPA1-S and PINK1 (by Western blot analysis); mRNA level of VDAC1, PINK1 and OPA1 (by Real time PCR); $\Delta\psi m$ (by mitotracker staining), calcium ion flux to mitochondria (using recombinant aequorin targeted to mitochondria), ROS level (through 2' 7'-dichlorofluorescein diacetate) and intracellular concentration of toxins. This last point will be fundamental. Indeed, the intracellular concentration of toxins represents the input of the dynamic model. To obtain an estimation of toxin intakes, which is a function of time, a computer simulation using cellular survival data will be used. This would be possible because we observed a biological effect (cell death) as a function of time and we assume that cell death depends on the intracellular toxin concentrations. To verify the obtained values, as a proof of principle, the intracellular concentration of DA will be experimentally evaluated by a spectrophotometric method. The absorbance at 600 nm of dopamine coordinated with Fe(III) will be monitored over time using a spectrophotometer. Therefore, the intracellular concentration of dopamine will be determined by lysing cells, adding Fe(III) and interpolating absorbance values with a calibration curve previously generated (Guo et al., 2009).

6.2

Conclusion

Neurodegenerative disorders, such as PD and ALS, represent a wide spectrum of pathologies characterized by the death of specific neuronal subtypes. The main clinical manifestation (movement disorders, cognitive impairment, and/or psychiatric disturbances) depends on the neuron population being primarily affected. ALS and PD aetiology and pathogenesis have not been completely characterized. To identify general and disease-specific patterns of neurodegeneration, a meta-analysis of the literature of all proteomics investigations about PD and ALS was performed. Regarding the ALS specific-pathways, the involvement of RNA processing was particularly evident: mRNA metabolism, transport, and splicing were all over-represented ontologies. Instead, PD-specific proteins were those involved in cellular response to stress, mitochondrion organization, mitophagy and protein synthesis.

Nevertheless, there is also an extensive evidence that demonstrates the close relationship between ALS and PD. Indeed, the frequency of extrapyramidal symptoms in ALS patients is significantly higher than in the general population. ALS patients showing parkinsonian signs and symptoms (ALS-PD) may evidence altered protein levels and pathways, which lead to the manifestation of both diseases. To characterize ALS patients who display parkinsonian signs, proteomics analysis of PBMCs of ALS-PD, ALS and PD patients was performed. This approach highlighted common alterations among ALS-PD subjects and ALS or PD patients. In particular, several proteins that have already associated to PD or ALS contributed to the multivariate classification of ALS-PD patients in PBMCs samples, such as SOD1 (involved in genetic form of ALS), FGG (correlated with PD state or with the disease duration) and FGB (protein levels already found to be reduced in T-lymphocytes of PD patients). Another interesting result was the alteration observed in the glycolytic process in ALS-PD patients. Indeed, it has already been reported that in PBMCs of PD patients, mitochondrial dysfunction causes an abnormal activation of glycolysis.

Again, mitochondria seem to have a pivotal role in PD pathogenesis. Although many neurodegenerative diseases are associated with alterations at the mitochondrial level, the impairment of the mitochondrial quality control seems to lead PD pathogenesis, since several molecular pathways implicated in PD aetiology converge on mitochondria. To focus on the main mitochondrial processes involved in PD, PD-specific proteins obtained by the meta-analysis were mapped on the functional mitochondrial human proteome network. This analysis highlighted that 31% of PD-specific proteins were mitochondrial proteins or associated with mitochondria. Moreover, ORA highlighted the central role of mitophagy, mitochondrial protein import and mitochondrial transport in PD.

Considering all the results so far obtained, it will be interesting to generate a dynamic model to describe what happens in mitochondria of PD patients. To this purpose, preliminary data were collected about several proteins involved in mitophagy, fusion and fission pathways, in cellular models of mitochondrial impairment due to mitochondrial toxins related to PD. Next goal will be to obtain more molecular information about mitochondrial dynamics and elimination. All these data will be used to generate membership functions of a fuzzy-model of the "PD mitochondrion", to be further used as a simulation platform. For instance, this model could be used to understand what happens at the mitochondrial level during PD pathogenesis and to simulate the action of drugs on the nodes to revert the process. For example, the reduced activity of PINK1 is linked to PD pathogenesis. Using this model, it could be possible to investigate the action of drugs able to activate PINK1 and estimate their rescue potential. However, this model has some limitations. First of all, it could be used only to evaluate the mitochondrial behaviour in neuronal cells after the treatment with mitochondrial toxins. Moreover, this model takes into account only three mitochondrial processes (mitophagy, fusion and fission), while mitochondrial network is involved in many other pathways. Additionally, only the PINK1/Parkin mitophagic process has been considered, while it has already been demonstrated that other proteins are involved in mitochondrial disposal (such as BNIP3).

To conclude, the main aim of this thesis was to identify the pathways involved specifically in PD pathogenesis using proteomics and bioinformatics. Proteomics provides a global snapshot at the molecular level, thus allowing for the identification of processes that regulate the pathogenetic process. In the last decade, the proteomic community focused its attention on neurodegenerative diseases. However, a relevant limitation so far observed was the lack of proper controls, aimed at filtering out aspecific pathways of neurodegeneration/neuroinflammation. Therefore, the solution proposed in the present thesis was the use of other neurodegenerative diseases as a "control", to remove all pathways that are involved in generic processes of neuronal death. Another limitation of proteomics studies on neurodegenerative disorders is the static view they convey. Indeed, investigated models are usually considered at a single time point, with no consideration for systems dynamics. Conversely, to obtain

a comprehensive image of altered processes in neurodegeneration, it would be important to observe how specific molecular factors and pathways are dysregulated during disease progression.

PART VII

References

Agosta F, Al-Chalabi A, Filippi M, Hardiman O, Kaji R, Meininger V, Nakano I, Shaw P, Shefner J, van den Berg LH, Ludolph A; WFN Research Group on ALS/MND. The El Escorial criteria: strengths and weaknesses. Amyotroph Lateral Scler Frontotemporal Degener. 2015 Mar;16(1-2):1-7. doi: 10.3109/21678421.2014.964258. Epub 2014 Dec 8. PubMed PMID: 25482030.

Alberio T, Bossi AM, Milli A, Parma E, Gariboldi MB, Tosi G, Lopiano L, Fasano M. Proteomic analysis of dopamine and α-synuclein interplay in a cellular model of Parkinson's disease pathogenesis. FEBS J. 2010 Dec;277(23):4909-19. doi: 10.1111/j.1742-4658.2010.07896.x. Epub 2010 Oct 26. PubMed PMID: 20977677.

Alberio T, Pippione AC, Zibetti M, Olgiati S, Cecconi D, Comi C, Lopiano L, Fasano M. Discovery and verification of panels of T-lymphocyte proteins as biomarkers of Parkinson's disease. Sci Rep. 2012;2:953. doi: 10.1038/srep00953. Epub 2012 Dec 11. PubMed PMID: 23233872.

Alberio T, Bondi H, Colombo F, Alloggio I, Pieroni L, Urbani A, Fasano M. Mitochondrial proteomics investigation of a cellular model of impaired dopamine homeostasis, an early step in Parkinson's disease pathogenesis. Mol Biosyst. 2014 Jun;10(6):1332-44. doi: 10.1039/c3mb70611g. Epub 2014 Mar 28. PubMed PMID:24675778.

Alberio T, Pieroni L, Ronci M, Banfi C, Bongarzone I, Bottoni P, Brioschi M, Caterino M, Chinello C, Cormio A, Cozzolino F, Cunsolo V, Fontana S, Garavaglia B, Giusti L, Greco V, Lucacchini A, Maffioli E, Magni F, Monteleone F, Monti M, Monti V, Musicco C, Petrosillo G, Porcelli V, Saletti R, Scatena R, Soggiu A, Tedeschi G, Zilocchi M, Roncada P, Urbani A, Fasano M. Toward the Standardization of Mitochondrial Proteomics: The Italian Mitochondrial Human Proteome Project Initiative. J Proteome Res. 2017 Dec 1;16(12):4319-4329. doi: 10.1021/acs.jproteome.7b00350. Epub 2017 Sep 13. PubMed PMID: 28828861.

Alm E, Arkin AP. Biological networks. Curr Opin Struct Biol. 2003 Apr;13(2):193-202. Review. PubMed PMID: 12727512.

Amo T, Saiki S, Sawayama T, Sato S, Hattori N. Detailed analysis of mitochondrial respiratory chain defects caused by loss of PINK1. Neurosci Lett. 2014 Sep 19;580:37-40. doi: 10.1016/j.neulet.2014.07.045. Epub 2014 Aug 1. PubMed PMID: 25092611.

Andersen PM, Al-Chalabi A. Clinical genetics of amyotrophic lateral sclerosis:what do we really know? Nat Rev Neurol. 2011 Oct 11;7(11):603-15. doi:10.1038/nrneurol.2011.150. Review. PubMed PMID: 21989245.

Anjo SI, Santa C, Manadas B. SWATH-MS as a tool for biomarker discovery: From basic research to clinical applications. Proteomics. 2017 Feb;17(3-4). doi:10.1002/pmic.201600278. Review. PubMed PMID: 28127880.

Annesi G, Savettieri G, Pugliese P, D'Amelio M, Tarantino P, Ragonese P, La Bella V, Piccoli T, Civitelli D, Annesi F, Fierro B, Piccoli F, Arabia G, Caracciolo M, Cirò Candiano IC, Quattrone A. DJ-1 mutations and parkinsonism-dementia-amyotrophic lateral sclerosis complex. Ann Neurol. 2005 Nov;58(5):803-7. PubMed PMID: 16240358.

Antonov AV, Dietmann S, Rodchenkov I, Mewes HW. PPI spider: a tool for the interpretation of proteomics data in the context of protein-protein interaction networks. Proteomics. 2009 May;9(10):2740-9. doi: 10.1002/pmic.200800612. PubMed PMID: 19405022.

Antonov AV. BioProfiling.de: analytical web portal for high-throughput cell biology. Nucleic Acids Res. 2011 Jul;39(Web Server issue):W323-7. doi: 10.1093/nar/gkr372. Epub 2011 May 23. PubMed PMID: 21609949.

Arthur KC, Calvo A, Price TR, Geiger JT, Chiò A, Traynor BJ. Projected increase in amyotrophic lateral sclerosis from 2015 to 2040. Nat Commun. 2016 Aug 11;7:12408. doi: 10.1038/ncomms12408. PubMed PMID: 27510634.

Assenov Y, Ramírez F, Schelhorn SE, Lengauer T, Albrecht M. Computing topological parameters of biological networks. Bioinformatics. 2008 Jan 15;24(2):282-4. Epub 2007 Nov 15. PubMed PMID: 18006545.

Baker MS, Ahn SB, Mohamedali A, Islam MT, Cantor D, Verhaert PD, Fanayan S, Sharma S, Nice EC, Connor M, Ranganathan S. Accelerating the search for the missing proteins in the human proteome. Nat Commun. 2017 Jan 24;8:14271. doi: 10.1038/ncomms14271. Review. PubMed PMID: 28117396.

Bartocci E, Lió P. Computational Modeling, Formal Analysis, and Tools for Systems Biology. PLoS Comput Biol. 2016 Jan 21;12(1):e1004591. doi: 10.1371/journal.pcbi.1004591. eCollection 2016 Jan. Review. PubMed PMID: 26795950; PubMed Central PMCID: PMC4721667.

Bastian M, Heymann S, Jacomy M. Gephi:an open source software for exploring and manipulating networks. International AAAI Conference on Weblogs and Social Media; 2009 May 17–20; San Jose (CA).

Beal MF. Mitochondrial dysfunction in neurodegenerative diseases. BiochimBiophys Acta. 1998 Aug 10;1366(1-2):211-23. Review. PubMed PMID: 9714810.

Belin J, Gordon PH, Guennoc AM, De Toffol B, Corcia P. Brait-Fahn-Schwarz disease: the missing link between ALS and Parkinson's disease. Amyotroph Lateral Scler Frontotemporal Degener. 2015 Mar;16(1-2):135-6. doi:10.3109/21678421.2014.948880. Epub 2014 Aug 15. PubMed PMID: 25125199.

Benabou R, Waters C. Hepatotoxic profile of catechol-O-methyltransferase inhibitors in Parkinson's disease. Expert Opin Drug Saf. 2003 May;2(3):263-7. Review. PubMed PMID: 12904105.

Benson DA, Karsch-Mizrachi I, Lipman DJ, Ostell J, Wheeler DL. GenBank. Nucleic Acids Res. 2005 Jan 1;33(Database issue):D34-8. PubMed PMID: 15608212.

Bienert S, Waterhouse A, de Beer TA, Tauriello G, Studer G, Bordoli L, Schwede T. The SWISS-MODEL Repository-new features and functionality. Nucleic Acids Res. 2017 Jan 4;45(D1):D313-D319. doi: 10.1093/nar/gkw1132. Epub 2016 Nov 29. PubMed PMID: 27899672.

Bizzarri M, Palombo A, Cucina A. Theoretical aspects of Systems Biology. Prog Biophys Mol Biol. 2013 May;112(1-2):33-43. doi: 10.1016/j.pbiomolbio.2013.03.019. Epub 2013 Apr 3. Review. PubMed PMID: 23562476.

Blandini F, Armentero MT. Animal models of Parkinson's disease. FEBS J. 2012 Apr;279(7):1156-66. doi: 10.1111/j.1742-4658.2012.08491.x. Epub 2012 Feb 28. Review. PubMed PMID: 22251459.

Blesa J, Trigo-Damas I, Quiroga-Varela A, Jackson-Lewis VR. Oxidative stress and Parkinson's disease. Front Neuroanat. 2015 Jul 8;9:91. doi:10.3389/fnana.2015.00091. eCollection 2015. Review. PubMed PMID: 26217195.

Bondi H, Zilocchi M, Mare MG, D'Agostino G, Giovannardi S, Ambrosio S, Fasano M, Alberio T. Dopamine induces mitochondrial depolarization without activating PINK1-mediated mitophagy. J Neurochem. 2015 Dec 28. doi: 10.1111/jnc.13506. [Epub ahead of print] PubMed PMID: 26710242.

Bonifati V, Rizzu P, Squitieri F, Krieger E, Vanacore N, van Swieten JC, Brice A, van Duijn CM, Oostra B, Meco G, Heutink P. DJ-1(PARK7), a novel gene for autosomal recessive, early onset parkinsonism. Neurol Sci. 2003 Oct;24(3):159-60. PubMed PMID: 14598065.

Bose A, Beal MF. Mitochondrial dysfunction in Parkinson's disease. J Neurochem. 2016 Oct;139 Suppl 1:216-231. doi: 10.1111/jnc.13731. Epub 2016 Aug 21. Review. PubMed PMID: 27546335.

Burns A, Iliffe S. Alzheimer's disease. BMJ. 2009 Feb 5;338:b158. doi:10.1136/bmj.b158. Review. Erratum in: BMJ. 2009 Apr 1. doi: 10.1136/bmj.b1349.PubMed PMID: 19196745.

Burté F, De Girolamo LA, Hargreaves AJ, Billett EE. Alterations in the mitochondrial proteome of neuroblastoma cells in response to complex 1 inhibition. J Proteome Res. 2011 Apr 1;10(4):1974-86. doi: 10.1021/pr101211k. Epub 2011 Mar 10. PubMed PMID: 21322648.

Byrne S, Bede P, Elamin M, Kenna K, Lynch C, McLaughlin R, Hardiman O. Proposed criteria for familial amyotrophic lateral sclerosis. Amyotroph Lateral Scler. 2011 May;12(3):157-9. doi: 10.3109/17482968.2010.545420. Epub 2011 Jan 5. PubMed PMID: 21208036.

Caudle WM, Richardson JR, Wang MZ, Taylor TN, Guillot TS, McCormack AL, Colebrooke RE, Di Monte DA, Emson PC, Miller GW. Reduced vesicular storage of dopamine causes progressive nigrostriatal neurodegeneration. J Neurosci. 2007 Jul 25;27(30):8138-48. PubMed PMID: 17652604.

Cerami EG, Gross BE, Demir E, Rodchenkov I, Babur O, Anwar N, Schultz N, Bader GD, Sander C. Pathway Commons, a web resource for biological pathway data. Nucleic Acids Res. 2011 Jan;39(Database issue):D685-90. doi: 10.1093/nar/gkq1039. Epub 2010 Nov 10. PubMed PMID: 21071392.

Chan DC. Dissecting mitochondrial fusion. Dev Cell. 2006 Nov;11(5):592-4. PubMed PMID: 17084350.

Chandramouli K, Qian PY. Proteomics: challenges, techniques and possibilities to overcome biological sample complexity. Hum Genomics Proteomics. 2009 Dec 8;2009. pii: 239204. doi: 10.4061/2009/239204. PubMed PMID: 20948568.

Chatr-Aryamontri A, Oughtred R, Boucher L, Rust J, Chang C, Kolas NK, O'Donnell L, Oster S, Theesfeld C, Sellam A, Stark C, Breitkreutz BJ, Dolinski K, Tyers M. The BioGRID interaction database: 2017 update. Nucleic Acids Res. 2017 Jan 4;45(D1):D369-D379. doi: 10.1093/nar/gkw1102. Epub 2016 Dec 14. PubMed PMID: 27980099.

Chaudhuri KR, Yates L, Martinez-Martin P. The non-motor symptom complex of Parkinson's disease: a comprehensive assessment is essential. Curr Neurol Neurosci Rep. 2005 Jul;5(4):275-83. Review. PubMed PMID: 15987611.

Cheah BC, Vucic S, Krishnan AV, Kiernan MC. Riluzole, neuroprotection and amyotrophic lateral sclerosis. Curr Med Chem. 2010;17(18):1942-199. Review. PubMed PMID: 20377511.

Chen C, Huang H, Wu CH. Protein Bioinformatics Databases and Resources. Methods Mol Biol. 2017;1558:3-39. doi: 10.1007/978-1-4939-6783-4_1. Review. PubMed PMID: 28150231.

Chen H, Chan DC. Critical dependence of neurons on mitochondrial dynamics. Curr Opin Cell Biol. 2006 Aug;18(4):453-9. Epub 2006 Jun 14. Review. PubMed PMID: 16781135.

Chen Y, Bodles AM. Amyloid precursor protein modulates beta-catenin degradation. J Neuroinflammation. 2007 Dec 10;4:29. PubMed PMID: 18070361.

Chen Y, Dorn GW 2nd. PINK1-phosphorylated mitofusin 2 is a Parkin receptor for culling damaged mitochondria. Science. 2013 Apr 26;340(6131):471-5. doi: 10.1126/science.1231031. PubMed PMID: 23620051.

Chiò A, Calvo A, Mazzini L, Cantello R, Mora G, Moglia C, Corrado L, D'Alfonso S, Majounie E, Renton A, Pisano F, Ossola I, Brunetti M, Traynor BJ, Restagno G; PARALS. Extensive genetics of ALS: a population-based study in Italy. Neurology.2012 Nov 6;79(19):1983-9. doi: 10.1212/WNL.0b013e3182735d36. Epub 2012 Oct 24. PubMed PMID: 23100398.

Chiò A, Canosa A, Gallo S, Cammarosano S, Moglia C, Fuda G, Calvo A, Mora G; PARALS group. ALS clinical trials: do enrolled patients accurately represent the ALS population? Neurology. 2011 Oct 11;77(15):1432-7. doi:10.1212/WNL.0b013e318232ab9b. Epub 2011 Sep 28. PubMed PMID: 21956723.

Chiò A, Logroscino G, Hardiman O, Swingler R, Mitchell D, Beghi E, Traynor BG; Eurals Consortium. Prognostic factors in ALS: A critical review. Amyotroph Lateral Scler. 2009 Oct-Dec;10(5-6):310-23. doi:10.3109/17482960802566824. Review. PubMed PMID: 19922118.

Cho DH, Nakamura T, Lipton SA. Mitochondrial dynamics in cell death and neurodegeneration. Cell Mol Life Sci. 2010 Oct;67(20):3435-47. doi: 10.1007/s00018-010-0435-2. Epub 2010 Jun 25. Review. PubMed PMID: 20577776.

Cistaro A, Cuccurullo V, Quartuccio N, Pagani M, Valentini MC, Mansi L. Role of PET and SPECT in the study of amyotrophic lateral sclerosis. Biomed Res Int. 2014;2014:237437. doi: 10.1155/2014/237437. Epub 2014 Apr 10. Review. PubMed PMID: 24818133.

Cobelli C, Dalla Man C, Toffolo G, Basu R, Vella A, Rizza R. The oral minimal model method. Diabetes. 2014 Apr;63(4):1203-13. doi: 10.2337/db13-1198. Review. PubMed PMID: 24651807.

Collins MA, An J, Hood BL, Conrads TP, Bowser RP. Label-Free LC-MS/MS Proteomic Analysis of Cerebrospinal Fluid Identifies Protein/Pathway Alterations and Candidate Biomarkers for Amyotrophic Lateral Sclerosis. J Proteome Res. 2015 Nov 6;14(11):4486-501. doi: 10.1021/acs.jproteome.5b00804. Epub 2015 Oct 8.PubMed PMID: 26401960

Conway KA, Rochet JC, Bieganski RM, Lansbury PT Jr. Kinetic stabilization of the alpha-synuclein protofibril by a dopamine-alpha-synuclein adduct. Science. 2001 Nov 9;294(5545):1346-9. PubMed PMID: 11701929.

Craig R, Cortens JP, Beavis RC. Open source system for analyzing, validating, and storing protein identification data. J Proteome Res. 2004 Nov-Dec;3(6):1234-42. PubMed PMID: 15595733.

Crosiers D, Theuns J, Cras P, Van Broeckhoven C. Parkinson disease: insights in clinical, genetic and pathological features of monogenic disease subtypes. J Chem Neuroanat. 2011 Oct;42(2):131-41. doi: 10.1016/j.jchemneu.2011.07.003. Epub 2011 Jul 26. Review. PubMed PMID: 21810464

Curti D, Malaspina A, Facchetti G, Camana C, Mazzini L, Tosca P, Zerbi F, Ceroni M. Amyotrophic lateral sclerosis: oxidative energy metabolism and calcium homeostasis in peripheral blood lymphocytes. Neurology. 1996 Oct;47(4):1060-4. PubMed PMID: 8857745.

Davidson B, Hadar R, Schlossberg A, Sternlicht T, Slipicevic A, Skrede M, Risberg B, Flørenes VA, Kopolovic J, Reich R. Expression and clinical role of DJ-1, a negative regulator of PTEN, in ovarian carcinoma. Hum Pathol. 2008 Jan;39(1):87-95. Epub 2007 Oct 18. PubMed PMID: 17949781.

Day JJ, Sweatt JD. Cognitive neuroepigenetics: a role for epigenetic mechanisms in learning and memory. Neurobiol Learn Mem. 2011 Jul;96(1):2-12. doi:10.1016/j.nlm.2010.12.008. Epub 2010 Dec 30. Review. PubMed PMID: 21195202.

de Lau LM, Breteler MM. Epidemiology of Parkinson's disease. Lancet Neurol. 2006 Jun;5(6):525-35. Review. PubMed PMID: 16713924.

Desai J, Swash M. Extrapyramidal involvement in amyotrophic lateral sclerosis: backward falls and retropulsion. J Neurol Neurosurg Psychiatry. 1999Aug;67(2):214-6. PubMed PMID: 10406993.

Deutsch EW, Csordas A, Sun Z, Jarnuczak A, Perez-Riverol Y, Ternent T, Campbell DS, Bernal-Llinares M, Okuda S, Kawano S, Moritz RL, Carver JJ, Wang M, Ishihama Y, Bandeira N, Hermjakob H, Vizcaíno JA. The ProteomeXchange consortium in 2017: supporting the cultural change in proteomics public data deposition. Nucleic Acids Res. 2017 Jan 4;45(D1):D1100-D1106. doi: 10.1093/nar/gkw936. Epub 2016 Oct 18. PubMed PMID: 27924013.

Deutsch EW, Sun Z, Campbell D, Kusebauch U, Chu CS, Mendoza L, Shteynberg D, Omenn GS, Moritz RL. State of the Human Proteome in 2014/2015 As Viewed through PeptideAtlas: Enhancing Accuracy and Coverage through the AtlasProphet. J Proteome Res. 2015 Sep 4;14(9):3461-73. doi: 10.1021/acs.jproteome.5b00500. Epub 2015 Jul 24. PubMed PMID: 26139527.

Dickson DW. Parkinson's disease and parkinsonism: neuropathology. Cold Spring Harb Perspect Med. 2012 Aug 1;2(8). pii: a009258. doi:10.1101/cshperspect.a009258. Review. PubMed PMID: 22908195.

Dimmer KS, Scorrano L. (De)constructing mitochondria: what for? Physiology (Bethesda). 2006 Aug;21:233-41. Review. PubMed PMID: 16868312.

Egan DF, Shackelford DB, Mihaylova MM, Gelino S, Kohnz RA, Mair W, Vasquez DS, Joshi A, Gwinn DM, Taylor R, Asara JM, Fitzpatrick J, Dillin A, Viollet B, Kundu M, Hansen M, Shaw RJ. Phosphorylation of ULK1 (hATG1) by AMP-activated protein kinase connects energy sensing to mitophagy. Science. 2011 Jan 28;331(6016):456-61. doi: 10.1126/science.1196371. Epub 2010 Dec 23. PubMed PMID: 21205641.

Eiyama A, Okamoto K. PINK1/Parkin-mediated mitophagy in mammalian cells. Curr Opin Cell Biol. 2015 Apr;33:95-101. doi: 10.1016/j.ceb.2015.01.002. Epub 2015 Feb 17. Review. PubMed PMID: 25697963.

Erol AM, Kilic AK, Celik A, Celik C, Basak AN. Brait-Fahn-Schwarz disease: Parkinson's disease and amyotrophic lateral sclerosis complex. Acta Neurol Belg. 2016 Sep;116(3):401-3. doi: 10.1007/s13760-015-0531-z. Epub 2015 Aug 29. PubMed PMID: 26319125.

Fabregat A, Jupe S, Matthews L, Sidiropoulos K, Gillespie M, Garapati P, Haw R, Jassal B, Korninger F, May B, Milacic M, Roca CD, Rothfels K, Sevilla C, Shamovsky V, Shorser S, Varusai T, Viteri G, Weiser J, Wu G, Stein L, Hermjakob H, D'Eustachio P. The Reactome Pathway Knowledgebase. Nucleic Acids Res. 2018 Jan 4;46(D1):D649-D655. doi: 10.1093/nar/gkx1132. PubMed PMID: 29145629.

Fasano M, Alberio T, Babu M, Lundberg E, Urbani A. Towards a functional definition of the mitochondrial human proteome. EuPA Open Proteom. 2016 Jan 7;10:24-27. doi: 10.1016/j.euprot.2016.01.004. eCollection 2016 Mar. PubMed PMID: 29900096.

Fasano M, Alberio T, Lopiano L. Peripheral biomarkers of Parkinson's disease as early reporters of central neurodegeneration. Biomark Med. 2008 Oct;2(5):465-78. doi: 10.2217/17520363.2.5.465. PubMed PMID: 20477424.

Fasano M, Monti C, Alberio T. A systems biology-led insight into the role of the proteome in neurodegenerative diseases. Expert Rev Proteomics. 2016 Sep;13(9):845-55. doi: 10.1080/14789450.2016.1219254. Epub 2016 Aug 22. Review. PubMed PMID: 27477319.

Fathinia P, Hermann A, Reuner U, Kassubek J, Storch A, Ludolph AC. Parkinson's disease-like midbrain hyperechogenicity is frequent in amyotrophic lateral sclerosis. J Neurol. 2013 Feb;260(2):454-7. doi: 10.1007/s00415-012-6654-8. Epub 2012 Aug 26. PubMed PMID: 22923257.

Fernández-Moriano C, González-Burgos E, Gómez-Serranillos MP. Mitochondria-Targeted Protective Compounds in Parkinson's and Alzheimer's Diseases. Oxid Med Cell Longev. 2015;2015:408927. doi: 10.1155/2015/408927. Epub 2015 Apr 29. Review. PubMed PMID: 26064418.

Gagliardi S, Zucca S, Pandini C, Diamanti L, Bordoni M, Sproviero D, Arigoni M, Olivero M, Pansarasa O, Ceroni M, Calogero R, Cereda C. Long non-coding and coding RNAs characterization in Peripheral Blood Mononuclear Cells and Spinal Cord from Amyotrophic Lateral Sclerosis patients. Sci Rep. 2018 Feb 5;8(1):2378. doi: 10.1038/s41598-018-20679-5. PubMed PMID: 29402919.

Gao F, Chen D, Si J, Hu Q, Qin Z, Fang M, Wang G. The mitochondrial protein BNIP3L is the substrate of PARK2 and mediates mitophagy in PINK1/PARK2 pathway. Hum Mol Genet. 2015 May 1;24(9):2528-38. doi: 10.1093/hmg/ddv017. Epub 2015 Jan 22. PubMed PMID: 25612572.

Gasser T. Molecular pathogenesis of Parkinson disease: insights from genetic studies. Expert Rev Mol Med. 2009 Jul 27;11:e22. doi: 10.1017/S1462399409001148. Review. PubMed PMID: 19631006.

Gaudet P, Michel PA, Zahn-Zabal M, Britan A, Cusin I, Domagalski M, Duek PD, Gateau A, Gleizes A, Hinard V, Rech de Laval V, Lin J, Nikitin F, Schaeffer M, Teixeira D, Lane L, Bairoch A. The neXtProt knowledgebase on human proteins: 2017 update. Nucleic Acids Res. 2017 Jan 4;45(D1):D177-D182. doi: 10.1093/nar/gkw1062. Epub 2016 Nov 29. PubMed PMID: 27899619.

Ghavami S, Shojaei S, Yeganeh B, Ande SR, Jangamreddy JR, Mehrpour M, Christoffersson J, Chaabane W, Moghadam AR, Kashani HH, Hashemi M, Owji AA, Łos MJ. Autophagy and apoptosis dysfunction in neurodegenerative disorders. Prog Neurobiol. 2014 Jan;112:24-49. doi: 10.1016/j.pneurobio.2013.10.004. Epub 2013 Nov 6. Review. PubMed PMID: 24211851.

Gilbert RM, Fahn S, Mitsumoto H, Rowland LP. Parkinsonism and motor neuron diseases: twenty-seven patients with diverse overlap syndromes. Mov Disord. 2010Sep 15;25(12):1868-75. doi: 10.1002/mds.23200. PubMed PMID: 20669307.

Glatter T, Wepf A, Aebersold R, Gstaiger M. An integrated workflow for charting the human interaction proteome: insights into the PP2A system. Mol Syst Biol. 2009;5:237. doi: 10.1038/msb.2008.75. Epub 2009 Jan 20. PubMed PMID:19156129.

Goedert M, Spillantini MG, Del Tredici K, Braak H. 100 years of Lewy pathology. Nat Rev Neurol. 2013 Jan;9(1):13-24. doi: 10.1038/nrneurol.2012.242. Epub 2012 Nov 27. Review. PubMed PMID: 23183883.

Goetz CG, Fahn S, Martinez-Martin P, Poewe W, Sampaio C, Stebbins GT, Stern MB, Tilley BC, Dodel R, Dubois B, Holloway R, Jankovic J, Kulisevsky J, Lang AE, Lees A, Leurgans S, LeWitt PA, Nyenhuis D, Olanow CW, Rascol O, Schrag A, Teresi JA, Van Hilten JJ, LaPelle N. Movement Disorder Society-sponsored revision of the Unified Parkinson's Disease Rating Scale (MDS-UPDRS): Process, format, and clinimetric testing plan. Mov Disord. 2007 Jan;22(1):41-7. PubMed PMID: 17115387.

Goh WW, Lee YH, Chung M, Wong L. How advancement in biological network analysis methods empowers proteomics. Proteomics. 2012 Feb;12(4-5):550-63. doi:10.1002/pmic.201100321. Epub 2012 Jan 19. Review. PubMed PMID: 22247042.

Goodsell DS, Dutta S, Zardecki C, Voigt M, Berman HM, Burley SK. The RCSB PDB "Molecule of the Month": Inspiring a Molecular View of Biology. PLoS Biol. 2015 May 5;13(5):e1002140. doi: 10.1371/journal.pbio.1002140. eCollection 2015 May. PubMed PMID: 25942442.

Gorman GS, Schaefer AM, Ng Y, Gomez N, Blakely EL, Alston CL, Feeney C, Horvath R, Yu-Wai-Man P, Chinnery PF, Taylor RW, Turnbull DM, McFarland R. Prevalence of nuclear and mitochondrial DNA mutations related to adult mitochondrial disease. Ann Neurol. 2015 May;77(5):753-9. doi: 10.1002/ana.24362. Epub 2015 Mar 28. PubMed PMID: 25652200.

Gui YX, Wang XY, Kang WY, Zhang YJ, Zhang Y, Zhou Y, Quinn TJ, Liu J, Chen SD. Extracellular signal-regulated kinase is involved in alpha-synuclein-induced mitochondrial dynamic disorders by regulating dynamin-like protein 1. Neurobiol Aging. 2012 Dec;33(12):2841-54. doi: 10.1016/j.neurobiolaging.2012.02.001. Epub 2012 Mar 22. PubMed PMID: 22445325.

Guo L, Zhang Y, Li Q. Spectrophotometric determination of dopamine hydrochloride in pharmaceutical, banana, urine and serum samples by potassium ferricyanide-Fe(III). Anal Sci. 2009 Dec;25(12):1451-5. PubMed PMID: 20009333.

Hastings TG. The role of dopamine oxidation in mitochondrial dysfunction: implications for Parkinson's disease. J Bioenerg Biomembr. 2009 Dec;41(6):469-72. doi: 10.1007/s10863-009-9257-z. PubMed PMID: 19967436.

Head B, Griparic L, Amiri M, Gandre-Babbe S, van der Bliek AM. Inducible proteolytic inactivation of OPA1 mediated by the OMA1 protease in mammalian cells. J Cell Biol. 2009 Dec 28;187(7):959-66. doi: 10.1083/jcb.200906083. PubMed PMID: 20038677.

Heberle H, Meirelles GV, da Silva FR, Telles GP, Minghim R. InteractiVenn: a web-based tool for the analysis of sets through Venn diagrams. BMC Bioinformatics. 2015 May 22;16:169. doi: 10.1186/s12859-015-0611-3. PubMed PMID: 25994840.

Hensley K, Mhatre M, Mou S, Pye QN, Stewart C, West M, Williamson KS. On the relation of oxidative stress to neuroinflammation: lessons learned from the G93A-SOD1 mouse model of amyotrophic lateral sclerosis. Antioxid Redox Signal.2006 Nov-Dec;8(11-12):2075-87. Review. PubMed PMID: 17034351.

Herrera A, Muñoz P, Steinbusch HWM, Segura-Aguilar J. Are Dopamine Oxidation Metabolites Involved in the Loss of Dopaminergic Neurons in the Nigrostriatal System in Parkinson's Disease? ACS Chem Neurosci. 2017 Apr 19;8(4):702-711. doi: 10.1021/acschemneuro.7b00034. Epub 2017 Mar 3. Review. PubMed PMID: 28233992.

Honig LS, Vellas B, Woodward M, Boada M, Bullock R, Borrie M, Hager K, Andreasen N, Scarpini E, Liu-Seifert H, Case M, Dean RA, Hake A, Sundell K, Poole Hoffmann V, Carlson C, Khanna R, Mintun M, DeMattos R, Selzler KJ, Siemers E. Trial of Solanezumab for Mild Dementia Due to Alzheimer's Disease. N Engl J Med. 2018 Jan 25;378(4):321-330. doi: 10.1056/NEJMoa1705971. PubMed PMID: 29365294.

Hosp F, Mann M. A Primer on Concepts and Applications of Proteomics in Neuroscience. Neuron. 2017 Nov 1;96(3):558-571. doi:10.1016/j.neuron.2017.09.025. Review. PubMed PMID: 29096073.

Hornburg D, Drepper C, Butter F, Meissner F, Sendtner M, Mann M. Deep proteomic evaluation of primary and cell line motoneuron disease models delineates major differences in neuronal characteristics. Mol Cell Proteomics. 2014 Dec;13(12):3410-20. doi: 10.1074/mcp.M113.037291. Epub 2014 Sep 5. PubMed PMID: 25193168

Hua G, Xiaolei L, Weiwei Y, Hao W, Yuangang Z, Dongmei L, Yazhuo Z, Hui Y. Protein phosphatase 2A is involved in the tyrosine hydroxylase phosphorylation regulated by α-synuclein. Neurochem Res. 2015 Mar;40(3):428-37. doi:10.1007/s11064-014-1477-x. Epub 2015 Jan 8. PubMed PMID: 25567480.

Imai Y, Soda M, Murakami T, Shoji M, Abe K, Takahashi R. A product of the human gene adjacent to parkin is a component of Lewy bodies and suppresses Pael receptor-induced cell death. J Biol Chem. 2003 Dec 19;278(51):51901-10. Epub 2003 Oct 7. PubMed PMID: 14532270.

Ingerman E, Perkins EM, Marino M, Mears JA, McCaffery JM, Hinshaw JE, Nunnari J. Dnm1 forms spirals that are structurally tailored to fit mitochondria. J Cell Biol. 2005 Sep 26;170(7):1021-7. PubMed PMID: 16186251.

Ingre C, Roos PM, Piehl F, Kamel F, Fang F. Risk factors for amyotrophic lateral sclerosis. Clin Epidemiol. 2015 Feb 12;7:181-93. doi: 10.2147/CLEP.S37505. eCollection 2015. Review. PubMed PMID: 25709501.

Itoh K, Nakamura K, Iijima M, Sesaki H. Mitochondrial dynamics in neurodegeneration. Trends Cell Biol. 2013 Feb;23(2):64-71. doi:10.1016/j.tcb.2012.10.006. Epub 2012 Nov 16. Review. PubMed PMID: 23159640

Jankovic J, Aguilar LG. Current approaches to the treatment of Parkinson's disease. Neuropsychiatr Dis Treat. 2008 Aug;4(4):743-57. PubMed PMID: 19043519.

Janković M, Svetel M, Kostić V. Frequency of REM sleep behavior disorders in patients with Parkinson's disease. Vojnosanit Pregl. 2015 May;72(5):442-6. PubMed PMID: 26165053.

Jin J, Meredith GE, Chen L, Zhou Y, Xu J, Shie FS, Lockhart P, Zhang J. Quantitative proteomic analysis of mitochondrial proteins: relevance to Lewy body formation and Parkinson's disease. Brain Res Mol Brain Res. 2005 Mar 24;134(1):119-38. Epub 2004 Nov 11. PubMed PMID: 15790536.

Johnson ME, Bobrovskaya L. An update on the rotenone models of Parkinson's disease: their ability to reproduce the features of clinical disease and model gene-environment interactions. Neurotoxicology. 2015 Jan;46:101-16. doi: 10.1016/j.neuro.2014.12.002. Epub 2014 Dec 13. Review. PubMed PMID: 25514659.

Johri A, Beal MF. Mitochondrial dysfunction in neurodegenerative diseases. J Pharmacol Exp Ther. 2012 Sep;342(3):619-30. doi: 10.1124/jpet.112.192138. Epub 2012 Jun 13. Review. PubMed PMID: 22700435.

Jorrin-Novo JV, Komatsu S, Sanchez-Lucas R, Rodríguez de Francisco LE. Gel electrophoresis-based plant proteomics: Past, present, and future. Happy 10th anniversary Journal of Proteomics! J Proteomics. 2018 Aug 29. pii: S1874-3919(18)30326-9. doi: 10.1016/j.jprot.2018.08.016. [Epub ahead of print] Review. PubMed PMID: 30170112.

Kageyama Y, Zhang Z, Sesaki H. Mitochondrial division: molecular machinery and physiological functions. Curr Opin Cell Biol. 2011 Aug;23(4):427-34. doi: 10.1016/j.ceb.2011.04.009. Epub 2011 May 10. Review. PubMed PMID: 21565481.

Kanehisa M, Furumichi M, Tanabe M, Sato Y, Morishima K. KEGG: new perspectives on genomes, pathways, diseases and drugs. Nucleic Acids Res. 2017 Jan 4;45(D1):D353-D361. doi: 10.1093/nar/gkw1092. Epub 2016 Nov 28. PubMed PMID: 27899662.

Kang Y, Fielden LF, Stojanovski D. Mitochondrial protein transport in health and disease. Semin Cell Dev Biol. 2018 Apr;76:142-153. doi:10.1016/j.semcdb.2017.07.028. Epub 2017 Jul 29. Review. PubMed PMID: 28765093.

Karren MA, Coonrod EM, Anderson TK, Shaw JM. The role of Fis1p-Mdv1p interactions in mitochondrial fission complex assembly. J Cell Biol. 2005 Oct 24;171(2):291-301. PubMed PMID: 16247028.

Khatri P, Sirota M, Butte AJ. Ten years of pathway analysis: current approaches and outstanding challenges. PLoS Comput Biol. 2012;8(2):e1002375. doi: 10.1371/journal.pcbi.1002375. Epub 2012 Feb 23. Review. PubMed PMID: 22383865.

Kiernan MC, Vucic S, Cheah BC, Turner MR, Eisen A, Hardiman O, Burrell JR, Zoing MC. Amyotrophic lateral sclerosis. Lancet. 2011 Mar 12;377(9769):942-55. doi: 10.1016/S0140-6736(10)61156-7. Epub 2011 Feb 4. Review. PubMed PMID: 21296405.

Kim RH, Peters M, Jang Y, Shi W, Pintilie M, Fletcher GC, DeLuca C, Liepa J, Zhou L, Snow B, Binari RC, Manoukian AS, Bray MR, Liu FF, Tsao MS, Mak TW. DJ-1, a novel regulator of the tumor suppressor PTEN. Cancer Cell. 2005 Mar;7(3):263-73. PubMed PMID: 15766664.

Kitano[a] H. Looking beyond the details: a rise in system-oriented approaches in genetics and molecular biology. Curr Genet. 2002 Apr;41(1):1-10. Epub 2002 Apr 4. Review. PubMed PMID: 12073094.

Kitano[b] H. Systems biology: a brief overview. Science. 2002 Mar 1;295(5560):1662-4. Review. PubMed PMID: 11872829.

Klionsky DJ, Abdelmohsen K, Abe A, Abedin MJ, Abeliovich H, Acevedo Arozena A, Adachi H, Adams CM, et al., Guidelines for the use and interpretation of assays for monitoring autophagy (3rd edition). Autophagy. 2016;12(1):1-222. doi: 10.1080/15548627.2015.1100356. Erratum in: Autophagy. 2016;12(2):443. Selliez, Iban [corrected to Seiliez, Iban]. PubMed PMID: 26799652

Kohl P, Crampin EJ, Quinn TA, Noble D. Systems biology: an approach. Clin Pharmacol Ther. 2010 Jul;88(1):25-33. doi: 10.1038/clpt.2010.92. Epub 2010 Jun 9. Review. PubMed PMID: 20531468.

Koopmans F, Ho JTC, Smit AB, Li KW. Comparative Analyses of Data Independent Acquisition Mass Spectrometric Approaches: DIA, WiSIM-DIA, and Untargeted DIA. Proteomics. 2018 Jan;18(1). doi: 10.1002/pmic.201700304. PubMed PMID: 29134766; PubMed Central PMCID: PMC5817406.

Körner S, Kollewe K, Ilsemann J, Müller-Heine A, Dengler R, Krampfl K, Petri S. Prevalence and prognostic impact of comorbidities in amyotrophic lateral sclerosis. Eur J Neurol. 2013 Apr;20(4):647-54. doi: 10.1111/ene.12015. Epub 2012Oct 25. PubMed PMID: 23094606.

Koshiba T, Detmer SA, Kaiser JT, Chen H, McCaffery JM, Chan DC. Structural basis of mitochondrial tethering by mitofusin complexes. Science. 2004 Aug 6;305(5685):858-62. PubMed PMID: 15297672.

Kubli DA, Gustafsson ÅB. Mitochondria and mitophagy: the yin and yang of cell death control. Circ Res. 2012 Oct 12;111(9):1208-21. doi:10.1161/CIRCRESAHA.112.265819. Review. PubMed PMID: 23065344.

L'Episcopo F, Tirolo C, Caniglia S, Testa N, Morale MC, Serapide MF, Pluchino S, Marchetti B. Targeting Wnt signaling at the neuroimmune interface for dopaminergic neuroprotection/repair in Parkinson's disease. J Mol Cell Biol. 2014 Feb;6(1):13-26. doi: 10.1093/jmcb/mjt053. Epub 2014 Jan 14. Review. PubMed PMID: 24431301

Ladd AC, Keeney PM, Govind MM, Bennett JP Jr. Mitochondrial oxidative phosphorylation transcriptome alterations in human amyotrophic lateral sclerosis spinal cord and blood. Neuromolecular Med. 2014 Dec;16(4):714-26. doi: 10.1007/s12017-014-8321-y. Epub 2014 Aug 1. PubMed PMID: 25081190.

Landgrave-Gómez J, Mercado-Gómez O, Guevara-Guzmán R. Epigenetic mechanisms in neurological and neurodegenerative diseases. Front Cell Neurosci. 2015 Feb 27;9:58. doi: 10.3389/fncel.2015.00058. eCollection 2015. Review. PubMed PMID:25774124.

Lane L, Bairoch A, Beavis RC, Deutsch EW, Gaudet P, Lundberg E, Omenn GS. Metrics for the Human Proteome Project 2013-2014 and strategies for finding missing proteins. J Proteome Res. 2014 Jan 3;13(1):15-20. doi: 10.1021/pr401144x. Epub 2013 Dec 23. PubMed PMID: 24364385

Laukens K, Naulaerts S, Berghe WV. Bioinformatics approaches for the functional interpretation of protein lists: from ontology term enrichment to network analysis. Proteomics. 2015 Mar;15(5-6):981-96. doi: 10.1002/pmic.201400296. Epub 2015 Feb 20. Review. PubMed PMID: 25430566.

Le Novère N. Quantitative and logic modelling of molecular and gene networks. Nat Rev Genet. 2015 Mar;16(3):146-58. doi: 10.1038/nrg3885. Epub 2015 Feb 3. Review. PubMed PMID: 25645874.

Li J, O W, Li W, Jiang ZG, Ghanbari HA. Oxidative stress and neurodegenerative disorders. Int J Mol Sci. 2013 Dec 16;14(12):24438-75. doi: 10.3390/ijms141224438. Review. PubMed PMID: 24351827.

Licker V, Turck N, Kövari E, Burkhardt K, Côte M, Surini-Demiri M, Lobrinus JA, Sanchez JC, Burkhard PR. Proteomic analysis of human substantia nigra identifies novel candidates involved in Parkinson's disease pathogenesis. Proteomics. 2014 Mar;14(6):784-94. doi: 10.1002/pmic.201300342. Epub 2014 Feb 18. PubMed PMID: 24449343.

Lionaki E, Gkikas I, Tavernarakis N. Differential Protein Distribution between the Nucleus and Mitochondria: Implications in Aging. Front Genet. 2016 Sep 16;7:162. eCollection 2016. Review. PubMed PMID: 27695477

Logroscino G, Traynor BJ, Hardiman O, Chiò A, Mitchell D, Swingler RJ, Millul A, Benn E, Beghi E; EURALS. Incidence of amyotrophic lateral sclerosis in Europe. J Neurol Neurosurg Psychiatry. 2010 Apr;81(4):385-90. doi:10.1136/jnnp.2009.183525. Epub 2009 Aug 25. PubMed PMID: 19710046.

Longo G, Miquel PA, Sonnenschein C, Soto AM. Is information a proper observable for biological organization? Prog Biophys Mol Biol. 2012 Aug;109(3):108-14. doi: 10.1016/j.pbiomolbio.2012.06.004. Epub 2012 Jul 13. Review. PubMed PMID: 22796169.

López OL, Dekosky ST. Clinical symptoms in Alzheimer's disease. Handb Clin Neurol. 2008;89:207-16. doi: 10.1016/S0072-9752(07)01219-5. PubMed PMID:18631745.

Luk KC, Kehm V, Carroll J, Zhang B, O'Brien P, Trojanowski JQ, Lee VM. Pathological α-synuclein transmission initiates Parkinson-like neurodegeneration in nontransgenic mice. Science. 2012 Nov 16;338(6109):949-53. doi:10.1126/science.1227157. PubMed PMID: 23161999.

Lunati A, Lesage S, Brice A. The genetic landscape of Parkinson's disease. Rev Neurol (Paris). 2018 Nov;174(9):628-643. doi: 10.1016/j.neurol.2018.08.004. Epub 2018 Sep 21. Review. PubMed PMID: 30245141.

Ma Y, Bao J, Zhao X, Shen H, Lv J, Ma S, Zhang X, Li Z, Wang S, Wang Q, Ji J. Activated cyclin-dependent kinase 5 promotes microglial phagocytosis of fibrillar β-amyloid by up-regulating lipoprotein lipase expression. Mol Cell Proteomics. 2013 Oct;12(10):2833-44. doi: 10.1074/mcp.M112.026864. Epub 2013 Jul 1. PubMed PMID: 23816988

Macron C, Lane L, Núñez Galindo A, Dayon L. Deep Dive on the Proteome of Human Cerebrospinal Fluid: A Valuable Data Resource for Biomarker Discovery and Missing Protein Identification. J Proteome Res. 2018 Aug 31. doi:10.1021/acs.jproteome.8b00300. [Epub ahead of print] PubMed PMID: 30124047.

MacVicar T, Langer T. OPA1 processing in cell death and disease - the long and short of it. J Cell Sci. 2016 Jun 15;129(12):2297-306. doi: 10.1242/jcs.159186. Epub 2016 May 17. Review. PubMed PMID: 27189080.

Małecki J, Jakobsson ME, Ho AYY, Moen A, Rustan AC, Falnes PØ. Uncovering human METTL12 as a mitochondrial methyltransferase that modulates citrate synthase activity through metabolite-sensitive lysine methylation. J Biol Chem. 2017 Oct 27;292(43):17950-17962. doi: 10.1074/jbc.M117.808451. Epub 2017 Sep 8. PubMed PMID: 28887308.

Manno C, Lipari A, Bono V, Taiello AC, La Bella V. Sporadic Parkinson disease and amyotrophic lateral sclerosis complex (Brait-Fahn-Schwartz disease). J Neurol Sci. 2013 Mar 15;326(1-2):104-6. doi: 10.1016/j.jns.2013.01.009. Epub 2013 Feb 4. PubMed PMID: 23380453.

Medina MÁ. Systems biology for molecular life sciences and its impact in biomedicine. Cell Mol Life Sci. 2013 Mar;70(6):1035-53. doi: 10.1007/s00018-012-1109-z. Epub 2012 Aug 19. Review. Erratum in: Cell Mol Life Sci. 2013 Sep;70(18):3475-80. PubMed PMID: 22903296.

Mena MA, Garcia de Yebenes J, Dwork A, Fahn S, Latov N, Herbert J, Flaster E, Slonim D. Biochemical properties of monoamine-rich human neuroblastoma cells. Brain Res. 1989 May 8;486(2):286-96. PubMed PMID: 2567196.

Menzies FM, Grierson AJ, Cookson MR, Heath PR, Tomkins J, Figlewicz DA, Ince PG, Shaw PJ. Selective loss of neurofilament expression in Cu/Zn superoxide dismutase (SOD1) linked amyotrophic lateral sclerosis. J Neurochem. 2002 Sep;82(5):1118-28. PubMed PMID: 12358759.

Mercado G, Castillo V, Soto P, Sidhu A. ER stress and Parkinson's disease: Pathological inputs that converge into the secretory pathway. Brain Res. 2016 Oct 1;1648(Pt B):626-632. doi: 10.1016/j.brainres.2016.04.042. Epub 2016 Apr 19. Review. PubMed PMID: 27103567.

Mila S, Albo AG, Corpillo D, Giraudo S, Zibetti M, Bucci EM, Lopiano L, Fasano M. Lymphocyte proteomics of Parkinson's disease patients reveals cytoskeletal protein dysregulation and oxidative stress. Biomark Med. 2009 Apr;3(2):117-28. doi: 10.2217/bmm.09.4. PubMed PMID: 20477505.

Minati L, Edginton T, Bruzzone MG, Giaccone G. Current concepts in Alzheimer's disease: a multidisciplinary review. Am J Alzheimers Dis Other Demen. 2009 Apr-May;24(2):95-121. doi: 10.1177/1533317508328602. Review. PubMed PMID:19116299.

Monti C, Colugnat I, Lopiano L, Chiò A, Alberio T. Network Analysis Identifies Disease-Specific Pathways for Parkinson's Disease. Mol Neurobiol. 2018 Jan;55(1):370-381. doi: 10.1007/s12035-016-0326-0. Epub 2016 Dec 21. PubMed PMID:28004338.

Monti C, Lane L, Fasano M, Alberio T. Update of the Functional Mitochondrial Human Proteome Network. J Proteome Res. 2018 Oct 8. doi:10.1021/acs.jproteome.8b00447. [Epub ahead of print] PubMed PMID: 30230342.

Monti C, Bondi H, Urbani A, Fasano M, Alberio T. Systems biology analysis of the proteomic alterations induced by MPP(+), a Parkinson's disease-related mitochondrial toxin. Front Cell Neurosci. 2015 Feb 2;9:14. doi: 10.3389/fncel.2015.00014. eCollection 2015. PubMed PMID: 25698928

Moors T, Paciotti S, Chiasserini D, Calabresi P, Parnetti L, Beccari T, van de Berg WD. Lysosomal Dysfunction and α-Synuclein Aggregation in Parkinson's Disease: Diagnostic Links. Mov Disord. 2016 Jun;31(6):791-801. doi:10.1002/mds.26562. Epub 2016 Feb 29. Review. PubMed PMID: 26923732.

Morais VA, Haddad D, Craessaerts K, De Bock PJ, Swerts J, Vilain S, Aerts L, Overbergh L, Grünewald A, Seibler P, Klein C, Gevaert K, Verstreken P, De Strooper B. PINK1 loss-of-function mutations affect mitochondrial complex I activity via NdufA10 ubiquinone uncoupling. Science. 2014 Apr 11;344(6180):203-7. doi: 10.1126/science.1249161. Epub 2014 Mar 20. PubMed PMID: 24652937.

Morris MK, Saez-Rodriguez J, Sorger PK, Lauffenburger DA. Logic-based models for the analysis of cell signaling networks. Biochemistry. 2010 Apr 20;49(15):3216-24. doi: 10.1021/bi902202q. Review. PubMed PMID: 20225868.

Mrvar A, Batagelj V. Analysis and visualization of large networks with program package Pajek. Complex Adaptive Systems Modeling. 2016;4:6. doi:10.1186/s40294-016-0017-8.

Naghdi S, Hajnóczky G. VDAC2-specific cellular functions and the underlying structure. Biochim Biophys Acta. 2016 Oct;1863(10):2503-14. doi:10.1016/j.bbamcr.2016.04.020. Epub 2016 Apr 23. Review. PubMed PMID: 27116927

Nardo G, Pozzi S, Mantovani S, Garbelli S, Marinou K, Basso M, Mora G, Bendotti C, Bonetto V. Nitroproteomics of peripheral blood mononuclear cells from patients and a rat model of ALS. Antioxid Redox Signal. 2009 Jul;11(7):1559-67. doi: 10.1089/ARS.2009.2548. PubMed PMID: 19290778.

Nardo G, Pozzi S, Pignataro M, Lauranzano E, Spano G, Garbelli S, Mantovani S, Marinou K, Papetti L, Monteforte M, Torri V, Paris L, Bazzoni G, Lunetta C, Corbo M, Mora G, Bendotti C, Bonetto V. Amyotrophic lateral sclerosis multiprotein biomarkers in peripheral blood mononuclear cells. PLoS One. 2011;6(10):e25545.doi: 10.1371/journal.pone.0025545. Epub 2011 Oct 5. PubMed PMID: 21998667.

Narendra DP, Jin SM, Tanaka A, Suen DF, Gautier CA, Shen J, Cookson MR, Youle RJ. PINK1 is selectively stabilized on impaired mitochondria to activate Parkin. PLoS Biol. 2010 Jan 26;8(1):e1000298. doi: 10.1371/journal.pbio.1000298. PubMed PMID: 20126261.

Navarro-Yepes J, Anandhan A, Bradley E, Bohovych I, Yarabe B, de Jong A, Ovaa H, Zhou Y, Khalimonchuk O, Quintanilla-Vega B, Franco R. Inhibition of Protein Ubiquitination by Paraquat and 1-Methyl-4-Phenylpyridinium Impairs Ubiquitin-Dependent Protein Degradation Pathways. Mol Neurobiol. 2016 Oct;53(8):5229-51. doi: 10.1007/s12035-015-9414-9. Epub 2015 Sep 26. PubMed PMID: 26409479.

NCBI Resource Coordinators . Database resources of the National Center for Biotechnology Information. Nucleic Acids Res. 2018 Jan 4;46(D1):D8-D13. doi: 10.1093/nar/gkx1095. PubMed PMID: 29140470.

Niemi NM, Lanning NJ, Klomp JA, Tait SW, Xu Y, Dykema KJ, Murphy LO, Gaither LA, Xu HE, Furge KA, Green DR, MacKeigan JP. MK-STYX, a catalytically inactive phosphatase regulating mitochondrially dependent apoptosis. Mol Cell Biol. 2011 Apr;31(7):1357-68. doi: 10.1128/MCB.00788-10. Epub 2011 Jan 24. PubMed PMID:21262771.

Niemi NM, Sacoman JL, Westrate LM, Gaither LA, Lanning NJ, Martin KR, MacKeigan JP. The pseudophosphatase MK-STYX physically and genetically interacts with the mitochondrial phosphatase PTPMT1. PLoS One. 2014 Apr 7;9(4):e93896. doi:10.1371/journal.pone.0093896. eCollection 2014. PubMed PMID: 24709986.

Noble D. The aims of systems biology: between molecules and organisms. Pharmacopsychiatry. 2011 May;44 Suppl 1:S9-S14. doi: 10.1055/s-0031-1271703. Epub 2011 May 4. PubMed PMID: 21544748.

Nutt JG, Wooten GF. Clinical practice. Diagnosis and initial management of Parkinson's disease. N Engl J Med. 2005 Sep 8;353(10):1021-7. Review. PubMed PMID: 16148287.

O'Leary NA, Wright MW, Brister JR, Ciufo S, Haddad D, McVeigh R, Rajput B, Robbertse B, Smith-White B, Ako-Adjei D, Astashyn A, Badretdin A, Bao Y, Blinkova O, Brover V, Chetvernin V, Choi J, Cox E, Ermolaeva O, Farrell CM, Goldfarb T, Gupta T, Haft D, Hatcher E, Hlavina W, Joardar VS, Kodali VK, Li W, Maglott D, Masterson P, McGarvey KM, Murphy MR, O'Neill K, Pujar S, Rangwala SH, Rausch D, Riddick LD, Schoch C, Shkeda A, Storz SS, Sun H, Thibaud-Nissen F, Tolstoy I, Tully RE, Vatsan AR, Wallin C, Webb D, Wu W, Landrum MJ, Kimchi A, Tatusova T, DiCuccio M, Kitts P, Murphy TD, Pruitt KD. Reference sequence (RefSeq) database at NCBI: current status, taxonomic expansion, and functional annotation. Nucleic Acids Res. 2016 Jan 4;44(D1):D733-45. doi: 10.1093/nar/gkv1189. Epub 2015 Nov 8. PubMed PMID: 26553804.

Olichon A, Baricault L, Gas N, Guillou E, Valette A, Belenguer P, Lenaers G. Loss of OPA1 perturbates the mitochondrial inner membrane structure and integrity, leading to cytochrome c release and apoptosis. J Biol Chem. 2003 Mar 7;278(10):7743-6. Epub 2002 Dec 31. PubMed PMID: 12509422.

Orchard S, Ammari M, Aranda B, Breuza L, Briganti L, Broackes-Carter F, Campbell NH, Chavali G, Chen C, del-Toro N, Duesbury M, Dumousseau M, Galeota E, Hinz U, Iannuccelli M, Jagannathan S, Jimenez R, Khadake J, Lagreid A, Licata L, Lovering RC, Meldal B, Melidoni AN, Milagros M, Peluso D, Perfetto L, Porras P, Raghunath A, Ricard-Blum S, Roechert B, Stutz A, Tognolli M, van Roey K, Cesareni G, Hermjakob H. The MIntAct project--IntAct as a common curation platform for 11 molecular interaction databases. Nucleic Acids Res. 2014 Jan;42(Database issue):D358-63. doi: 10.1093/nar/gkt1115. Epub 2013 Nov 13. PubMed PMID: 24234451.

Orchard S, Kerrien S, Abbani S, Aranda B, Bhate J, Bidwell S, Bridge A, Briganti L, Brinkman FS, Cesareni G, Chatr-aryamontri A, Chautard E, Chen C, Dumousseau M, Goll J, Hancock RE, Hannick LI, Jurisica I, Khadake J, Lynn DJ, Mahadevan U, Perfetto L, Raghunath A, Ricard-Blum S, Roechert B, Salwinski L, Stümpflen V, Tyers M, Uetz P, Xenarios I, Hermjakob H. Protein interaction data curation: the International Molecular Exchange (IMEx) consortium. Nat Methods. 2012 Apr;9(4):345-50. doi: 10.1038/nmeth.1931. Erratum in: Nat Methods. 2012 Jun;9(6):626. Brinkman, Fiona [corrected to Brinkman, Fiona S L]; Hancock, Robert [corrected to Hancock, Robert E W]. PubMed PMID: 22453911.

Ordureau A, Sarraf SA, Duda DM, Heo JM, Jedrychowski MP, Sviderskiy VO, Olszewski JL, Koerber JT, Xie T, Beausoleil SA, Wells JA, Gygi SP, Schulman BA, Harper JW. Quantitative proteomics reveal a feedforward mechanism for mitochondrial PARKIN translocation and ubiquitin chain synthesis. Mol Cell. 2014 Nov 6;56(3):360-75. doi: 10.1016/j.molcel.2014.09.007. Epub 2014 Oct 2. Erratum in: Mol Cell. 2014 Nov 6;56(3):462. PubMed PMID: 25284222.

Otera H, Wang C, Cleland MM, Setoguchi K, Yokota S, Youle RJ, Mihara K. Mff is an essential factor for mitochondrial recruitment of Drp1 during mitochondrial fission in mammalian cells. J Cell Biol. 2010 Dec 13;191(6):1141-58. doi:10.1083/jcb.201007152. PubMed PMID: 21149567.

Pacheco R, Prado CE, Barrientos MJ, Bernales S. Role of dopamine in the physiology of T-cells and dendritic cells. J Neuroimmunol. 2009 Nov30;216(1-2):8-19. doi: 10.1016/j.jneuroim.2009.07.018. Epub 2009 Sep 4. Review. PubMed PMID: 19732962.

Pal R, Alves G, Larsen JP, Møller SG. New insight into neurodegeneration: the role of proteomics. Mol Neurobiol. 2014 Jun;49(3):1181-99. doi:10.1007/s12035-013-8590-8. Epub 2013 Dec 10. Review. PubMed PMID: 24323427.

Pallanck LJ. Culling sick mitochondria from the herd. J Cell Biol. 2010 Dec 27;191(7):1225-7. doi: 10.1083/jcb.201011068. PubMed PMID: 21187326.

Palmer CS, Osellame LD, Laine D, Koutsopoulos OS, Frazier AE, Ryan MT. MiD49 and MiD51, new components of the mitochondrial fission machinery. EMBO Rep. 2011 Jun;12(6):565-73. doi: 10.1038/embor.2011.54. Epub 2011 Apr 21. PubMed PMID:21508961.

Paris I, Perez-Pastene C, Cardenas S, Iturriaga-Vasquez P, Muñoz P, Couve E, Caviedes P, Segura-Aguilar J. Aminochrome induces disruption of actin, alpha-, and beta-tubulin cytoskeleton networks in substantia-nigra-derived cell line. Neurotox Res. 2010 Jul;18(1):82-92. doi: 10.1007/s12640-009-9148-4. Epub 2010 Jan 20. Erratum in: Neurotox Res. 2010 Jul;18(1):93. Iturra, Patricio [corrected to Iturriaga-Vasquez, Patricio]. PubMed PMID: 20087799.

Park HK, Lim YM, Kim JS, Lee MC, Kim SM, Kim BJ, Kim KK. Nigrostriatal dysfunction in patients with amyotrophic lateral sclerosis and parkinsonism. J Neurol Sci. 2011 Feb 15;301(1-2):12-3. doi: 10.1016/ /j.jns.2010.11.017. Epub 2010 Dec 16. PubMed PMID: 21167502.

Parone PA, Da Cruz S, Tondera D, Mattenberger Y, James DI, Maechler P, Barja F, Martinou JC. Preventing mitochondrial fission impairs mitochondrial function and leads to loss of mitochondrial DNA. PLoS One. 2008 Sep 22;3(9):e3257. doi:10.1371/journal.pone.0003257. PubMed PMID: 18806874

Paupe V, Prudent J, Dassa EP, Rendon OZ, Shoubridge EA. CCDC90A (MCUR1) is a cytochrome c oxidase assembly factor and not a regulator of the mitochondrial calcium uniporter. Cell Metab. 2015 Jan 6;21(1):109-16. doi:10.1016/j.cmet.2014.12.004. PubMed PMID: 25565209.

Pennisi E. Systems biology. Tracing life's circuitry. Science. 2003 Dec 5;302(5651):1646-9. PubMed PMID: 14657470.

Perier C, Vila M. Mitochondrial biology and Parkinson's disease. Cold Spring Harb Perspect Med. 2012 Feb;2(2):a009332. doi: 10.1101/cshperspect.a009332. Review. PubMed PMID: 22355801.

Perkins G, Bossy-Wetzel E, Ellisman MH. New insights into mitochondrial structure during cell death. Exp Neurol. 2009 Aug;218(2):183-92. doi:10.1016/j.expneurol.2009.05.021. Epub 2009 May 21. Review. PubMed PMID: 19464290.

Perl A, Hanczko R, Telarico T, Oaks Z, Landas S. Oxidative stress, inflammation and carcinogenesis are controlled through the pentose phosphate pathway by transaldolase. Trends Mol Med. 2011 Jul;17(7):395-403. doi:10.1016/j.molmed.2011.01.014. Epub 2011 Mar 2. Review. PubMed PMID: 21376665

Picard M, Wallace DC, Burelle Y. The rise of mitochondria in medicine. Mitochondrion. 2016 Sep;30:105-16. doi: 10.1016/j.mito.2016.07.003. Epub 2016 Jul 14. Review. PubMed PMID: 27423788.

Pickles S, Vigié P, Youle RJ. Mitophagy and Quality Control Mechanisms in Mitochondrial Maintenance. Curr Biol. 2018 Feb 19;28(4):R170-R185. doi:10.1016/j.cub.2018.01.004. Review. PubMed PMID: 29462587.

Pickrell AM, Youle RJ. The roles of PINK1, parkin, and mitochondrial fidelity in Parkinson's disease. Neuron. 2015 Jan 21;85(2):257-73. doi: 10.1016/j.neuron.2014.12.007. Review. PubMed PMID: 25611507.

Piñero J, Queralt-Rosinach N, Bravo À, Deu-Pons J, Bauer-Mehren A, Baron M, Sanz F, Furlong LI. DisGeNET: a discovery platform for the dynamical exploration of human diseases and their genes. Database (Oxford). 2015 Apr 15;2015:bav028. doi: 10.1093/database/bav028. Print 2015. PubMed PMID: 25877637.

Plum S, Steinbach S, Abel L, Marcus K, Helling S, May C. Proteomics in neurodegenerative diseases: Methods for obtaining a closer look at the neuronal proteome. Proteomics Clin Appl. 2015 Oct;9(9-10):848-71. doi: 10.1002/prca.201400030. Epub 2014 Nov 10. Review. PubMed PMID: 25195870.

Polyzos AA, McMurray CT. The chicken or the egg: mitochondrial dysfunction as a cause or consequence of toxicity in Huntington's disease. Mech Ageing Dev. 2017 Jan;161(Pt A):181-197. doi: 10.1016/j.mad.2016.09.003. Epub 2016 Sep 12. Review. PubMed PMID: 27634555.

Poulopoulou C, Davaki P, Koliaraki V, Kolovou D, Markakis I, Vassilopoulos D. Reduced expression of metabotropic glutamate receptor 2mRNA in T cells of ALS patients. Ann Neurol. 2005 Dec;58(6):946-9. PubMed PMID: 16240362.

Querfurth HW, LaFerla FM. Alzheimer's disease. N Engl J Med. 2010 Jan 28;362(4):329-44. doi: 10.1056/NEJMra0909142. Review. Erratum in: N Engl J Med. 2011 Feb 10;364(6):588. PubMed PMID: 20107219.

Qureshi AI, Wilmot G, Dihenia B, Schneider JA, Krendel DA. Motor neuron disease with parkinsonism. Arch Neurol. 1996 Oct;53(10):987-91. PubMed PMID:8859060.

Rabilloud T, Lelong C. Two-dimensional gel electrophoresis in proteomics: a tutorial. J Proteomics. 2011 Sep 6;74(10):1829-41. doi: 10.1016/j.jprot.2011.05.040. Epub 2011 Jun 12. PubMed PMID: 21669304.

Ramanan VK, Shen L, Moore JH, Saykin AJ. Pathway analysis of genomic data: concepts, methods, and prospects for future development. Trends Genet. 2012 Jul;28(7):323-32. doi: 10.1016/j.tig.2012.03.004. Epub 2012 Apr 3. Review. PubMed PMID: 22480918.

Ramonet D, Perier C, Recasens A, Dehay B, Bové J, Costa V, Scorrano L, Vila M. Optic atrophy 1 mediates mitochondria remodeling and dopaminergic neurodegeneration linked to complex I deficiency. Cell Death Differ. 2013 Jan;20(1):77-85. doi: 10.1038/cdd.2012.95. Epub 2012 Aug 3. PubMed PMID: 22858546.

Ramsay RR, Salach JI, Dadgar J, Singer TP. Inhibition of mitochondrial NADH dehydrogenase by pyridine derivatives and its possible relation to experimental and idiopathic parkinsonism. Biochem Biophys Res Commun. 1986 Feb 26;135(1):269-75. PubMed PMID: 3485428.

Rhein VF, Carroll J, Ding S, Fearnley IM, Walker JE. Human METTL12 is a mitochondrial methyltransferase that modifies citrate synthase. FEBS Lett. 2017 Jun;591(12):1641-1652. doi: 10.1002/1873-3468.12649. Epub 2017 Apr 27. PubMed PMID: 28391595.

Rivero-Ríos P, Gómez-Suaga P, Fdez E, Hilfiker S. Upstream deregulation of calcium signaling in Parkinson's disease. Front Mol Neurosci. 2014 Jun 17;7:53. doi: 10.3389/fnmol.2014.00053. eCollection 2014. Review. PubMed PMID: 24987329.

Rizzu P, Hinkle DA, Zhukareva V, Bonifati V, Severijnen LA, Martinez D, Ravid R, Kamphorst W, Eberwine JH, Lee VM, Trojanowski JQ, Heutink P. DJ-1 colocalizes with tau inclusions: a link between parkinsonism and dementia. Ann Neurol. 2004 Jan;55(1):113-8. PubMed PMID: 14705119.

Roche JC, Rojas-Garcia R, Scott KM, Scotton W, Ellis CE, Burman R, Wijesekera L, Turner MR, Leigh PN, Shaw CE, Al-Chalabi A. A proposed staging system for amyotrophic lateral sclerosis. Brain. 2012 Mar;135(Pt 3):847-52. doi: 10.1093/brain/awr351. Epub 2012 Jan 23. PubMed PMID: 22271664.

Ross JM, Olson L, Coppotelli G. Mitochondrial and Ubiquitin Proteasome System Dysfunction in Ageing and Disease: Two Sides of the Same Coin? Int J Mol Sci. 2015 Aug 17;16(8):19458-76. doi: 10.3390/ijms160819458. Review. PubMed PMID:26287188.

Ross PL, Huang YN, Marchese JN, Williamson B, Parker K, Hattan S, Khainovski N, Pillai S, Dey S, Daniels S, Purkayastha S, Juhasz P, Martin S, Bartlet-Jones M, He F, Jacobson A, Pappin DJ. Multiplexed protein quantitation in Saccharomyces cerevisiae using amine-reactive isobaric tagging reagents. Mol Cell Proteomics. 2004 Dec;3(12):1154-69. Epub 2004 Sep 22. PubMed PMID: 15385600.

Roy S, Zhang B, Lee VM, Trojanowski JQ. Axonal transport defects: a common theme in neurodegenerative diseases. Acta Neuropathol. 2005 Jan;109(1):5-13. Epub 2005 Jan 12. Review. PubMed PMID: 15645263.

Saccon RA, Bunton-Stasyshyn RK, Fisher EM, Fratta P. Is SOD1 loss of function involved in amyotrophic lateral sclerosis? Brain. 2013 Aug;136(Pt 8):2342-58. doi: 10.1093/brain/awt097. Epub 2013 May 17. Review. PubMed PMID: 23687121.

Santiago JA, Potashkin JA. System-based approaches to decode the molecular links in Parkinson's disease and diabetes. Neurobiol Dis. 2014 Dec;72 Pt A:84-91. doi: 10.1016/j.nbd.2014.03.019. Epub 2014 Apr 6. Review. PubMed PMID: 24718034.

Santos AL, Lindner AB. Protein Posttranslational Modifications: Roles in Aging and Age-Related Disease. Oxid Med Cell Longev. 2017;2017:5716409. doi:10.1155/2017/5716409. Epub 2017 Aug 15. Review. PubMed PMID: 28894508.

Scarmeas N, Hadjigeorgiou GM, Papadimitriou A, Dubois B, Sarazin M, Brandt J, Albert M, Marder K, Bell K, Honig LS, Wegesin D, Stern Y. Motor signs during the course of Alzheimer disease. Neurology. 2004 Sep 28;63(6):975-82. PubMed PMID:15452286.

Scarpulla RC. Nucleus-encoded regulators of mitochondrial function: integration of respiratory chain expression, nutrient sensing and metabolic stress. Biochim Biophys Acta. 2012 Sep-Oct;1819(9-10):1088-97. doi:10.1016/j.bbagrm.2011.10.011. Epub 2011 Nov 4. PubMed PMID: 22080153.

Schapira AH, Jenner P. Etiology and pathogenesis of Parkinson's disease. Mov Disord. 2011 May;26(6):1049-55. doi: 10.1002/mds.23732. Review. PubMed PMID: 21626550.

Schneider CA, Rasband WS, Eliceiri KW. NIH Image to ImageJ: 25 years of image analysis. Nat Methods. 2012 Jul;9(7):671-5. PubMed PMID: 22930834.

Schulte C, Gasser T. Genetic basis of Parkinson's disease: inheritance, penetrance, and expression. Appl Clin Genet. 2011 Jun 1;4:67-80. doi:10.2147/TACG.S11639. Print 2011. PubMed PMID: 23776368.

Segura-Aguilar J, Paris I, Muñoz P, Ferrari E, Zecca L, Zucca FA. Protective and toxic roles of dopamine in Parkinson's disease. J Neurochem. 2014 Jun;129(6):898-915. doi: 10.1111/jnc.12686. Epub 2014 Mar 18. Review. PubMedPMID: 24548101.

Seilhean D, Cazeneuve C, Thuriès V, Russaouen O, Millecamps S, Salachas F, Meininger V, Leguern E, Duyckaerts C. Accumulation of TDP-43 and alpha-actin in an amyotrophic lateral sclerosis patient with the K17I ANG mutation. Acta Neuropathol. 2009 Oct;118(4):561-73. doi: 10.1007/s00401-009-0545-9. Epub 2009 May 16. PubMed PMID: 19449021.

Shalhoub J, Sikkel MB, Davies KJ, Vorkas PA, Want EJ, Davies AH. Systems biology of human atherosclerosis. Vasc Endovascular Surg. 2014 Jan;48(1):5-17. doi: 10.1177/1538574413510628. Epub 2013 Nov 7. Review. PubMed PMID: 24212404.

Shannon P, Markiel A, Ozier O, Baliga NS, Wang JT, Ramage D, Amin N, Schwikowski B, Ideker T. Cytoscape: a software environment for integrated models of biomolecular interaction networks. Genome Res. 2003 Nov;13(11):2498-504.PubMed PMID: 14597658.

Sitaram RT, Cairney CJ, Grabowski P, Keith WN, Hallberg B, Ljungberg B, Roos G. The PTEN regulator DJ-1 is associated with hTERT expression in clear cell renal cell carcinoma. Int J Cancer. 2009 Aug 15;125(4):783-90. doi: 10.1002/ijc.24335. PubMed PMID: 19384955.

Slenter DN, Kutmon M, Hanspers K, Riutta A, Windsor J, Nunes N, Mélius J, Cirillo E, Coort SL, Digles D, Ehrhart F, Giesbertz P, Kalafati M, Martens M, Miller R, Nishida K, Rieswijk L, Waagmeester A, Eijssen LMT, Evelo CT, Pico AR, Willighagen EL. WikiPathways: a multifaceted pathway database bridging metabolomics to other omics research. Nucleic Acids Res. 2018 Jan 4;46(D1):D661-D667. doi: 10.1093/nar/gkx1064. PubMed PMID: 29136241.

Smith AC, Robinson AJ. MitoMiner v3.1, an update on the mitochondrial proteomics database. Nucleic Acids Res. 2016 Jan 4;44(D1):D1258-61. doi: 10.1093/nar/gkv1001. Epub 2015 Oct 1. PubMed PMID: 26432830.

Smith LM, Kelleher NL; Consortium for Top Down Proteomics. Proteoform: a single term describing protein complexity. Nat Methods. 2013 Mar;10(3):186-7. doi: 10.1038/nmeth.2369. PubMed PMID: 23443629; PubMed Central PMCID: PMC4114032.

Smith AM, Depp C, Ryan BJ, Johnston GI, Alegre-Abarrategui J, Evetts S, Rolinski M, Baig F, Ruffmann C, Simon AK, Hu MTM, Wade-Martins R. Mitochondrial dysfunction and increased glycolysis in prodromal and early Parkinson's blood cells. Mov Disord. 2018 Oct 7. doi: 10.1002/mds.104. [Epub ahead of print] PubMed PMID: 30294923.

Song Z, Ghochani M, McCaffery JM, Frey TG, Chan DC. Mitofusins and OPA1 mediate sequential steps in mitochondrial membrane fusion. Mol Biol Cell. 2009 Aug;20(15):3525-32. doi: 10.1091/mbc.E09-03-0252. Epub 2009 May 28. PubMed PMID: 19477917.

Staats KA, Van Den Bosch L. Astrocytes in amyotrophic lateral sclerosis: direct effects on motor neuron survival. J Biol Phys. 2009 Oct;35(4):337-46. doi:10.1007/s10867-009-9141-4. Epub 2009 Mar 21. PubMed PMID: 19669429.

Stefanis L. α-Synuclein in Parkinson's disease. Cold Spring Harb Perspect Med. 2012 Feb;2(2):a009399. doi: 10.1101/cshperspect.a009399. Review. PubMed PMID:22355802.

Strange K. The end of "naive reductionism": rise of systems biology or renaissance of physiology? Am J Physiol Cell Physiol. 2005 May;288(5):C968-74. Review. PubMed PMID: 15840560.

Strong MJ. The evidence for altered RNA metabolism in amyotrophic lateral sclerosis (ALS). J Neurol Sci. 2010 Jan 15;288(1-2):1-12. doi:10.1016/j.jns.2009.09.029. Epub 2009 Oct 18. Review. PubMed PMID: 19840884.

Su T, Turnbull DM, Greaves LC. Roles of Mitochondrial DNA Mutations in Stem Cell Ageing. Genes (Basel). 2018 Mar 27;9(4). pii: E182. doi:10.3390/genes9040182. Review. PubMed PMID: 29584704.

Sun M, Latourelle JC, Wooten GF, Lew MF, Klein C, Shill HA, Golbe LI, Mark MH, Racette BA, Perlmutter JS, Parsian A, Guttman M, Nicholson G, Xu G, Wilk JB, Saint-Hilaire MH, DeStefano AL, Prakash R, Williamson S, Suchowersky O, Labelle N, Growdon JH, Singer C, Watts RL, Goldwurm S, Pezzoli G, Baker KB, Pramstaller PP, Burn DJ, Chinnery PF, Sherman S, Vieregge P, Litvan I, Gillis T, MacDonald ME, Myers RH, Gusella JF. Influence of heterozygosity for parkin mutation on onset age in familial Parkinson disease: the GenePD study. Arch Neurol. 2006 Jun;63(6):826-32. PubMed PMID: 16769863.

Sun Y, Vashisht AA, Tchieu J, Wohlschlegel JA, Dreier L. Voltage-dependent anion channels (VDACs) recruit Parkin to defective mitochondria to promote mitochondrial autophagy. J Biol Chem. 2012 Nov 23;287(48):40652-60. doi: 10.1074/jbc.M112.419721. Epub 2012 Oct 11. PubMed PMID: 23060438.

Szklarczyk D, Morris JH, Cook H, Kuhn M, Wyder S, Simonovic M, Santos A, Doncheva NT, Roth A, Bork P, Jensen LJ, von Mering C. The STRING database in 2017: quality-controlled protein-protein association networks, made broadly accessible. Nucleic Acids Res. 2017 Jan 4;45(D1):D362-D368. doi: 10.1093/nar/gkw937. Epub 2016 Oct 18. PubMed PMID: 27924014.

Takahashi H, Snow BJ, Bhatt MH, Peppard R, Eisen A, Calne DB. Evidence for a dopaminergic deficit in sporadic amyotrophic lateral sclerosis on positron emission scanning. Lancet. 1993 Oct 23;342(8878):1016-8. PubMed PMID: 8105264.

Tang B, Xiong H, Sun P, Zhang Y, Wang D, Hu Z, Zhu Z, Ma H, Pan Q, Xia JH, Xia K, Zhang Z. Association of PINK1 and DJ-1 confers digenic inheritance of early-onset Parkinson's disease. Hum Mol Genet. 2006 Jun 1;15(11):1816-25. Epub 2006 Apr 21. PubMed PMID: 16632486.

Tatton WG, Chalmers-Redman RM, Ju WY, Wadia J, Tatton NA. Apoptosis in neurodegenerative disorders: potential for therapy by modifying gene transcription. J Neural Transm Suppl. 1997;49:245-68. Review. PubMed PMID:9266433.

The Gene Ontology Consortium. Expansion of the Gene Ontology knowledgebase and resources. Nucleic Acids Res. 2017 Jan 4;45(D1):D331-D338. doi: 10.1093/nar/gkw1108. Epub 2016 Nov 29. PubMed PMID: 27899567.

Thul PJ, Lindskog C. The human protein atlas: A spatial map of the human proteome. Protein Sci. 2018 Jan;27(1):233-244. doi: 10.1002/pro.3307. Epub 2017 Oct 10. PubMed PMID: 28940711.

Thul PJ, Åkesson L, Wiking M, Mahdessian D, Geladaki A, Ait Blal H, Alm T, Asplund A, Björk L, Breckels LM, Bäckström A, Danielsson F, Fagerberg L, Fall J, Gatto L, Gnann C, Hober S, Hjelmare M, Johansson F, Lee S, Lindskog C, Mulder J, Mulvey CM, Nilsson P, Oksvold P, Rockberg J, Schutten R, Schwenk JM, Sivertsson Å, Sjöstedt E, Skogs M, Stadler C, Sullivan DP, Tegel H, Winsnes C, Zhang C, Zwahlen M, Mardinoglu A, Pontén F, von Feilitzen K, Lilley KS, Uhlén M, Lundberg E. A subcellular map of the human proteome. Science. 2017 May 26;356(6340). pii: eaal3321. doi: 10.1126/science.aal3321. Epub 2017 May 11. PubMed PMID: 28495876.

Tillman JE, Yuan J, Gu G, Fazli L, Ghosh R, Flynt AS, Gleave M, Rennie PS, Kasper S. DJ-1 binds androgen receptor directly and mediates its activity in hormonally treated prostate cancer cells. Cancer Res. 2007 May 15;67(10):4630-7. PubMed PMID: 17510388.

Tomar D, Dong Z, Shanmughapriya S, Koch DA, Thomas T, Hoffman NE, Timbalia SA, Goldman SJ, Breves SL, Corbally DP, Nemani N, Fairweather JP, Cutri AR, Zhang X, Song J, Jaña F, Huang J, Barrero C, Rabinowitz JE, Luongo TS, Schumacher SM, Rockman ME, Dietrich A, Merali S, Caplan J, Stathopulos P, Ahima RS, Cheung JY, Houser SR,

Koch WJ, Patel V, Gohil VM, Elrod JW, Rajan S, Madesh M. MCUR1 Is a Scaffold Factor for the MCU Complex Function and Promotes Mitochondrial Bioenergetics. Cell Rep. 2016 May 24;15(8):1673-85. doi: 10.1016/j.celrep.2016.04.050. Epub 2016 May 12. PubMed PMID: 27184846.

Triplett JC, Zhang Z, Sultana R, Cai J, Klein JB, Büeler H, Butterfield DA. Quantitative expression proteomics and phosphoproteomics profile of brain from PINK1 knockout mice: insights into mechanisms of familial Parkinson's disease. J Neurochem. 2015 Jun;133(5):750-65. doi: 10.1111/jnc.13039. Epub 2015 Mar 1. PubMed PMID: 25626353.

Turner MR, Hardiman O, Benatar M, Brooks BR, Chio A, de Carvalho M, Ince PG, Lin C, Miller RG, Mitsumoto H, Nicholson G, Ravits J, Shaw PJ, Swash M, Talbot K, Traynor BJ, Van den Berg LH, Veldink JH, Vucic S, Kiernan MC. Controversies and priorities in amyotrophic lateral sclerosis. Lancet Neurol. 2013 Mar;12(3):310-22. doi: 10.1016/S1474-4422(13)70036-X. Review. PubMed PMID:23415570.

Vakifahmetoglu-Norberg H, Ouchida AT, Norberg E. The role of mitochondria in metabolism and cell death. Biochem Biophys Res Commun. 2017 Jan 15;482(3):426-431. doi: 10.1016/j.bbrc.2016.11.088. Epub 2017 Feb 3. Review. PubMed PMID: 28212726.

van der Bliek AM, Shen Q, Kawajiri S. Mechanisms of mitochondrial fission and fusion. Cold Spring Harb Perspect Biol. 2013 Jun 1;5(6). pii: a011072. doi:10.1101/cshperspect.a011072. Review. PubMed PMID: 23732471

Van Regenmortel MH. Reductionism and complexity in molecular biology. Scientists now have the tools to unravel biological and overcome the limitations of reductionism. EMBO Rep. 2004 Nov;5(11):1016-20. PubMed PMID: 15520799; PubMed Central PMCID: PMC1299179.

Villoslada P, Steinman L, Baranzini SE. Systems biology and its application to the understanding of neurological diseases. Ann Neurol. 2009 Feb;65(2):124-39. doi: 10.1002/ana.21634. Review. PubMed PMID: 19260029.

Vogels OJ, Veltman J, Oyen WJ, Horstink MW. Decreased striatal dopamine D2 receptor binding in amyotrophic lateral sclerosis (ALS) and multiple system atrophy (MSA): D2 receptor down-regulation versus striatal cell degeneration. J Neurol Sci. 2000 Nov 1;180(1-2):62-5. PubMed PMID: 11090866.

Wang J, Vasaikar S, Shi Z, Greer M, Zhang B. WebGestalt 2017: a more comprehensive, powerful, flexible and interactive gene set enrichment analysis toolkit. Nucleic Acids Res. 2017 Jul 3;45(W1):W130-W137. doi: 10.1093/nar/gkx356. PubMed PMID: 28472511.

Wilson TJ, Slupe AM, Strack S. Cell signaling and mitochondrial dynamics: Implications for neuronal function and neurodegenerative disease. Neurobiol Dis. 2013 Mar;51:13-26. doi: 10.1016/j.nbd.2012.01.009. Epub 2012 Jan 24. Review. PubMed PMID: 22297163

Winter DL, Wilkins MR, Donald WA. Differential Ion Mobility-Mass Spectrometry for Detailed Analysis of the Proteome. Trends Biotechnol. 2018 Sep 4. pii:S0167-7799(18)30209-9. doi: 10.1016/j.tibtech.2018.07.018. [Epub ahead of print] Review. PubMed PMID: 30193737.

Wu J, Lou H, Alerte TN, Stachowski EK, Chen J, Singleton AB, Hamilton RL, Perez RG. Lewy-like aggregation of α-synuclein reduces protein phosphatase 2A activity in vitro and in vivo. Neuroscience. 2012 Apr 5;207:288-97. doi:10.1016/j.neuroscience.2012.01.028. Epub 2012 Jan 25. PubMed PMID: 22326202

Wu X, Hasan MA, Chen JY. Pathway and network analysis in proteomics. J Theor Biol. 2014 Dec 7;362:44-52. doi: 10.1016/j.jtbi.2014.05.031. Epub 2014 Jun 6. Review. PubMed PMID: 24911777.

Würstle ML, Zink E, Prehn JH, Rehm M. From computational modelling of the intrinsic apoptosis pathway to a systems-based analysis of chemotherapy resistance: achievements, perspectives and challenges in systems medicine. Cell Death Dis. 2014 May 29;5:e1258. doi: 10.1038/cddis.2014.36. Review. PubMed PMID: 24874730.

Wynn ML, Consul N, Merajver SD, Schnell S. Logic-based models in systems biology: a predictive and parameter-free network analysis method. Integr Biol (Camb). 2012 Nov;4(11):1323-37. doi: 10.1039/c2ib20193c. Review. PubMed PMID: 23072820.

Yang H, Wittnam JL, Zubarev RA, Bayer TA. Shotgun brain proteomics reveals early molecular signature in presymptomatic mouse model of Alzheimer's disease. J Alzheimers Dis. 2013;37(2):297-308. doi: 10.3233/JAD-130476. PubMed PMID: 24018289.

Yokota O, Tsuchiya K, Oda T, Ishihara T, de Silva R, Lees AJ, Arai T, Uchihara T, Ishizu H, Kuroda S, Akiyama H. Amyotrophic lateral sclerosis with dementia: an autopsy case showing many Bunina bodies, tau-positive neuronal and astrocytic plaque-like pathologies, and pallido-nigral degeneration. Acta Neuropathol. 2006 Nov;112(5):633-45. Epub 2006 Sep 26. PubMed PMID: 17021751.

Youle RJ, Narendra DP. Mechanisms of mitophagy. Nat Rev Mol Cell Biol. 2011 Jan;12(1):9-14. doi: 10.1038/nrm3028. Review. PubMed PMID: 21179058.

Yu LR, Zhu Z, Chan KC, Issaq HJ, Dimitrov DS, Veenstra TD. Improved titanium dioxide enrichment of phosphopeptides from HeLa cells and high confident phosphopeptide identification by cross-validation of MS/MS and MS/MS/MS spectra. J Proteome Res. 2007 Nov;6(11):4150-62. Epub 2007 Oct 9. PubMed PMID: 17924679.

Zahid S, Oellerich M, Asif AR, Ahmed N. Phosphoproteome profiling of substantia nigra and cortex regions of Alzheimer's disease patients. J Neurochem. 2012 Jun;121(6):954-63. doi: 10.1111/j.1471-4159.2012.07737.x. Epub 2012 Apr 24. PubMed PMID: 22436009.

Zahid S, Khan R, Oellerich M, Ahmed N, Asif AR. Differential S-nitrosylation of proteins in Alzheimer's disease. Neuroscience. 2014 Jan 3;256:126-36. doi: 10.1016/j.neuroscience.2013.10.026. Epub 2013 Oct 22. PubMed PMID: 24157928.

Zhou ZD, Lim TM. Dopamine (DA) induced irreversible proteasome inhibition via DA derived quinones. Free Radic Res. 2009 Apr;43(4):417-30. doi:10.1080/10715760902801533. Epub 2009 Mar 17. PubMed PMID: 19291591.

Zilocchi M, Finzi G, Lualdi M, Sessa F, Fasano M, Alberio T. Mitochondrial alterations in Parkinson's disease human samples and cellular models. Neurochem Int. 2018 Sep;118:61-72. doi: 10.1016/j.neuint.2018.04.013. Epub 2018 Apr 26. PubMed PMID: 29704589.

Zoccolella S, Palagano G, Fraddosio A, Russo I, Ferrannini E, Serlenga L, Maggio F, Lamberti S, Iliceto G. ALS-plus: 5 cases of concomitant amyotrophic lateral sclerosis and parkinsonism. Neurol Sci. 2002 Sep;23 Suppl 2:S123-4. PubMed PMID: 12548374.

PART VIII

Supplemental Information

8.1

Supplemental Tables

Supplementary Table 2.1. PMIDs of studies used to generate "_Proteins" input lists. Colours indicate the organism used in the proteomics analysis. Blue: Homo Sapiens, Red: Mus musculus and Green: other organisms.

	PMID
AD	11747211, 15756939, 15797529, 16519965, 17050040, 17111439, 17309106, 18648492, 18648646, 19241155, 20061648, 21237293, 21368863, 21388376, 21699958, 21883897, 21954051, 22559202, 22634250, 22926577, 23050487, 23154051, 23211594, 23231993, 23276639, 23391701, 23424162, 23457027, 23512986, 23537733, 23963966, 24306222, 24606058, 24893329, 25108202, 25457556, 25756589, 25818006, 25958317, 26059363
PD	15526345, 15755676, 15790536, 16150055, 16565515, 16889417, 17203978, 17490626, 17532186, 17705834, 18173235, 18226537, 18270577, 18338827, 18353766, 18384645, 18782562, 19498008, 19725078, 20155936, 20334438, 20403401, 20563739, 20594931, 20977677, 21136655, 21296869, 21296869, 21322648, 21960009, 21988495, 22315971, 22410244, 22445325, 23562983, 24040246, 24449343, 24675778, 24737941, 24806433, 24834013, 24841483, 25626353, 25683516, 25865804, 26468903
ALS	17979159, 17196550, 16847061, 15863242, 15501831, 19357085, 12475980, 25743254

Supplementary Table 2.2. Summary of the protein level variations in PD complexes. ↓ indicates a down-regulation of the protein in PD, ↑ indicates up-regulation of proteins in PD.

	Gene Symbol	Expression	Pubmed ID	Model used
Respiratory chain	**UQCRB**	↓	24449343	Human SN
	UQCRC1	↓	24841483	Striatum in unilateral 6-OHDA-rat model
		↑	22445325	α-synuclein overexpression in SH-SY5Y cells
	UQCRC2	↓	22410244	Human SN
		↓	18338827	Ventral midbrain in MPTP-treated L1cam transgenic mice (1 day)
		↑	18338827	Ventral midbrain in MPTP-treated L1cam transgenic mice (7 days)
	UQCRH	↑	21960009	Nigrostriatal area in A53T and wt α-synuclein mice
		↓	15790536	SN in mice treated chronically with MPTP for 5 weeks
	UQCRSF1	↑	20403401	SN in 6-OHDA rat model
		↓	18270577	Striatum in MPTP macaque model
		↑	16565515	Human SN
	CYC1	↑	18173235	Striatum in MPTP and METH mice models
		↓	15790536	SN in mice treated chronically with MPTP for 5 weeks
CCT complex	**TCP1**	↑	16150055	Cortical and striatal tissue of PARK2 knockout mice
		↑	25865804	mutant parkin (Q311R and A371T) overexpression in SH-SY5Y cells
	CCT4	↑	18338827	Ventral midbrain in MPTP-treated L1cam transgenic mice (1 day)
		↑	18173235	Striatum in MPTP mice model
		↑	18173235	Striatum in METH mice model

Continue →

	Gene Symbol	Expression	Pubmed ID	Model used
CCT complex	**CCT5**	↓	22445325	α-synuclein overexpression in SH-SY5Y cells
		↑	21322648	MPTP-treated N2a cells
		↓	15790536	SN in mice treated chronically with MPTP for 5 weeks
		↑	25626353	Whole brain in PINK1 knockout mice
	CCT6A	↑	18338827	Ventral midbrain in MPTP-treated L1cam transgenic mice (1 day)
	CCT7	↑	22445325	α-synuclein overexpression in SH-SY5Y cells
		↑	18338827	Ventral midbrain in MPTP-treated L1cam transgenic mice (1 day)
PPP2A complex	**PPP2CA**	↓	24449343	Human SN
	PPP2CB	↑	16150055	Cortical and striatal tissue in PARK2 knockout mice
		↑	26468903	α-synuclein fibrils-exposed SH-SY5Y cells
	PPP2R4	↓	20403401	SN in 6-OHDA rat model
		↑	20403401	SN in 6-OHDA rat model
	PPP2R5A	↓	15790536	SN in mice treated chronically with MPTP for 5 weeks
Proteasome complex	**PSMB1**	↑	21296869	Parkin-expressing SH-SY5Y cells treated with CCCP
	PSMB3	↑	21296869	Parkin-expressing SH-SY5Y cells treated with CCCP
	PSMB5	↑	21296869	Parkin-expressing SH-SY5Y cells treated with CCCP
		↑	16150055	Cortical and striatal tissue in PARK2 knockout mice
	PSMA1	↑	22315971	Co-expression of wt or mutated LRRK2 and Tau in C. elegans
		↑	21296869	Parkin-expressing SH-SY5Y cells treated with CCCP

Continue →

	Gene Symbol	Expression	Pubmed ID	Model used
Proteasome complex	**PSMA3**	↑	21960009	Nigrostriatal area in A53T and wt α-synuclein mice
		↑	21296869	Parkin-expressing SH-SY5Ycells treated with CCCP
	PSMA7, PSMA5	↑	21296869	Parkin-expressing SH-SY5Ycells treated with CCCP
		↓	18338827	Ventral midbrain in MPTP-treated L1cam transgenic mice (1 day)
	PSMC2	↓	20403401	SN in 6-OHDA rat model
		↓	22445325	α-synuclein overexpression in SH-SY5Y cells
	PSMC1	↓	15790536	SN in mice treated chronically with MPTP for 5 weeks
	PSMC3	↓	18338827	Ventral midbrain in MPTP-treated L1cam transgenic mice (1 day)
	UCHL5	↓	17705834	Rotenone-treated MES cells
	USP14	↑	18173235	Striatum in MPTP and METH mice models

6-OHDA: 6-hydroxydopamine, LRRK2: Leucine-rich repeat kinase 2, MES cells: dopaminergic neuronal cell line, METH: methamphetamine, MPTP:1-methyl-4-phenyl-1,2,3,6-tetrahydropyridine, N2a cells: murine neuroblastoma cell line, PARK2: Parkin gene, PINK1: PTEN-induced putative kinase 1, SH-SY5Ycells: human neuroblastoma cell line.

Supplementary Table 3.1. Gender and age distributions.

Patients	Genetic analysis	Riluzole	ALSFRS Score	Gender	Birth date
ALS_r1	wt	50mgx2/d	28	M	1954
ALS_r2	wt	50mgx2/d	33	M	1959
ALS_r3	wt	50mg/d	29	F	1943
ALS_r4	C9orf72	50mg/d	16	F	1949
ALS_r5	SOD1	50mgx2/d	25	F	1950
ALS_r6	wt	50mgx2/d	26	M	1941
ALS_r7	wt	50mgx2/d	40	M	1953
ALS_r8	wt	50mg/d	39	M	1951
ALS_r9	wt	50mgx2/d	37	M	1943
ALS_r10	wt	50mgx2/d	31	F	1941
ALS_r11	wt	50mgx2/d	44	M	1960
ALS_r12	wt	50mgx2/d	29	F	1940
ALS_r13	wt	50mgx2/d	21	M	1941
ALS_r14	wt	50mgx2/d	24	F	1943
ALS_r15	wt	50mgx2/d	16	F	1965
ALS_r16	wt	50mg/d	42	F	1955
ALS_r17	wt	50mgx2/d	MISS	F	1964
ALS_r18	wt	50mgx2/d	22	M	1943
ALS_r19	C9orf72	50mgx2/d	37	F	1946
ALS_r20	N.D.	50mgx2/d	36	M	1976
ALS1	wt	NO	43	M	1943
ALS2	wt	50mgx2/d	45	M	1960
ALS3	wt	50mgx2/d	40	M	1947
ALS4	wt	50mgx2/d	39	M	1947
ALS5	wt	50mgx2/d	39	F	1946
ALS6	N.D.	NO	45	M	1948
ALS7	wt	NO	25	F	1974
ALS8	wt	50mgx2/d	43	M	1948
ALS9	wt	50mgx2/d	33	M	1952
ALS10	wt	50mgx2/d	37	M	1962
ALS11	wt	20ml/d	41	F	1934
ALS12	wt	NO	25	F	1960
ALS13	wt	50mgx2/d	25	M	1940
ALS14	N.D.	NO	37	M	1946
ALS15	N.D.	50mgx2/d	47	M	1946
ALS16	wt	50mgx2/d	40	M	1953
ALS17	wt	50mgx2/d	47	M	1959
ALS18	wt	50mgx2/d	31	F	1938
ALS19	wt	50mgx2/d	42	F	1943
ALS20	wt	50mgx2/d	28	F	1931
PD1				M	1943
PD2				F	1946

Continue →

Patients	Genetic analysis	Riluzole	ALSFRS Score	Gender	Birth date
PD3				F	1946
PD4				F	1943
PD5				M	1947
PD6				M	1947
PD7				M	1958
PD8				F	1961
PD9				M	1971
PD10				F	1969
PD11				M	1966
PD12				F	1966
PD13				M	1951
PD14				F	1963
PD15				F	1942
PD16				M	1946
PD17				F	1950
PD18				F	1958
PD19				M	1940
PD20				F	1948
ALS-PD1	wt	50mgx2/d	27	M	1936
ALS-PD2	wt	50mgx2/d	41	F	1951
ALS-PD3	wt	NO	38	F	1939
ALS-PD4	N.D.	NO	34	M	1944
ALS-PD5	N.D.	50mgx2/d	29	F	1958
ALS-PD6	wt	50mgx2/d	19	M	1942
ALS-PD7	wt	50mgx2/d	20	M	1941
ALS-PD8	N.D.	50mgx2/d	29	M	1956
ALS-PD9	wt	MISS	26	M	1952

Supplemental Table 3.2. Coefficients of linear correlations of riluzole-sensitive spots with ALSFRS score.

Spots N°	Coefficients ALSFRS	Pearson correlation
498	0.037	p = 0.814
507	-0.138	p = 0.415
567	-0.130	p = 0.380
580	0.003	p = 0.986
603	0.073	p = 0.648
624	0.212	p = 0.208
631	0.356	p = 0.016
648	0.101	p = 0.513
649	-0.075	p = 0.619
681	0.105	p = 0.476
684	-0.297	p = 0.047
728	0.207	p = 0.167
787	-0.014	p = 0.935

Supplemental Table 3.3. All pathways significantly (FRD<0.001) over-represented using Reactome as reference database.

Pathway Name	Entities					Reactions		
	Found	Total	Ratio	Pvalue	FDR	Found	Total	Ratio
Prefoldin mediated transfer of substrate to CCT/TriC	6	28	0.002019	1.25E-10	2.58E-08	2	2	1.72E-04
Cooperation of Prefoldin and TriC/CCT in actin and tubulin folding	6	36	0.002596	5.57E-10	5.74E-08	6	6	5.15E-04
Platelet degranulation	8	137	0.009878	2.14E-09	8.65E-08	2	11	9.45E-04
Signaling by high-kinase activity BRAF mutants	6	46	0.003317	2.38E-09	8.65E-08	4	6	5.15E-04
MAP2K and MAPK activation	6	47	0.003389	2.70E-09	8.65E-08	4	8	6.87E-04
Signaling by moderate kinase activity BRAF mutants	6	48	0.003461	3.06E-09	8.65E-08	4	7	6.01E-04
Response to elevated platelet cytosolic Ca2+	8	144	0.010383	3.15E-09	8.65E-08	2	14	0.001202
Paradoxical activation of RAF signaling by kinase inactive BRAF	6	49	0.003533	3.46E-09	8.65E-08	4	7	6.01E-04
Hemostasis	14	806	0.058115	5.60E-09	1.23E-07	31	327	0.028086
Recycling pathway of L1	6	54	0.003894	6.14E-09	1.23E-07	7	14	0.001202
Signaling by RAS mutants	6	61	0.004398	1.26E-08	2.27E-07	4	8	6.87E-04
Signaling by BRAF and RAF fusions	6	68	0.004903	2.39E-08	3.90E-07	4	5	4.29E-04
HSP90 chaperone cycle for steroid hormone receptors (SHR)	6	69	0.004975	2.60E-08	3.90E-07	9	12	0.001031
Immune System	22	2638	0.190208	3.20E-08	4.48E-07	22	1470	0.126256
RHO GTPases activate IQGAPs	5	35	0.002524	3.62E-08	4.70E-07	2	5	4.29E-04
Gene and protein expression by JAK-STAT signaling after Interleukin-12 stimulation	6	74	0.005336	3.92E-08	4.70E-07	3	36	0.003092
L1CAM interactions	7	129	0.009301	3.97E-08	4.76E-07	10	54	0.004638
Cellular responses to stress	11	511	0.036845	4.33E-08	4.77E-07	34	184	0.015803
Interleukin-12 signaling	6	85	0.006129	8.82E-08	8.82E-07	3	56	0.00481

Continue →

Pathway Name	Entities					Reactions		
	Found	Total	Ratio	Pvalue	FDR	Found	Total	Ratio
Oncogenic MAPK signaling	6	87	0.006273	1.01E-07	1.01E-06	20	34	0.00292
Interleukin-12 family signaling	6	97	0.006994	1.90E-07	1.69E-06	3	114	0.009791
Gap junction trafficking	5	50	0.003605	2.09E-07	1.69E-06	7	20	0.001718
Cellular responses to external stimuli	11	598	0.043118	2.11E-07	1.69E-06	34	254	0.021816
Chaperonin-mediated protein folding	6	99	0.007138	2.14E-07	1.72E-06	6	19	0.001632
GRB2:SOS provides linkage to MAPK signaling for Integrins	4	20	0.001442	2.46E-07	1.72E-06	2	2	1.72E-04
Microtubule-dependent trafficking of connexons from Golgi to the plasma membrane	4	21	0.001514	2.98E-07	2.09E-06	1	2	1.72E-04
Protein folding	6	105	0.007571	3.02E-07	2.11E-06	15	28	0.002405
Gap junction trafficking and regulation	5	54	0.003894	3.05E-07	2.14E-06	7	24	0.002061
p130Cas linkage to MAPK signaling for integrins	4	22	0.001586	3.58E-07	2.15E-06	3	3	2.58E-04
Transport of connexons to the plasma membrane	4	22	0.001586	3.58E-07	2.15E-06	1	3	2.58E-04
Post-chaperonin tubulin folding pathway	4	24	0.00173	5.05E-07	3.03E-06	9	9	7.73E-04
COPI-independent Golgi-to-ER retrograde traffic	5	62	0.00447	6.00E-07	3.11E-06	2	7	6.01E-04
Platelet activation, signaling and aggregation	8	288	0.020766	6.22E-07	3.11E-06	22	114	0.009791
Formation of tubulin folding intermediates by CCT/TriC	4	29	0.002091	1.07E-06	5.34E-06	2	2	1.72E-04
Translocation of SLC2A4 (GLUT4) to the plasma membrane	5	78	0.005624	1.83E-06	9.17E-06	3	15	0.001288
Integrin alphaIIb beta3 signaling	4	39	0.002812	3.43E-06	1.71E-05	20	24	0.002061
Integrin signaling	4	39	0.002812	3.43E-06	1.71E-05	20	24	0.002061
Gap junction assembly	4	39	0.002812	3.43E-06	1.71E-05	3	16	0.001374

Continue →

Pathway Name	Entities					Reactions		
	Found	Total	Ratio	Pvalue	FDR	Found	Total	Ratio
COPI-mediated anterograde transport	5	106	0.007643	8.07E-06	3.23E-05	2	12	0.001031
Carboxyterminal post-translational modifications of tubulin	4	51	0.003677	9.80E-06	3.92E-05	6	6	5.15E-04
Factors involved in megakaryocyte development and platelet production	6	193	0.013916	9.88E-06	3.95E-05	5	43	0.003693
Platelet Aggregation (Plug Formation)	4	53	0.003821	1.14E-05	4.56E-05	20	27	0.002319
Intraflagellar transport	4	55	0.003966	1.32E-05	5.27E-05	6	12	0.001031
Kinesins	4	67	0.004831	2.84E-05	1.13E-04	2	14	0.001202
Golgi-to-ER retrograde transport	5	147	0.010599	3.83E-05	1.53E-04	4	18	0.001546
MHC class II antigen presentation	5	147	0.010599	3.83E-05	1.53E-04	1	26	0.002233
RHO GTPases Activate Formins	5	148	0.010671	3.96E-05	1.58E-04	9	27	0.002319
The role of GTSE1 in G2/M progression after G2 checkpoint	4	82	0.005912	6.19E-05	1.86E-04	3	10	8.59E-04
ER to Golgi Anterograde Transport	5	163	0.011753	6.24E-05	1.87E-04	2	39	0.00335
RAF/MAP kinase cascade	6	270	0.019468	6.42E-05	1.93E-04	4	39	0.00335
MAPK1/MAPK3 signaling	6	277	0.019973	7.39E-05	2.22E-04	4	46	0.003951
Regulation of TLR by endogenous ligand	3	31	0.002235	7.54E-05	2.26E-04	1	12	0.001031
Common Pathway of Fibrin Clot Formation	3	34	0.002452	9.90E-05	2.97E-04	4	29	0.002491
Axon guidance	8	582	0.041964	1.01E-04	3.03E-04	13	297	0.025509
Recruitment of NuMA to mitotic centrosomes	4	96	0.006922	1.13E-04	3.40E-04	1	2	1.72E-04
COPI-dependent Golgi-to-ER retrograde traffic	4	106	0.007643	1.65E-04	4.96E-04	2	11	9.45E-04
Glycolysis	4	108	0.007787	1.77E-04	5.32E-04	3	24	0.002061
MAPK family signaling cascades	6	328	0.02365	1.85E-04	5.55E-04	4	86	0.007386
Mitotic Anaphase	5	207	0.014925	1.90E-04	5.70E-04	3	11	9.45E-04
Mitotic Metaphase and Anaphase	5	208	0.014997	1.94E-04	5.81E-04	3	12	0.001031

Continue →

Pathway Name	Entities					Reactions		
	Found	Total	Ratio	Pvalue	FDR	Found	Total	Ratio
Signaling by Interleukins	8	640	0.046146	1.94E-04	5.81E-04	4	491	0.042171
Intra-Golgi and retrograde Golgi-to-ER traffic	5	217	0.015646	2.36E-04	5.81E-04	4	48	0.004123
Transport to the Golgi and subsequent modification	5	218	0.015719	2.41E-04	5.81E-04	2	60	0.005153
Hedgehog 'off' state	4	123	0.008869	2.90E-04	5.81E-04	2	32	0.002748
Formation of Fibrin Clot (Clotting Cascade)	3	52	0.003749	3.43E-04	6.86E-04	4	57	0.004896
Resolution of Sister Chromatid Cohesion	4	133	0.00959	3.90E-04	7.80E-04	4	8	6.87E-04
Glucose metabolism	4	139	0.010022	4.60E-04	9.20E-04	5	50	0.004294

Supplemental Table 4.1: ORA of PD sub-cluster. Reactome and GO BP were used as reference.

Reactome		GO BP		
Pathway name	**FDR**	**Pathway name**	**Fold enrichment**	**FDR**
Pink/Parkin Mediated Mitophagy	3.92E-04	establishment of mitochondrion localization, microtubule-mediated (GO:0034643)	30.64	1.87E-05
Mitochondrial protein import	4.82E-04	mitochondrion transport along microtubule (GO:0047497)	30.64	1.89E-05
Mitophagy	8.02E-04	establishment of mitochondrion localization (GO:0051654)	25.54	4.07E-05
		mitochondrion localization (GO:0051646)	22.7	4.12E-08
		GTP metabolic process (GO:0046039)	22.34	1.22E-05
		guanosine-containing compound metabolic process (GO:1901068)	19.15	8.35E-07
		protein targeting to mitochondrion (GO:0006626)	14.86	2.02E-05
		regulation of cellular response to heat (GO:1900034)	13.62	6.61E-04
		purine ribonucleoside metabolic process (GO:0046128)	13.13	1.06E-05
		purine nucleoside metabolic process (GO:0042278)	12.59	1.36E-05
		protein localization to mitochondrion (GO:0070585)	12.1	1.74E-05
		establishment of protein localization to mitochondrion (GO:0072655)	11.67	8.78E-05
		mitochondrial membrane organization (GO:0007006)	11.44	3.23E-08
		aerobic respiration (GO:0009060)	11.19	1.13E-04
		regulation of membrane permeability (GO:0090559)	10.48	1.63E-04
		regulation of mitochondrial membrane permeability (GO:0046902)	10.21	6.71E-04
		organelle transport along microtubule (GO:0072384)	9.93	7.82E-04
		ribonucleoside metabolic process (GO:0009119)	9.89	6.78E-05
		mitochondrial transport (GO:0006839)	8.81	1.94E-08
		purine ribonucleoside triphosphate metabolic process (GO:0009205)	8.28	1.53E-08
		respiratory electron transport chain (GO:0022904)	8.17	7.07E-04
		ribonucleoside triphosphate metabolic process (GO:0009199)	8.06	1.91E-08
		purine nucleoside triphosphate metabolic process (GO:0009144)	8.03	1.97E-08
		mitochondrion organization (GO:0007005)	7.95	2.46E-16

Continue →

Reactome		GO BP		
Pathway name	**FDR**	**Pathway name**	**Fold enrichment**	**FDR**
		oxidative phosphorylation (GO:0006119)	7.93	8.32E-04
		nucleoside metabolic process (GO:0009116)	7.73	3.35E-04
		nucleoside triphosphate metabolic process (GO:0009141)	7.38	4.54E-08
		regulation of neurotransmitter transport (GO:0051588)	6.91	7.08E-04
		positive regulation of cell morphogenesis involved in differentiation (GO:0010770)	6.86	2.78E-04
		macroautophagy (GO:0016236)	6.66	8.86E-04
		response to glucose (GO:0009749)	6.57	9.64E-04
		cellular respiration (GO:0045333)	6.55	3.86E-04
		regulation of mitochondrion organization (GO:0010821)	6.46	1.70E-04
		energy derivation by oxidation of organic compounds (GO:0015980)	6.33	1.36E-05
		purine ribonucleoside monophosphate metabolic process (GO:0009167)	6.27	1.48E-05
		cytoskeleton-dependent intracellular transport (GO:0030705)	6.27	5.36E-04
		purine nucleoside monophosphate metabolic process (GO:0009126)	6.24	1.50E-05
		ribonucleoside monophosphate metabolic process (GO:0009161)	5.91	2.61E-05
		ATP metabolic process (GO:0046034)	5.88	3.48E-04
		electron transport chain (GO:0022900)	5.77	9.53E-04
		purine ribonucleotide metabolic process (GO:0009150)	5.55	3.06E-08
		regulation of stress-activated MAPK cascade (GO:0032872)	5.55	2.46E-04
		regulation of stress-activated protein kinase signaling cascade (GO:0070302)	5.52	2.55E-04
		purine nucleotide metabolic process (GO:0006163)	5.51	1.95E-08
		regulation of Ras protein signal transduction (GO:0046578)	5.5	2.65E-04
		nucleoside monophosphate metabolic process (GO:0009123)	5.42	6.12E-05
		ribose phosphate metabolic process (GO:0019693)	5.36	2.61E-08
		ribonucleotide metabolic process (GO:0009259)	5.36	4.78E-08
		cellular response to peptide hormone stimulus (GO:0071375)	5.27	1.72E-04

Continue →

Reactome		GO BP		
Pathway name	**FDR**	**Pathway name**	**Fold enrichment**	**FDR**
		regulation of cell morphogenesis involved in differentiation (GO:0010769)	5.16	4.51E-05
		apoptotic signaling pathway (GO:0097190)	5.16	9.96E-05
		regulation of protein polymerization (GO:0032271)	5.15	9.59E-04
		cellular response to peptide (GO:1901653)	5.11	5.02E-05
		purine-containing compound metabolic process (GO:0072521)	5.09	4.99E-08
		regulation of small GTPase mediated signal transduction (GO:0051056)	5.06	2.60E-05

8.2

Supplemental Figures

Supplementary Figure 2.1: Physical interaction network of "_Proteins" lists. Network-based analysis of the (A) "AD_Proteins" list, (B) "PD_Proteins" list and (C) "ALS_Proteins" list, using the IntAct database as the reference set (PPI spider). network is statistically significant ($p < 0.01$).

(A)

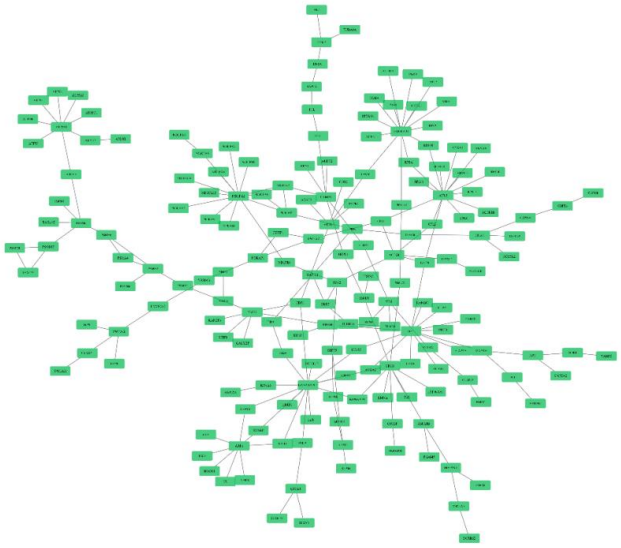

(B)

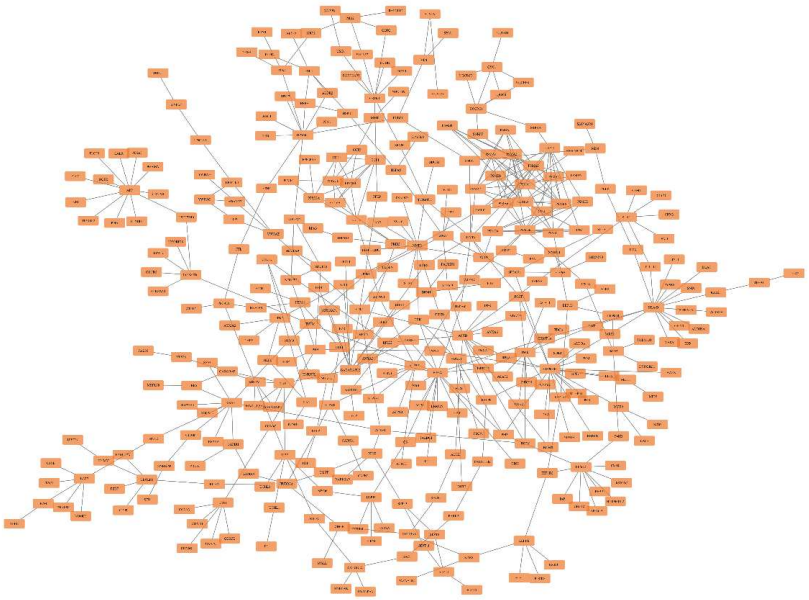

(C)

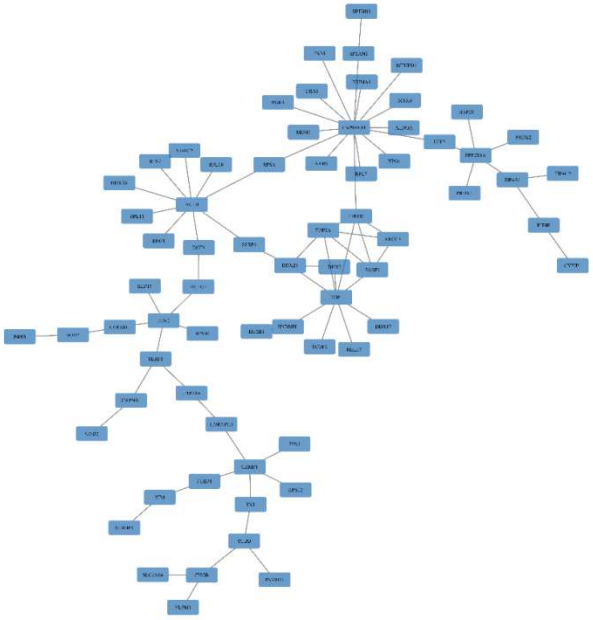

Supplementary Figure 2.2: Merged PPI networks. Network obtained by the union of AD, PD and ALS PPI networks (View Supplementary Figure 1). The colour code indicates which nodes are disease-specific and which nodes are shared by different diseases.

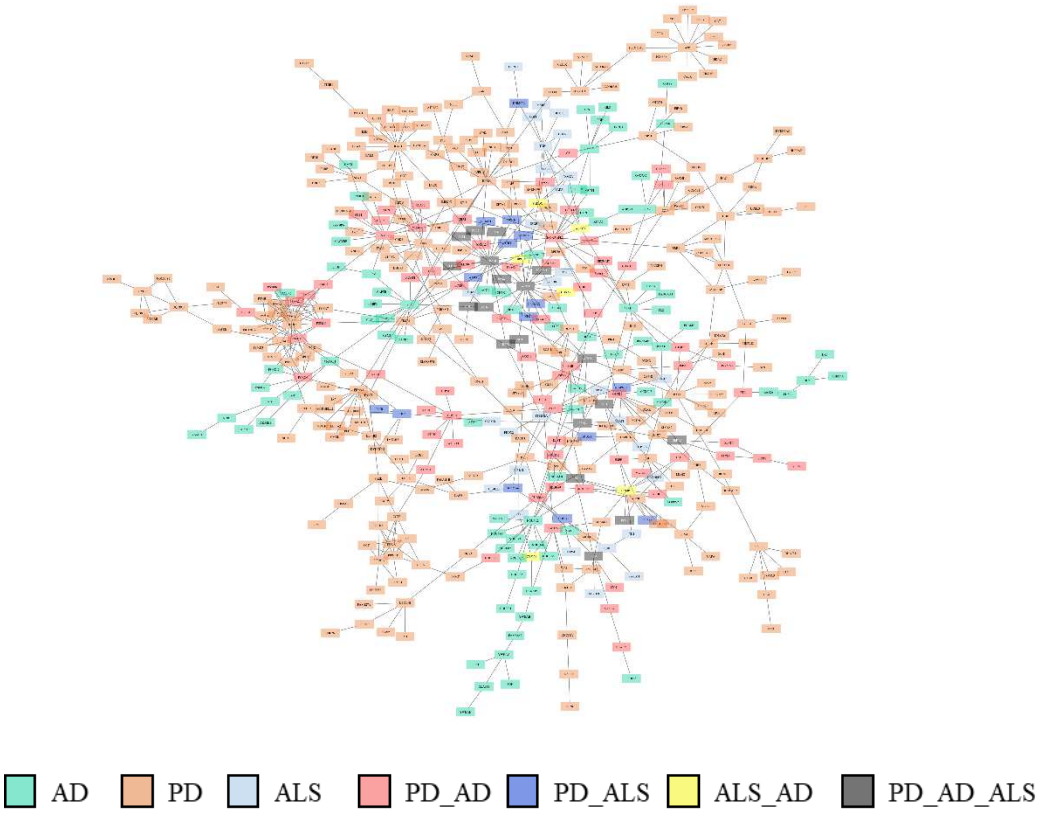

Supplemental Figure 3.1: Distribution density of the sum of common spot volumes

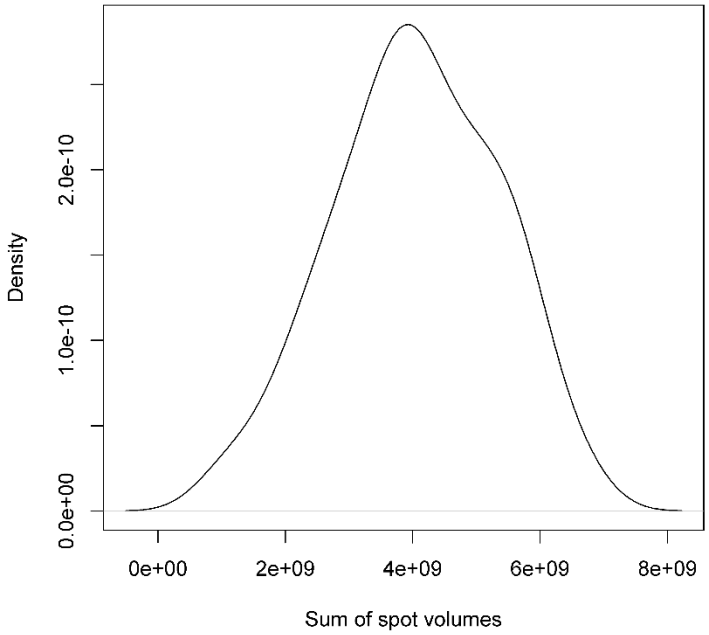

Supplemental Figure 3.2: Distribution of missing values. The horizontal line represents the chosen threshold of 24 missing values.

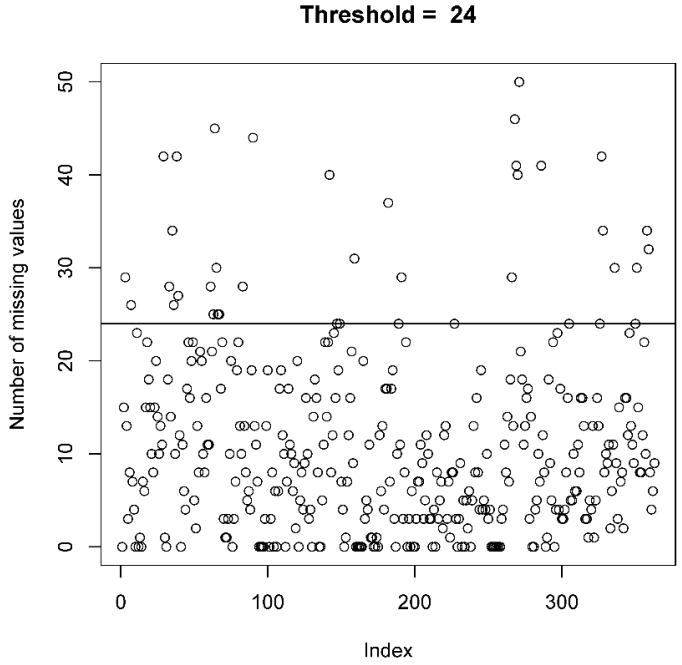

Supplemental Figure 3.3: (A) Scatter plot of a pair of gels belonging to the same group. The Pearson correlation coefficient is reported under the plot, together with the slope of the straight line. (B) Quantile-quantile plot for the residuals of the linear fit in panel A. A linear correlation between t quantiles and studentized residuals indicates that gels are comparable.

A

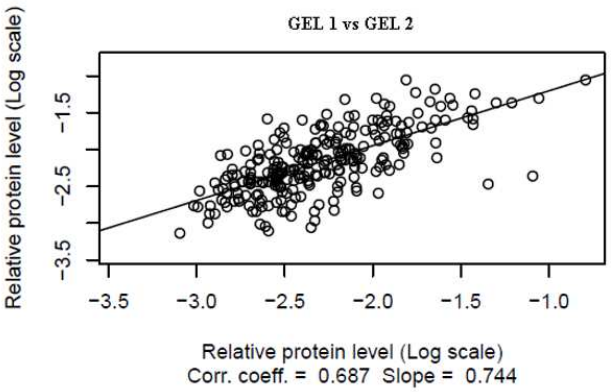

B

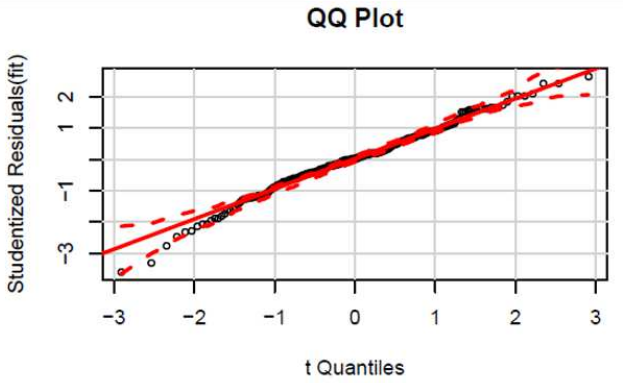

Supplemental Figure 3.4: 7 spots gender-sensible Box plot relative to the spots that significantly correlate with the gender by the Wilcoxon test ($p<0.01$). In "pink" are reported female patients, while in "light blue" are represented male patients.

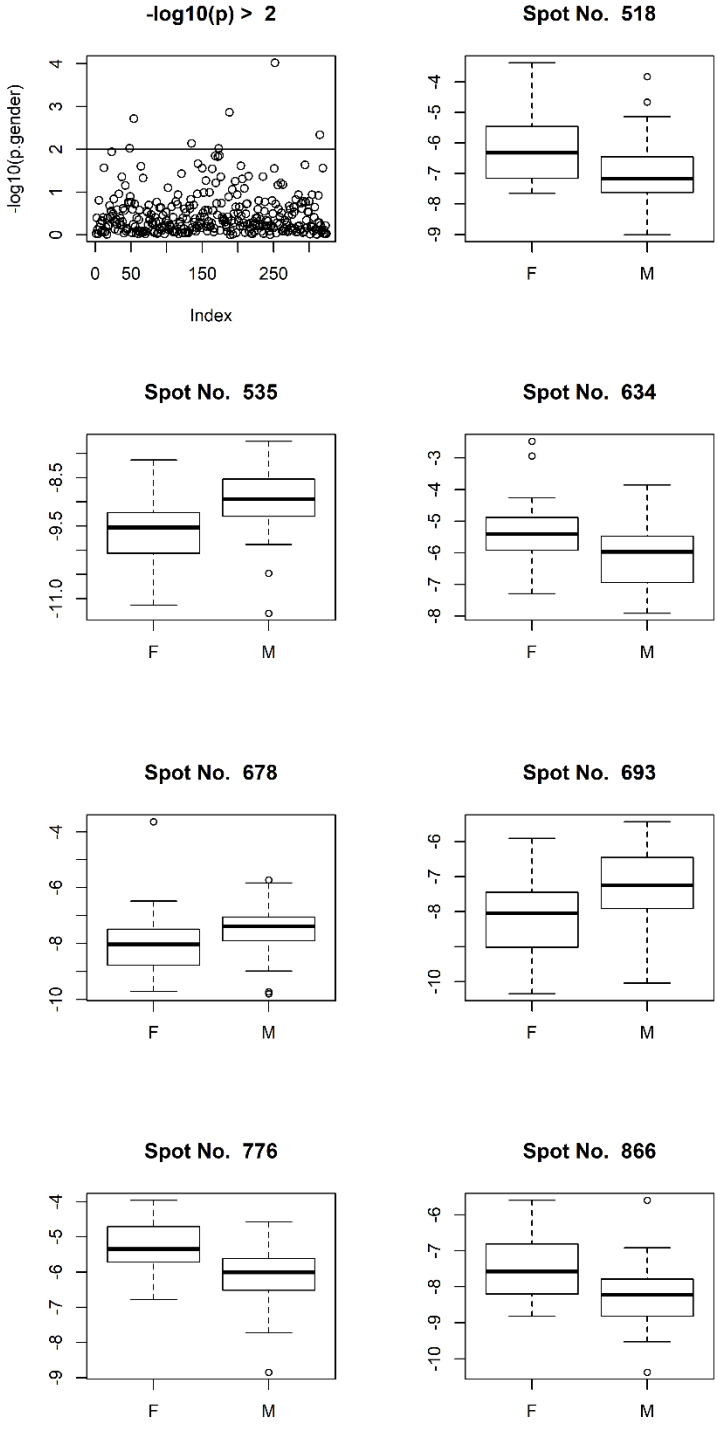

Supplemental Figure 3.5: 21 spots age-sensible Pearson correlation relative to the spots that significantly correlate (p<0.01) with age of patient at the withdrawal. In "yellow" are reported ALS patients, in "red" ALS_r patients, in "green" PD patients while in "blue" are displayed ALS-PD patients.

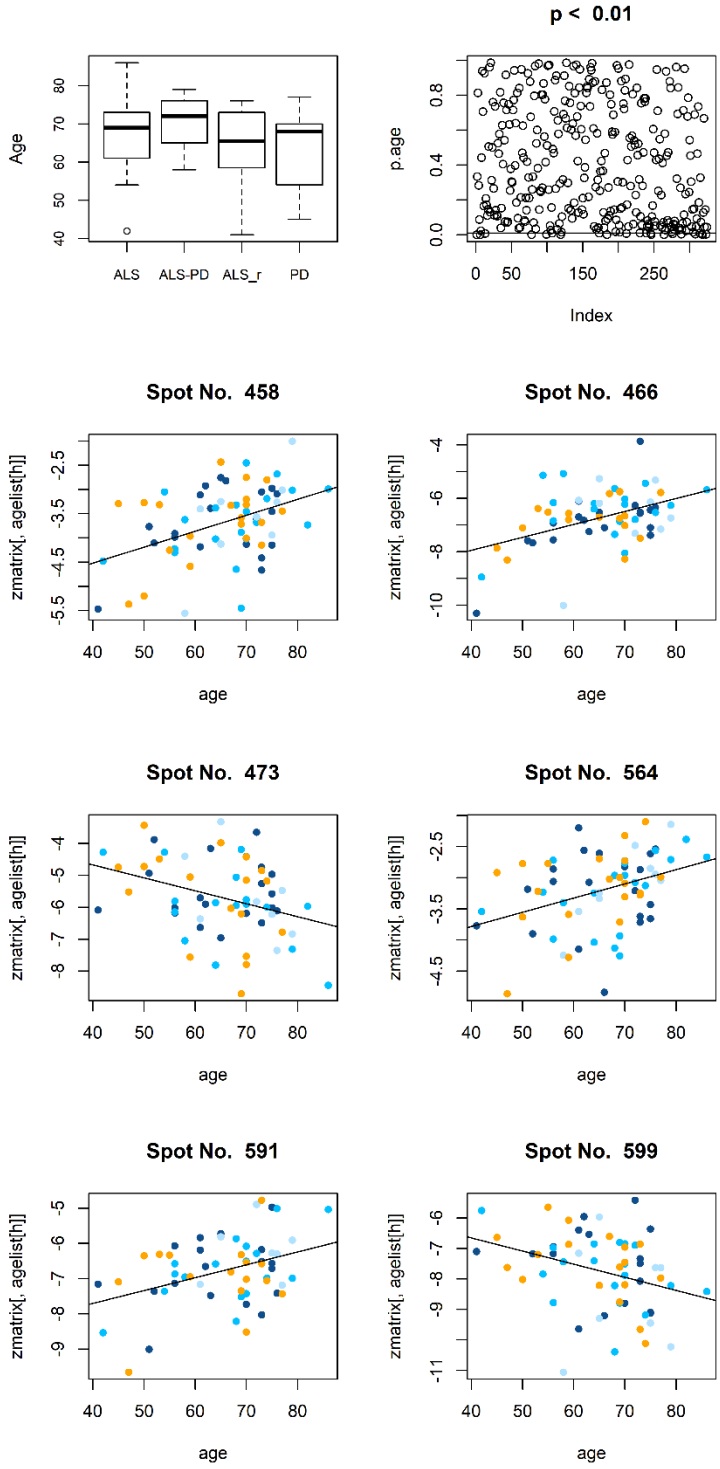

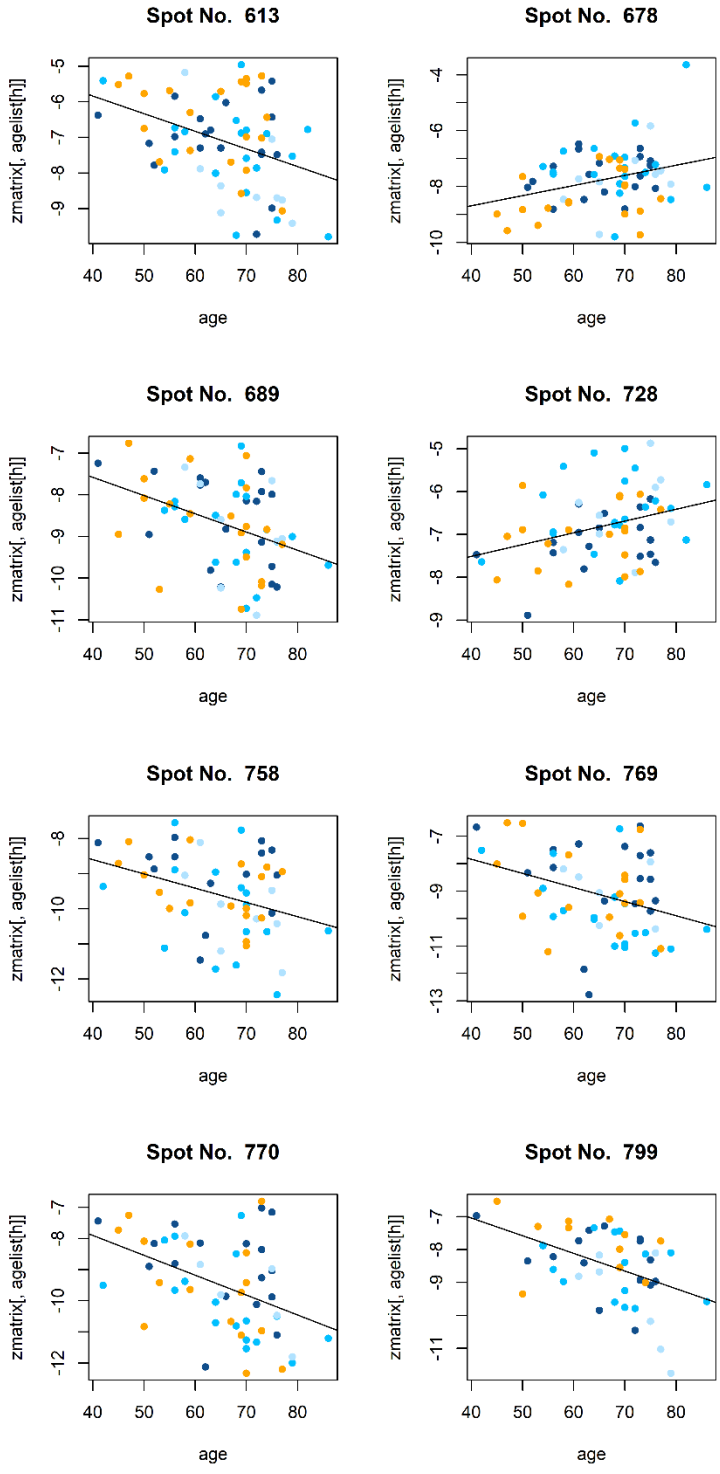
Spot No. 613
Spot No. 678
Spot No. 689
Spot No. 728
Spot No. 758
Spot No. 769
Spot No. 770
Spot No. 799
zmatrix[, agelist[h]]
age

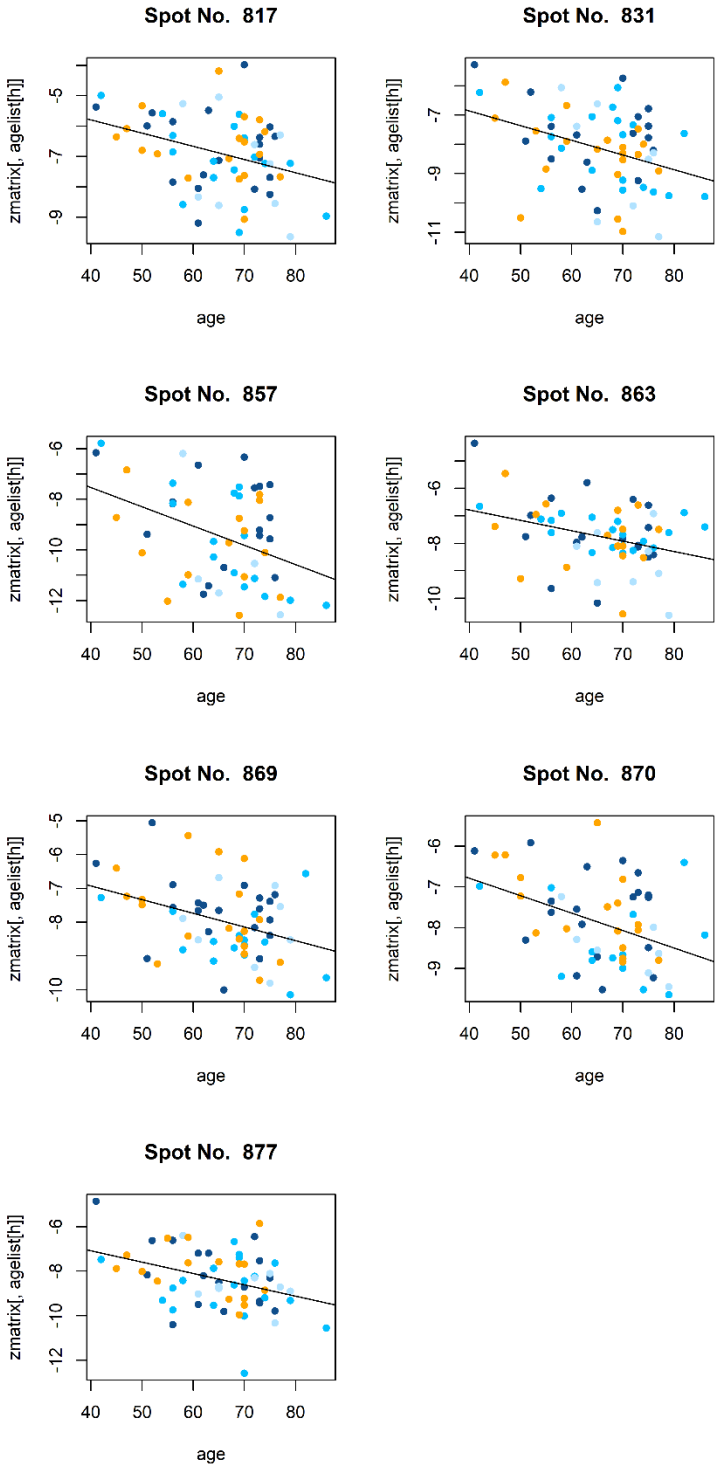
Spot No. 817
Spot No. 831
Spot No. 857
Spot No. 863
Spot No. 869
Spot No. 870
Spot No. 877
zmatrix[, agelist[h]]
age

Supplemental Figure 3.6: 13 spots riluzole-sensible Box plot relative to the spots that significantly correlate by the Student T test ($p<0.01$) with drug treatment. In "yellow" are reported ALS patients and in "red" ALS_r patients.

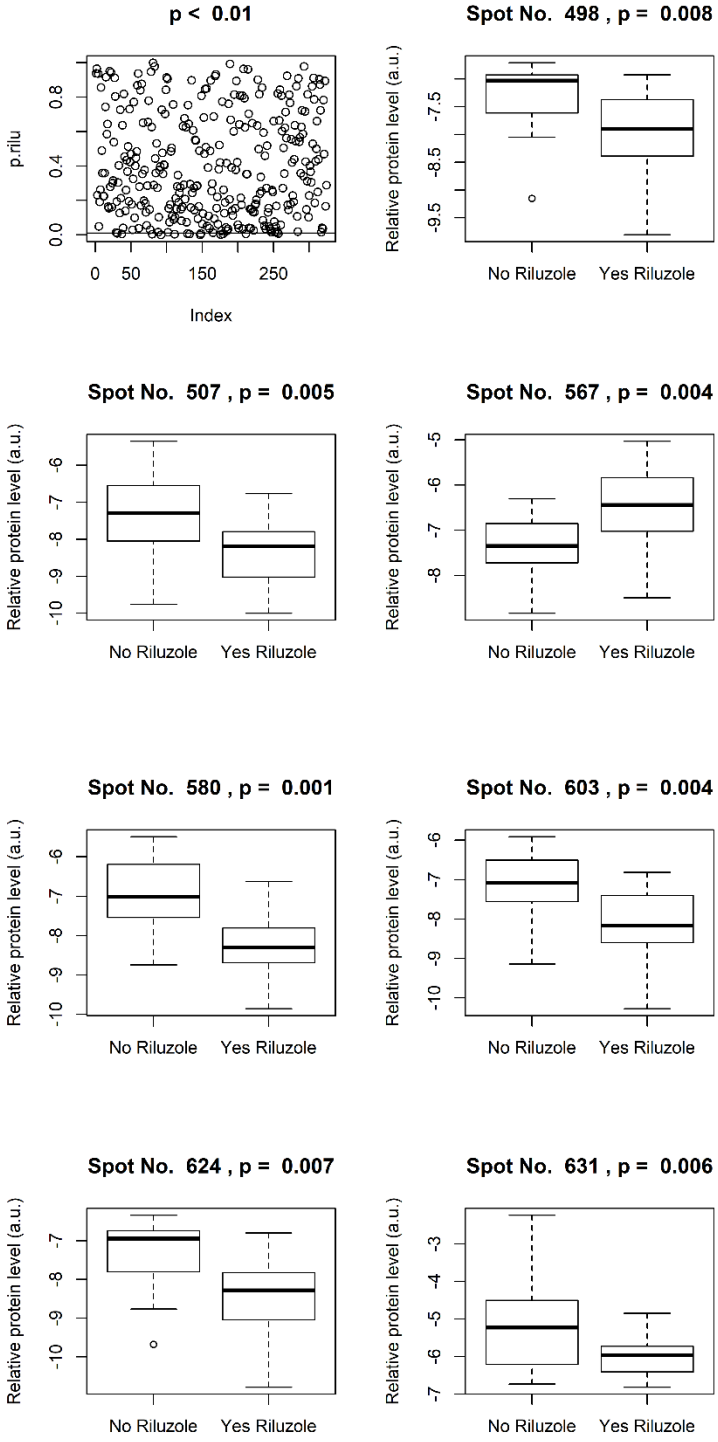

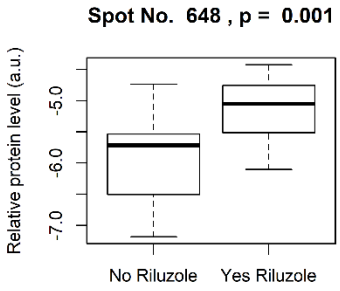
Spot No. 648 , p = 0.001
Relative protein level (a.u.)
-5.0
-6.0
-7.0
No Riluzole
Yes Riluzole

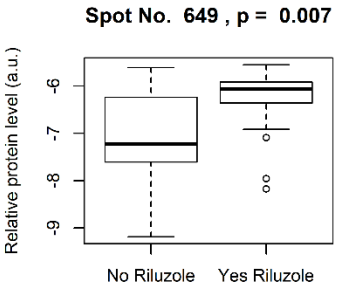
Spot No. 649 , p = 0.007
Relative protein level (a.u.)
-6
-7
-8
-9
No Riluzole
Yes Riluzole

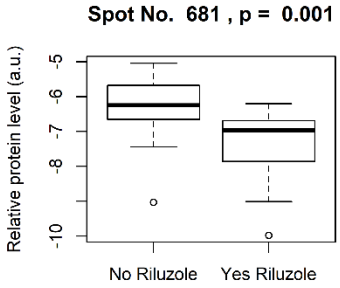
Spot No. 681 , p = 0.001
Relative protein level (a.u.)
-5
-6
-7
-8
-10
No Riluzole
Yes Riluzole

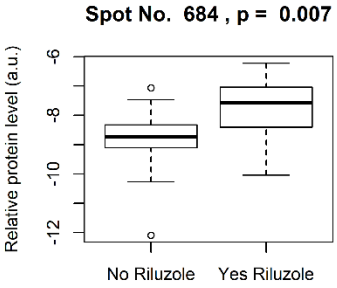
Spot No. 684 , p = 0.007
Relative protein level (a.u.)
-6
-8
-10
-12
No Riluzole
Yes Riluzole

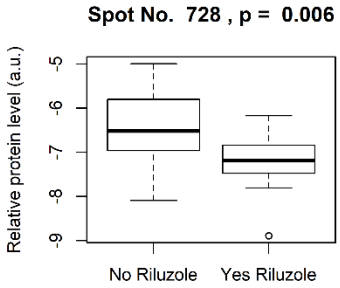
Spot No. 728 , p = 0.006
Relative protein level (a.u.)
-5
-6
-7
-8
-9
No Riluzole
Yes Riluzole

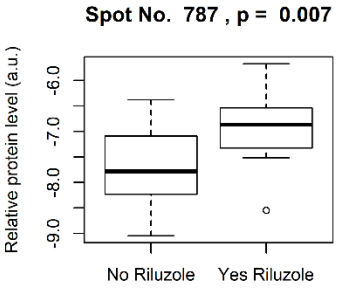
Spot No. 787 , p = 0.007
Relative protein level (a.u.)
-6.0
-7.0
-8.0
-9.0
No Riluzole
Yes Riluzole

Supplemental Figure 3.7: (A) Cross-validation performed with the Leave-one-out process. (B) Cross-validation obtained by the k-fold method. In "black" the percentage relative to the sensibility of each model is reported, in "dark gray" the specificity and in "light gray" the area under the ROC curve. The dashed line indicates the 33 spot model chosen because of the best performance.

A

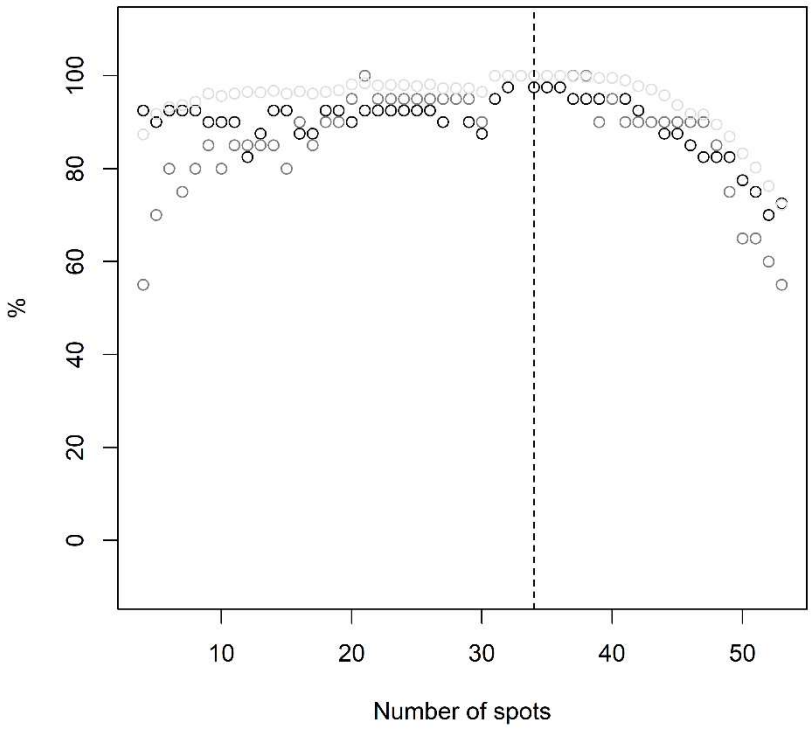

B

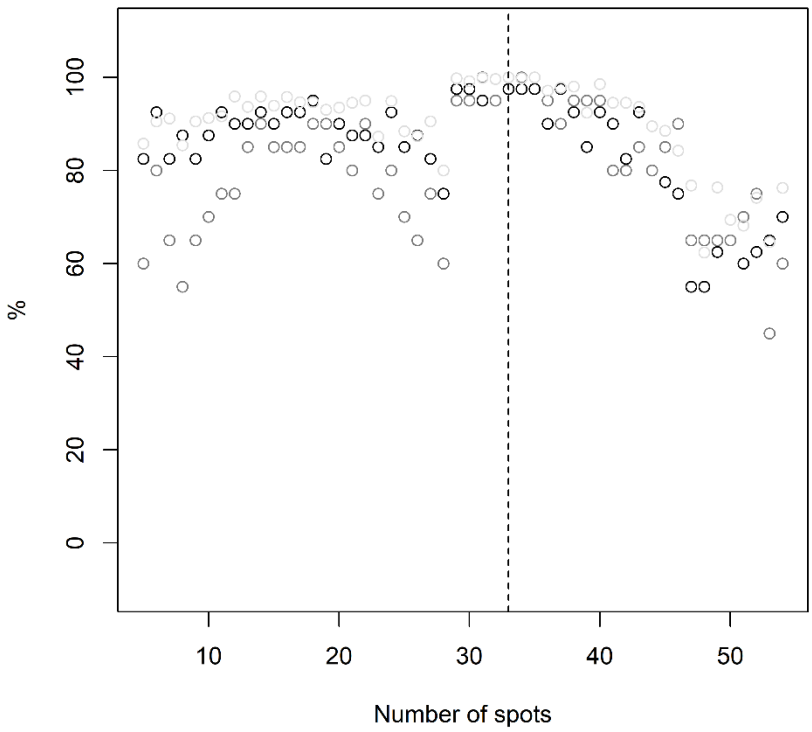

Supplemental Figure 3.8: graphical representation of PCA. The 5 ALS-PD patients classified as PD (blue spots) and the 4 ALS-PD patients classified as ALS (red spots) were discriminate for 25.4% by PC1.

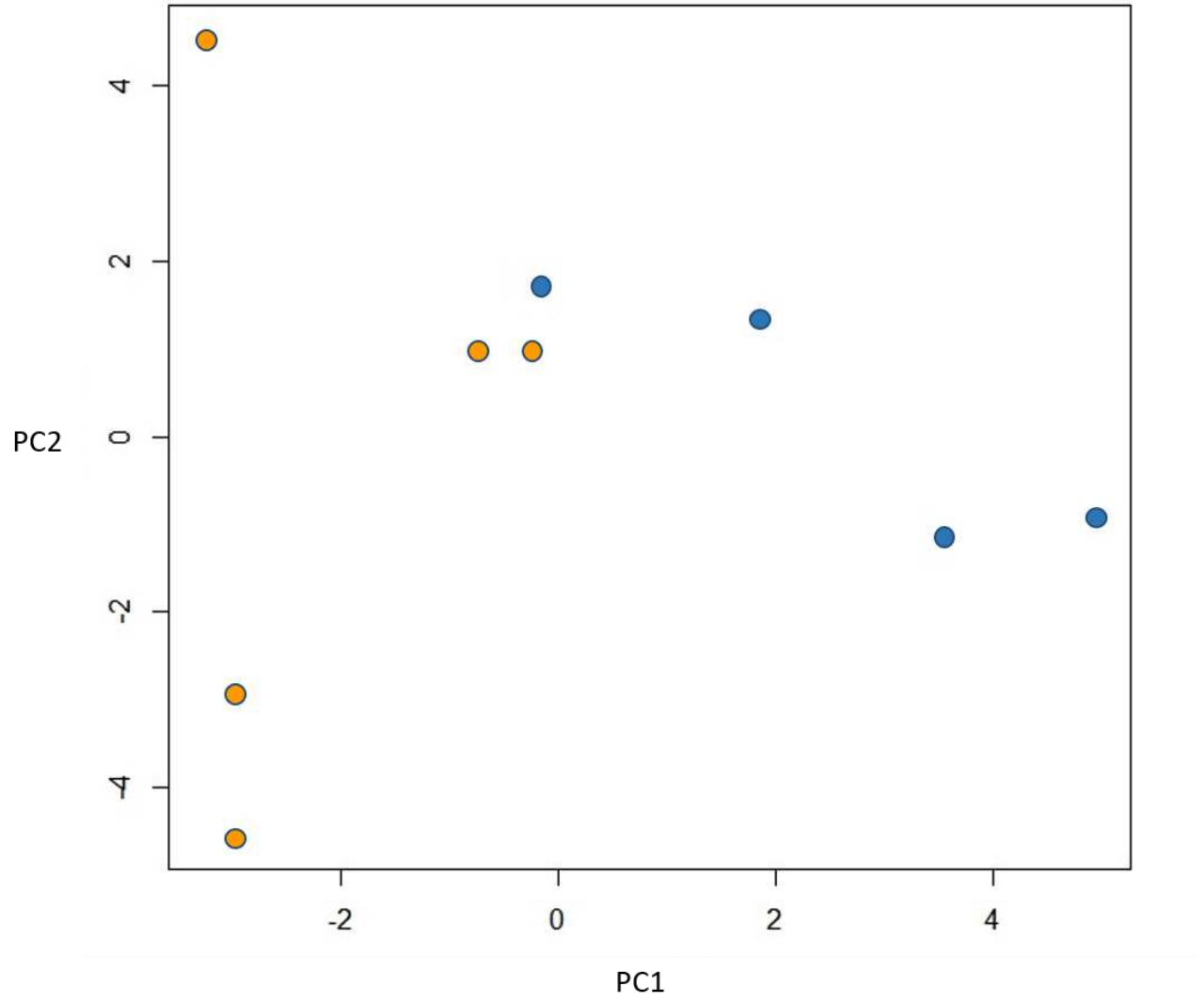

Supplemental Figure 5.1: Representative images of SH-SY5Y cells treated for 24 hours with different mitochondrial toxins. Red (Mitotracker) indicates mitochondria with intact Δψm.

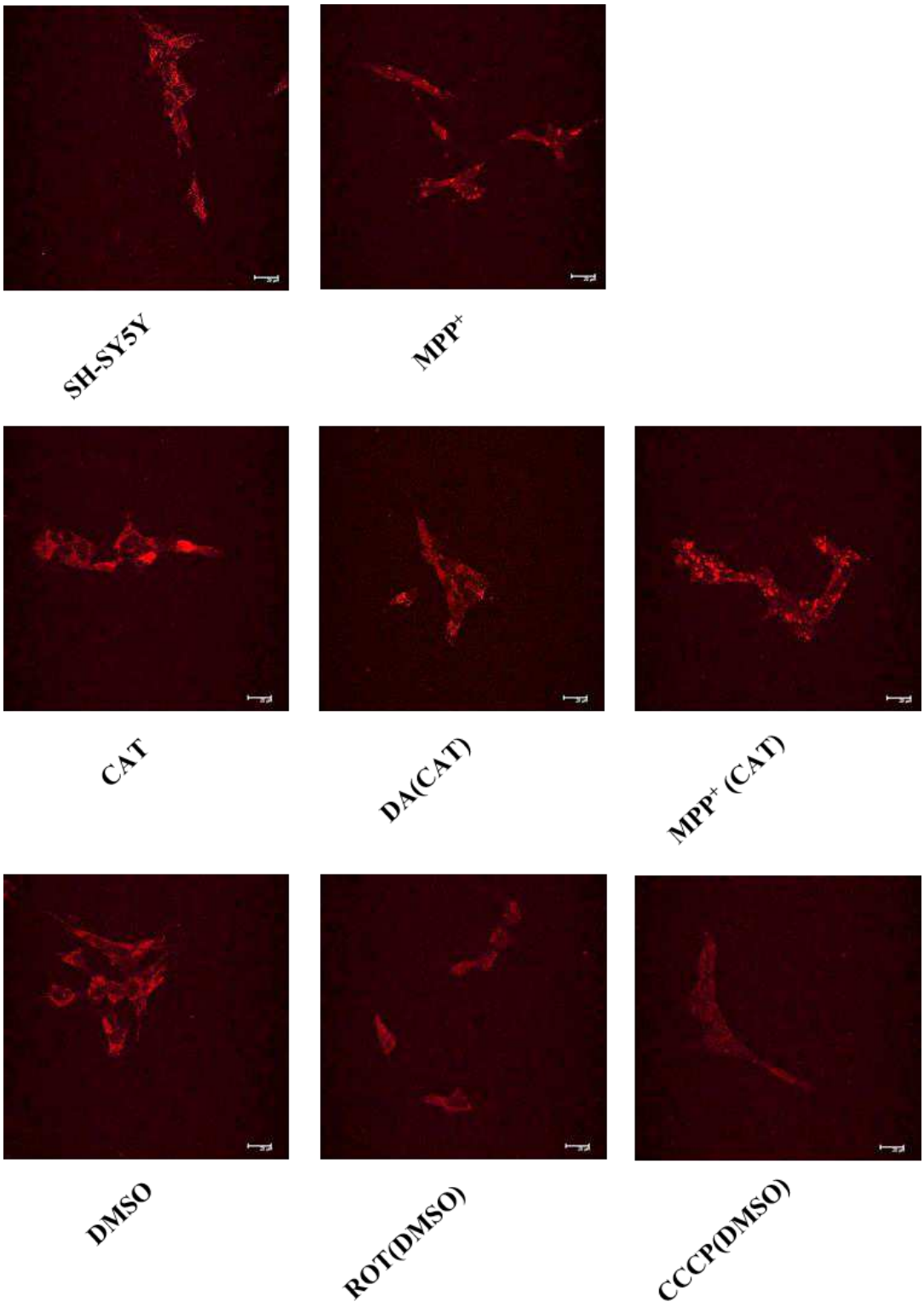

8.3

Supplemental Data

Supplemental Data 4.1: query to obtain all mitochondrial proteins. Data was extracted from neXtProt using the advanced search functionality based on SPARQL language on the neXtProt SNORQL interface

```
select distinct ?entry ?interactant where {
   values ?entry { #This is to replace with MITO list entries entry:NX_….
entry:NX_….
          }
       ?entry :isoform /:binaryInteraction ?interaction.
?interaction :interactant ?interactant, :quality :GOLD.
?interactant a :Entry.
}
```

Supplemental Data 4.2: query to obtain all gold protein-protein interactions from the protein interaction section. Information was extracted from neXtProt using the advanced search functionality based on SPARQL language on the neXtProt SNORQL interface

```
select distinct ?entry ?comment where {
  values ?entry { entry: #This is to replace with MITO list entries
}
  ?entry :isoform ?iso.
  ?iso :interactionInfo /rdfs:comment ?comment.
}
```

Supplemental Data 4.3: query to obtain subcellular location data. Information was extracted from neXtProt using the advanced search functionality based on SPARQL language on the neXtProt SNORQL interface

```
select distinct ?entry where {
   values ?mitoloc {cv:#Uniprot code cv:GO code}
       ?entry :isoform ?iso.
       ?iso :cellularComponent ?loc .
       ?loc :term/:childOf ?mitoloc .
       ?loc :evidence / :quality :GOLD .
       filter not exists {?loc :negativeEvidence ?_.}
}
```

Supplemental Data 4.4: query to obtain mitochondrial with unknown function. Data was extracted from neXtProt using the advanced search functionality based on SPARQL language on the neXtProt SNORQL interface

```
select distinct ?entry where {
 ?entry :isoform ?iso.
 filter not exists { ?iso :functionInfo ?_ . }
 filter not exists { ?iso :function ?func .
                     optional {?func :term ?fterm1 .}
                     filter(!bound(?fterm1)) #eliminates functions from
pathways
                   }
 filter not exists {
                       ?iso :function / :term ?fterm .
                       filter(?fterm != cv:GO_0005524 && ?fterm !=
cv:GO_0000287 && ?fterm != cv:GO_0005515 && ?fterm != cv:GO_0042802
                              && ?fterm != cv:GO_0008270 && ?fterm !=
cv:GO_0051260 && ?fterm != cv:GO_0005509
                              && ?fterm != cv:GO_0003676 && ?fterm !=
cv:GO_0003824 && ?fterm != cv:GO_0007165 && ?fterm != cv:GO_0035556)
                     # eliminates proteins whose ONLY GO functions are
one of ATP-binding, magnesium-binding, calcium-binding, zinc-binding,
                     # nucleic acid binding, protein-binding, identical
protein binding, protein homooligomerization, catalytic activity, signal
transduction,
                   }
}
```

PART IX

Publications, Posters and Awards

PUBLICATIONS:

Monti C, Lane L, Fasano M, Alberio T. Update of the Functional Mitochondrial Human Proteome Network. J Proteome Res. 2018 Oct 8. doi: 10.1021/acs.jproteome.8b00447. [Epub ahead of print] PubMed PMID: 30230342.

Monti C, Zilocchi M, Colugnat I, Alberio T. Proteomics turns functional. J Proteomics. 2018 Dec 13. pii: S1874-3919(18)30441-X. doi: 10.1016/j.jprot.2018.12.012. [Epub ahead of print] PubMed PMID: 30553948.

POSTERS:

2018

Oral presentation XII Italian Proteomic Association congress in Como. "An update of the functional mitochondrial human proteome network.". **Monti C.**, Lane L., Fasano M., Alberio T.

Poster XII European Proteomics Association congress in Santiago De Compostela. "THE FUNCTIONAL MITOCHONDRIAL HUMAN PROTEOME NETWORK". **Monti C.**, Lane L., Fasano M., Alberio T.

AWARD:

Travel grant for Young European Proteomics Researchers to attend XII European Proteomics Association congress in Santiago De Compostela

PUBLICATIONS:

Monti C, Colugnat I, Lopiano L, Chiò A, Alberio T. Network Analysis Identifies Disease-Specific Pathways for Parkinson's Disease. Mol Neurobiol. 2018 Jan;55(1):370-381. doi: 10.1007/s12035-016-0326-0. Epub 2016 Dec 21. PubMed PMID:28004338.

POSTERS:

Poster XVI HUman Proteome Organization congress in Dublin. "ProLiPALS: Proteomics of Lymphocytes of Parkinson's disease and Amyotrophic Lateral Sclerosis patients". **Monti C.**, Colugnat I., Sironi C., Lopiano L., Chiò A., Di Pierro A., Fasano M., Alberio T.

2017

Poster XI Italian Proteomic Association congress in Lecce. "MARNORA: a tool to perform Meta-Analysis, Reaction Network, Over Representation Analysis". **Monti C.**, Fasano M., Tini S., Alberio T.

Oral presentation Annual Swiss Proteomics Meeting 2017 in Thun. "Proteomics analysis of lymphocytes from Parkinson's disease and Amyotrophic Lateral Sclerosis patients to highlight a comorbidity protein signature". **Monti C.**, Colugnat I., Di Pierro A., Sironi C., Chiò A., Lopiano L., Comi C., Fasano M., Alberio T.

AWARDS:

Travel grant for Young European Proteomics Researchers to attend Annual Swiss Proteomics Meeting 2017 in Thun,

Travel grant for Young European Proteomics Researchers to attend XI Italian Proteomic Association Congress in Lecce

Travel grant for Young European Proteomics Researchers to attend XVI Human Proteome Organization Congress in Dublin.

PUBBLICATIONS:

Fasano M, **Monti C**, Alberio T. A systems biology-led insight into the role of the proteome in neurodegenerative diseases. Expert Rev Proteomics. 2016 Sep;13(9):845-55. doi: 10.1080/14789450.2016.1219254. Epub 2016 Aug 22. Review. PubMed PMID: 27477319.

Di Pierro A, Bondi H, **Monti C**, Pieroni L, Cilio E, Urbani A, Alberio T, Fasano M, Ronci M. Experimental setup for the identification of mitochondrial protease substrates by shotgun and top-down proteomics. EuPA Open Proteom. 2016 Feb 22;11:1-3. doi: 10.1016/j.euprot.2016.02.002. eCollection 2016 Jun. PubMed PMID: 29900104; PubMed Central PMCID: PMC5988556.

2016

POSTERS:

Poster X Italian Proteomic Association congress in Perugia "Proteomics analysis of lymphocyte from Parkinson's disease and Amyotrophic Lateral Sclerosis patients". **Monti C**., Colugnat I., Lopiano L., Chiò A., Fasano M., Alberio T.

Poster Applaied Bioinformatics in Life Sciences congress in Leuven. "Systems biology analysis of the proteomic alterations in Parkinson's disease and Amyotrophic Lateral Sclerosis". **Monti C**., Colugnat I., Fasano M., Alberio T.